Understanding the Efficiency of Hydraulic Actuation Systems Using the Concept of Cyclic Performance Index

by

Jaykumar Patel

A Thesis submitted to the

Faculty of Graduate and Postdoctoral Studies of
the University of Manitoba

in partial fulfillment of the requirements for the degree of

Master of Science

Department of Mechanical Engineering
University of Manitoba
Winnipeg, Manitoba, Canada

Abstract

This research develops and applies a new approach for evaluating the performance of hydraulic systems, with particular emphasis on those incorporating Energy Storage and Reutilization (ESR) circuits. Hydraulic systems are widely used in industry for their high-power density and versatility. Yet, current performance evaluation methods, such as energy-saving ratios, relative efficiency, and Sankey flow diagrams, are limited. These methods do not adequately account for stored and reutilized energy, making it difficult to fairly compare systems or accurately assess the benefits of energy recovery. To address this problem, the study applies the Cyclic Performance Index (CPI), a metric introduced by Costa and Sepehri [1], which evaluates all energy flows in the system. The CPI incorporates input energy from the prime mover, recoverable energy from the load, and energy losses during operation, thereby providing a more comprehensive framework for performance assessment.

The CPI methodology is validated through MATLAB simulations of Electro-Hydrostatic Actuators (EHA) configured with and without Energy Storage and Reutilization (ESR) circuits. This approach allows direct comparison between standard configurations and those equipped with energy recovery capability. The results show that, when ESR circuits are integrated, overall energy performance improved by approximately 40%, with CPI values increasing from 0.15 to 0.21. These results confirm the practical utility of CPI for capturing the impact of energy storage and reuse. The study also identifies limitations, especially where some stored energy is not fully reutilized due to system losses. This highlights the need for further optimization of ESR circuit design to enhance recovery efficiency.

In conclusion, the CPI offers a standardized and reliable tool for evaluating hydraulic systems with or without energy recovery. By measuring the balance of energy consumption, storage, and reuse, it allows for more precise comparisons between different system configurations. This research supports the development of energy-efficient and sustainable hydraulic technologies by illustrating both the advantages of ESR integration and the value of CPI as a performance evaluation metric.

Acknowledgements

I would like to express my sincere gratitude to my advisor, Dr. Nariman Sepehri, for his guidance, encouragement, and patience throughout this research. His expertise and steady support have been invaluable, and I am genuinely grateful for the opportunity to work under his supervision.

I am also grateful to Dr. Gustavo Koury Costa for his insightful feedback and technical suggestions, which significantly enhanced the quality of this work. I would like to express my appreciation to Dr. Subramaniam Balakrishnan for serving on my examining committee and for providing thoughtful comments on my thesis.

I sincerely appreciate the support of my colleagues in the Fluid Power and Telerobotics Research Laboratory, including Soleiman Hosseinpour, Hossam ElWehishy, and Narges Ghobadi, whose discussions and encouragement made this journey both productive and enjoyable.

My heartfelt thanks go to my friends for their support and understanding throughout my studies. I owe special thanks to Rohan Patel and Sneh Makwana, whose encouragement and positivity helped me stay focused during challenging times.

Finally, I would like to express my deepest gratitude to my parents for their unwavering love and support. I also extend my heartfelt thanks to my wife, whose patience, understanding, and constant encouragement gave me the strength to complete this work.

Table of Contents

List of Figures

List of Tables

Nomenclatures and Abbreviations

Nomenclatures

Variable	Definition
t	Time (s)
$[t_1, t_2]$	Time interval for integration (s)
x	Piston displacement (m)
A_{piston}	Piston cross-sectional area (m^2)
A_{rod}	Rod cross-sectional area (m^2)
Q_1	Pump flow rate (m^3/s)
Q_2	Piston-side flow rate (m^3/s)
Q_3	Rod-side flow rate (m^3/s)
p_1	Pump outlet pressure (Pa)
p_2	Piston-side pressure after the valve (Pa)
p_3	Piston-chamber pressure (Pa)
p_4	Rod-side pressure after the valve (Pa)
p_5	Rod-chamber pressure (Pa)
p_T	Return (tank) pressure (Pa)
Δp	Pressure differential of the pump/motor (Pa)
$P_{pump,out}$	Hydraulic output power of the pump (W)
P_{piston}	Power delivered at the actuator (piston) (W)
P_{hose}	Power loss in hoses (W)
P_{valve}	Power loss in throttling valves (W)
$E_{in,1}$	Input energy of the conventional system (J)
$E_{in,2}$	Effective input energy of the IEHEC-based system (J)
$E_{pump,out}$	Useful pump output energy (J)
E_{valve}	Energy lost in valves (J)
E_{hose}	Energy lost in hoses (J)
E_{out}	Useful output energy at the actuator (J)

Variable	Definition
E_{gen}	Generator drive losses (J)
E_{es}	Energy storage losses (J)
E_{fq}	Frequency converter losses (J)
E_{cable}	Cable losses (J)
E_{IEHEC}	Internal losses of the IEHEC unit (J)
E_{brake}	Energy recovered during lowering/braking (J)
E_{mot}	Electrical input energy to the motor/drive (J)
E_{old}	Energy consumption without recovery (J)
E_{new}	Energy consumption with recovery (J)
$E_{Act,pos}$	Positive actuator energy (useful actuator work) (J)
$E_{Act,neg}$	Recoverable actuator energy (from lowering/deceleration) (J)
$E_{Act,net}$	Net actuator energy (J)
E_{Diesel}	Diesel input energy (J)
E_{pump}	Energy delivered by a hydraulic pump (J)
$\eta_{cycle}(t)$	Cycle efficiency over $[t_1, t_2]$
Γ_s	Energy-saving ratio
η_{Hyd}	Hydraulic efficiency
$\eta_{Tot,Gross}$	Gross fuel efficiency
$\eta_{Tot,net}$	Net fuel efficiency
η_v	Volumetric efficiency (generic)
η_{v_p}, η_{v_m}	Volumetric efficiency in pump/motor mode
η_t	Torque efficiency (generic)
η_{t_p}, η_{t_m}	Torque efficiency in pump/motor mode
$\eta_{rt}(i)$	Round-trip efficiency for cycle *i*
i_{brake}	Braking current through resistor bank (A)
R_{brake}	Braking resistor value (Ω)
i_a, i_b, i_c	Phase currents of the motor/drive (A)
u_a, u_b, u_c	Phase voltages of the motor/drive (V)
I	Conductor current (A)
r	Conductor resistance per unit length (Ω/m)

Variable	Definition
l	Cable length (m)
C_s	Laminar leakage coefficient
C_{st}	Turbulent leakage coefficient
C_v	Viscous loss coefficient
C_f	Frictional loss coefficient
C_h	Hydrodynamic loss coefficient
β	Fluid bulk modulus of elasticity (Pa)
T_i, T_a	Ideal and actual torque (Nm)
Q_i, Q_a	Ideal and actual flow rate (m^3/s)
F_R	Cylinder force (N)
v	Piston velocity (m/s)
p_p	Piston-side pressure (Pa)
p_a	Rod-side pressure (Pa)
P_L	Load pressure (Pa)
S	Useful energy transferred to the load during lifting (J)
ε_1	Internal losses during lifting (J)
ε_2	Energy losses during lowering (J)
S_p	Extra input energy from prime mover to counterbalance load (J)
P_{in}	Input power from prime mover (W)
P_{out}	Output power at the actuator (W)
T_e	Electromagnetic torque (Nm)
T_L	Load torque (Nm)
J	Shaft/machine inertia (kgm^2)
B	Viscous damping coefficient (Nms/rad)
ω_m	Servomotor angular speed (rad/s)
ω_{P_S}	Pump/motor shaft angular speed (rad/s)
$D_{P/M}$	Pump/motor displacement ($\mathrm{m}^3/\mathrm{rev}$)
D_{P_S}	Pump/motor displacement (accumulator side) ($\mathrm{m}^3/\mathrm{rev}$)
P_{acc}	Accumulator pressure (Pa)
T_{P_S}	Torque associated with accumulator energy exchange (Nm)

Variable	Definition
t_{1k}, t_{2k}	Start/end times of the k-th pumping interval (s)
t_{1j}, t_{2j}	Start/end times of the j-th operation (pumping or motoring) (s)
U	Applied voltage to servomotor (V)
I_{ac}	AC current to servomotor (A)
V_b	Back electromotive force (EMF) (V)
R	Motor winding resistance (Ω)
L	Motor winding inductance
K_B	Back EMF constant (Vs/rad)
K_T	Motor torque constant (Nm/A)
PM_1	Primary pump/motor
PM_2	Secondary pump/motor for ESR circuit
D_{PM_1}	Displacement of primary pump/motor ($\mathrm{m}^3/\mathrm{rev}$)
D_{PM_2}	Displacement of secondary pump/motor ($\mathrm{m}^3/\mathrm{rev}$)
Q_{pm}	Flow through secondary pump/motor (m^3/s)
T_{PM_2}	Torque of secondary pump/motor (Nm)
P_{PM_1}, P_{PM_2}	Hydraulic power of $\mathrm{PM}_1/\mathrm{PM}_2$ (W)
P_{cy}	Cylinder power (W)
P_{cp}	Charge pump power (W)
Q_{cp}	Charge pump flow rate (m^3/s)
P_{or}	Charge pump outlet (relief) pressure (Pa)
c_{vi}	Valve flow coefficient
sg	Specific gravity of hydraulic fluid
A_a	Piston (cap-side) area (m^2)
A_b	Rod-side area (m^2)
p_a, p_b	Pressures at the cap and rod sides of the actuator (Pa)
Q_a, Q_b	Flow rates into cap and rod sides (m^3/s)
Q_{ac}, Q_{bc}	Compensation flow rates (m^3/s)
V_a, V_b	Pipe volumes at cylinder ports (m^3)
x_p	Piston position (m)
P_{acc}	Accumulator pressure (Pa)

Variable	Definition
P_{EPPRV}	Outlet pressure of electro-proportional pressure reducing valve (Pa)
SOC_V	Volume-based state of charge
SOC_P	Pressure-based state of charge
SOC_{RTH}	Reutilization threshold for SOC
SOC_{STH}	Storage threshold for SOC
T_{PM_1}	Torque from PM_1 (Nm)
T_e	Servomotor torque (Nm)
T_L	Load torque (Nm)
$\eta_{pumping}$	Efficiency during pumping mode
$\eta_{motoring}$	Efficiency during motoring mode

Abbreviations

Abbreviation	Full Form
EHA	Electro-Hydrostatic Actuator
ESR	Energy Storage and Reutilization
CPI	Cyclic Performance Index
IEHEC	Integrated Electro-Hydraulic Energy Converter
ICE	Internal Combustion Engine
PMSM	Permanent Magnet Synchronous Motor
TC-PMSM	Tooth-Coil Permanent Magnet Synchronous Motor
DTC	Direct Torque Control
PERS	Potential Energy Recovery System
EPPRV	Electro-Proportional Pressure Reducing Valve
SOC	State of Charge (of the accumulator)
P_s	Pump/motor unit
LP	Low Pressure

Symbols

Actuators, pumps, and motors

Double-acting, single-rod cylinder

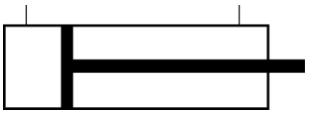

Fixed-displacement pump

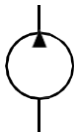

Fixed-displacement, bidirectional pump

Variable-displacement pump

Variable-displacement, bidirectional pump

Fixed-displacement motor

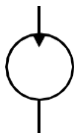

Fixed-displacement, bidirectional motor

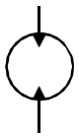

Variable-displacement motor

Variable-displacement, bidirectional motor

Fixed-displacement pump-motor

Fixed-displacement, bidirectional pump-motor 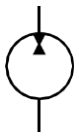

Fixed-displacement, bidirectional pump-motor 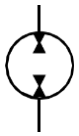

Variable-displacement, bidirectional pump- motor 

Power transmissions

Engine 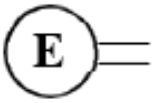

Electric motor 

Generator 

Servomotor 

Shaft 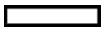

Clutch - open 

Clutch - closed 

Hydraulic conduits/lines

Working line

Crossing lines 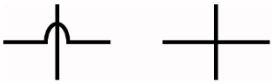

Tank 

Flow and pressure control

Pressure transducer 

Flow sensor 

Flow resistor (Orifice) 

Flow control valve (Variable Orifice) 

Pressure relief valve 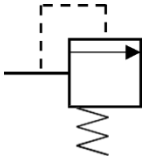

Check valve 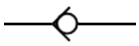

Directional valves

Two-way, two-position (2 × 2) normally closed solenoid-activated valve (spring returned) 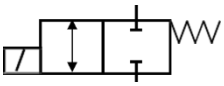

Two-way, two-position (2 × 2) normally open (unidirectional) solenoid-activated valve (spring returned) 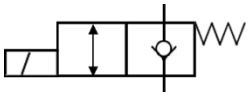

Three-way, two-position (3 × 2) solenoid-activated valve (spring returned) 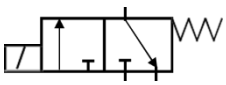

Three-way, three-position (3 × 3) solenoid-activated valve with closed centre (spring-centred) 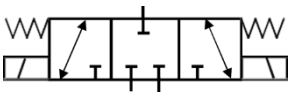

Four-way, three-position (4 × 3) solenoid-activated valve with closed centre (spring-centred) 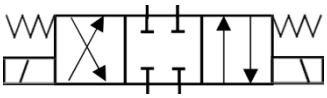

Four-way, three-position (4 × 3) solenoid-activated valve with float centre (spring-centred)

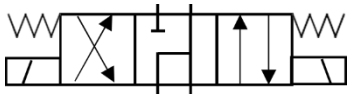

Energy storage component

Hydraulic Accumulator

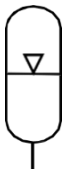

Chapter 1 Introduction

1.1 Motivation

Energy efficiency is a major concern in hydraulic systems, especially as industries seek ways to reduce power consumption while maintaining system performance. Traditional hydraulic systems lose a significant portion of energy through viscous losses. Several methods have been developed to evaluate energy efficiency in hydraulic systems, such as energy-saving ratio, relative efficiency and Sankey flow diagrams. While these methods provide useful insights, they are limited when applied to systems with energy storage and reutilization, as they do not accurately account for stored or reused energy. This limitation makes it difficult to compare different systems fairly.

The gap in current evaluation methods creates uncertainty in assessing how effectively energy storage and reutilization systems improve efficiency. This research is motivated by the need for a clear and standardized approach to evaluating hydraulic system performance, especially for systems that incorporate energy recovery. To address this gap, the Cyclic Performance Index (CPI) was introduced by Costa and Sepehri [1] as a new method to provide a more accurate and reliable way to assess performance in terms of energy consumption. CPI helps to compare different hydraulic systems more effectively, ensuring fair performance evaluations and guiding future improvements in hydraulic design.

1.2 Thesis Objectives

The objective of this thesis is to improve the evaluation of energy performance in hydraulic systems, particularly those with energy storage and reutilization capabilities. Current efficiency evaluation methods often fail to provide accurate assessments, making it difficult to compare different systems. This thesis addresses this gap by testing the Cyclic Performance Index (CPI) as a more reliable and standardized metric. The specific objectives of this thesis are:

1. Analyze current efficiency methods – Review commonly used methods for evaluating hydraulic system efficiency and apply them to a simulation model of an Electro-Hydrostatic Actuator (EHA) with and without an Energy Storage and Reutilization (ESR) circuit and identify their potential and limitations.
2. Validate the Cyclic Performance Index (CPI) – Apply the CPI, as proposed in [1], to the same simulation model of the EHA with and without the ESR circuit to verify its practical effectiveness.

By achieving these objectives, this thesis will provide a standardized and accurate method to evaluate energy efficiency in hydraulic systems, ensuring fair comparisons between different system configurations.

1.3 Thesis Organization

Chapter 2 reviews current efficiency evaluation methods and highlights their limitations, especially for systems with energy storage and reutilization. Chapter 3 describes the Cyclic Performance Index (CPI) as a new method for evaluating energy performance and investigates its theoretical foundation. Chapter 4 describes the Electro-Hydrostatic Actuator (EHA) with and without Energy Storage and Reutilization (ESR) circuit, which serves as the case study for evaluating energy efficiency methods. Chapter 5 applies current efficiency methods, as well as CPI, to the EHA with and without an ESR circuit, comparing the results to demonstrate CPI's advantages over conventional methods. Chapter 6 summarizes key findings, contributions, and potential future research directions. This structure provides clear progression from understanding existing challenges to inducing and validating the new CPI energy evaluation approach.

Chapter 2 Literature Review

Hydraulic systems are fundamental to a wide range of industrial, construction, and aerospace applications due to their high-power density, reliability, and ability to provide precise motion control. Despite these advantages, traditional valve-controlled hydraulic designs face significant challenges with energy inefficiency. Large amounts of input energy are lost through throttling, leakage, and pressure drops. These losses not only raise operational costs but also lead to higher fuel consumption and increased environmental emissions.

In recent years, researchers have proposed several solutions to enhance the energy efficiency of hydraulic systems. Some methods focus on redesigning circuit architectures to minimize losses in transmission lines, while others integrate electrical drives and storage technologies to enable energy recovery and reuse. Each of these developments addresses a specific weakness of conventional systems, providing valuable insights into how efficiency can be enhanced. At the same time, the variety of approaches and evaluation methods makes it challenging to compare systems directly or determine the most effective solutions.

This chapter reviews several major contributions in the field of energy-efficient hydraulics. Section 2.1 discusses the Integrated Electro-Hydraulic Energy Converter (IEHEC), which addresses losses in long-boom applications by eliminating lengthy hydraulic lines. Section 2.2 examines direct electric drive pump control, an approach that replaces servo valves with permanent magnet synchronous motors to reduce throttling losses and enable energy recovery. Section 2.3 focuses on hydraulic excavators, highlighting the issue of fuel efficiency and exploring how energy can be saved or recovered during different phases of the operating cycle. Section 2.4 reviews hydraulic energy regeneration systems, which capture kinetic or potential energy during deceleration and reuse it to reduce power demand in subsequent operations.

Through this review, the chapter builds a foundation for understanding how energy efficiency in hydraulic systems has been addressed so far. By analyzing these contributions in detail, it becomes possible to identify both the strengths of existing methods and the limitations that continue to challenge the development of highly efficient hydraulic technologies.

2.1 Improving Hydraulic Efficiency using Integrated Electro-Hydraulic Energy Converter

Hydraulic systems are commonly used in heavy off-highway vehicles because of their high-power density and reliability. However, in long-boom applications such as cranes, telescopic handlers, and excavators, they face significant energy efficiency issues. Typically, actuators at the boom end are supplied through lengthy pipelines, hoses, and control valves connected to a centralized hydraulic pump. This design results in multiple sources of inefficiency.

First, valve throttling losses occur when control valves restrict flow to match actuator demand. In doing so, they convert hydraulic energy directly into heat [2]. Second, hose and pipeline losses occur due to pressure drops as fluid travels long distances through flexible hoses. These losses become more pronounced under high-flow conditions, typical in long-boom operations. Together, these losses not only waste energy but also require large cooling systems to manage the heat generated, further increasing parasitic power consumption [3], [4].

Figure 2-1 illustrates the problem in conventional long-boom hydraulics. The diagram shows how the actuator at the end of the boom is supplied with hydraulic energy from a centralized pump via long hoses and valves. As fluid flows along this path, pressure drops in the hoses and throttling across the valves cause significant energy losses before the power reaches the actuator.

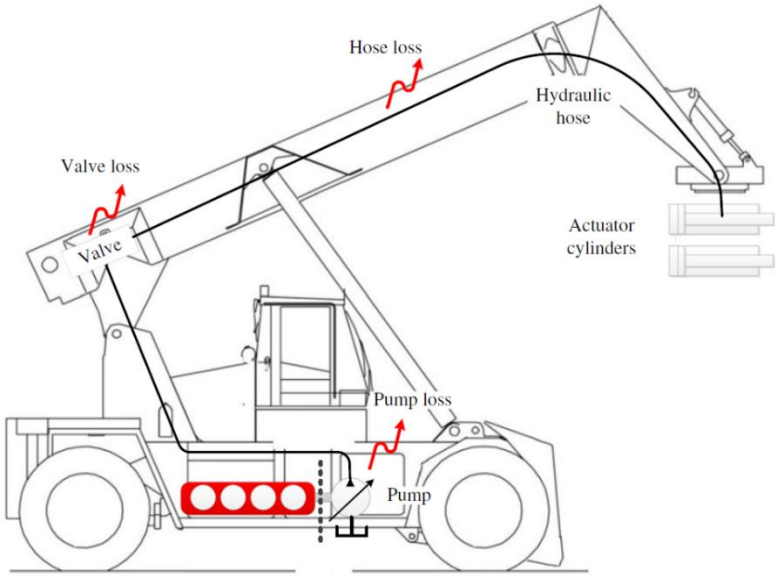

Figure 2-1: Schematic diagram of conventional telescopic boom end actuator (reproduced from [5], © 2020 Elsevier Ltd., with permission. License No. 6135211150907).

The outcome of this design is clear. A large part of the input energy is lost as heat and resistance losses before it can be transformed into useful work at the actuator. This inefficiency encourages the development of alternative system architectures that lessen transmission losses and enhance overall energy efficiency.

One such alternative is the Integrated Electro-Hydraulic Energy Converter (IEHEC). The IEHEC concept eliminates the need for long hydraulic hoses by using electrical power transmission instead of supplying pressurized fluid from a central pump. Electrical energy is transmitted through cables along the boom, where it is converted locally into hydraulic power near the actuator. Since electrical cables experience minimal transmission losses compared to hydraulic hoses, this approach greatly reduces the parasitic losses that characterize conventional long-boom systems [5].

Figure 2-2 illustrates the configuration of an IEHEC-based actuation system. The internal combustion engine (ICE) drives a generator that supplies electrical energy to the frequency converter. The converter regulates voltage and frequency and provides controlled electrical energy to the IEHEC. At the boom end, the IEHEC consists of a tooth-coil permanent magnet synchronous motor (TC-PMSM) integrated directly with a hydraulic pump. The motor converts electrical energy into mechanical torque, which is then used by the hydraulic pump to pressurize fluid and operate the actuator cylinders. During operations such as lowering, the flow direction reverses, and the hydraulic machine operates in motoring mode, converting hydraulic energy back into electrical energy that can be stored in energy storage devices, such as ultra-capacitors or lithium-titanate batteries.

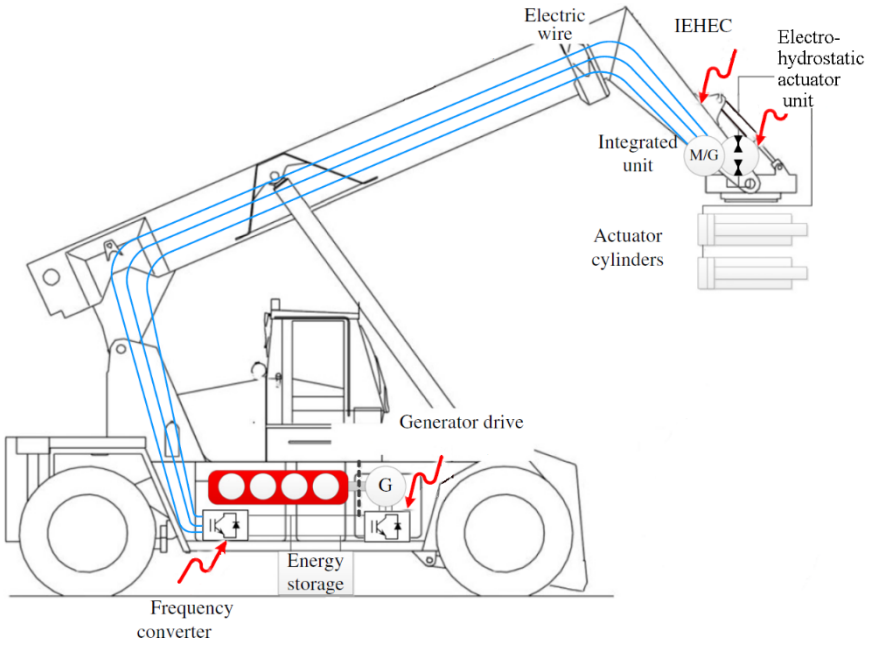

Figure 2-2: Integrated electro-hydrostatic actuation with diesel engine, generator, and energy storage (reproduced from [5], © 2020 Elsevier Ltd., with permission. License No. 6135211150907).

The IEHEC structure offers several benefits. Because energy conversion occurs close to the actuators, the need for long hydraulic lines is eliminated, reducing both pressure drop and throttling losses. The integrated design is also compact and lightweight. Compared with conventional motor–pump assemblies, the IEHEC is reported to be 61% shorter and 51% lighter, which makes it suitable for mobile machines where space and weight are critical [5]. Furthermore, the liquid-cooled design of the TC-PMSM allows for high power density operation even under heavy-duty cycles. These features make the IEHEC well-suited for hybrid diesel-electric working vehicles, in which energy can be drawn either from the generator or from onboard energy storage systems.

At the core of the IEHEC is the tooth-coil permanent magnet synchronous motor, whose internal configuration is illustrated in Figure 2-3. Unlike traditional distributed-winding synchronous machines, the TC-PMSM employs concentrated windings around each stator tooth. This design reduces the length of end windings, minimizing copper losses and improving efficiency. The compact winding arrangement also increases power density and shortens the overall machine length, which directly contributes to the reduced size of the IEHEC. Additionally, the TC-PMSM is mechanically robust, an important property for mobile machinery that must withstand vibration

and heavy loading. Its direct immersion liquid cooling enhances thermal performance, enabling continuous operation at high power levels. Due to its compact geometry, the TC-PMSM can be mounted directly on the shaft of the hydraulic pump without couplings or gears, thereby reducing additional losses and improving system reliability [6], [7].

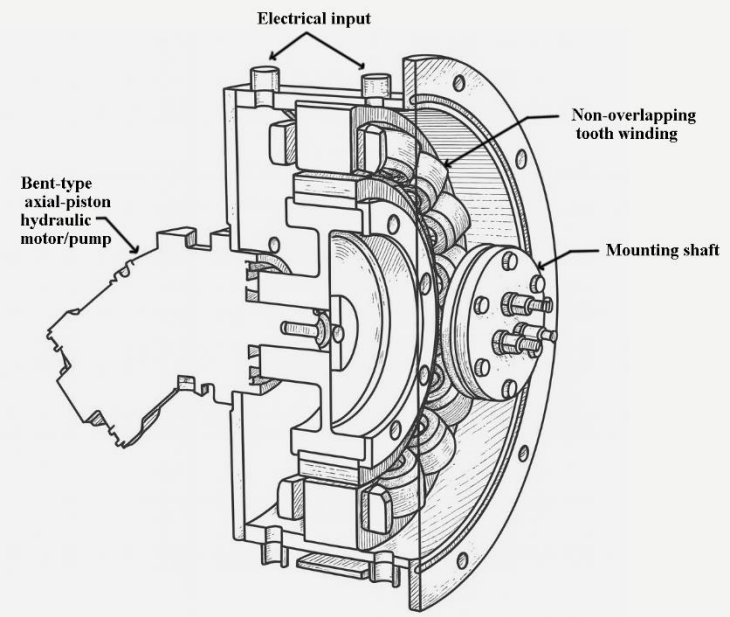

Figure 2-3: Cross-sectional view of integrated electro-hydraulic energy converter (reproduced from [5], © 2020 Elsevier Ltd., with permission. License No. 6135211150907).

The working principle of the IEHEC can be explained through the flow of energy across the actuator system. In pumping mode, the TC-PMSM drives the hydraulic pump, which generates fluid power to actuate the piston. In motoring mode, when external loads drive the actuator, the hydraulic machine converts fluid power back into mechanical and then electrical energy, which can be stored or reused. This bidirectional capability makes the IEHEC more versatile and efficient compared with conventional systems.

The efficiency of the IEHEC is determined by analyzing the flow of energy and losses that occur at different stages of the system. To carry out this analysis, pressure and flow rate measurements are required at key points along the circuit, as shown in Figure 2-4. In this schematic, p_T denotes the tank pressure, which is considered zero. These measurement points provide the basis for quantifying input power, output power, and losses across hoses and valves.

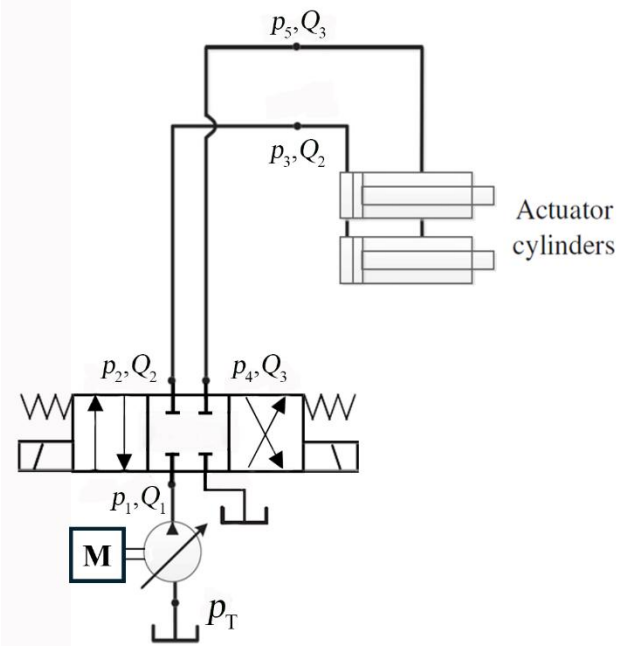

Figure 2-4: Simplified hydraulic system schematic for conventional stacking gripper (reproduced from [5], © 2020 Elsevier Ltd., with permission. License No. 6135211150907).

The flow-rate and power equations used here are adapted from the formulation provided in [5]. The mathematical formulation begins with the flow rate equations. The piston-side flow rate is expressed as

$$Q_2 = \frac{dx}{dt} A_{piston} \tag{2.1}$$

and the rod-side flow rate as

$$Q_3 = \frac{dx}{dt} A_{rod} \tag{2.2}$$

where x is the piston displacement, A_{piston} is the full effective area on the cap side of the cylinder; and A_{rod} represents the annular (reduced) area on the rod side, obtained by subtracting the rod cross-sectional area from the piston area. The total pump flow rate depends on the motion of the piston and is given by

$$Q_1 = \begin{cases} Q_2, & if \ \frac{dx}{dt} \geq 0 \\ Q_3, & if \ \frac{dx}{dt} < 0 \end{cases} \tag{2.3}$$

The hydraulic output power of the pump is then defined as

$$P_{pump,out} = p_1 Q_1 \tag{2.4}$$

and the power delivered by the actuator is expressed as

$$P_{piston} = \begin{cases} p_3 Q_2 - p_5 Q_3, & if \;\; Q_2 \geq 0 \\ p_5 Q_3 - p_3 Q_2, & if \;\; Q_2 < 0 \end{cases} \tag{2.5}$$

In conventional long-boom hydraulics, significant losses occur due to throttling at the valves. These losses can be quantified using the following equations. The hose losses are

$$P_{hose} = \begin{cases} (p_2 - p_3) Q_2 + (p_5 - p_4) Q_3, & if \;\; Q_2 \geq 0 \\ (p_4 - p_5) Q_3 + (p_3 - p_2) Q_2, & if \;\; Q_2 < 0 \end{cases} \tag{2.6}$$

and valve losses are expressed as

$$P_{valve} = \begin{cases} (p_1 - p_2) Q_2 + (p_4 - p_T) Q_3, & if \;\; Q_2 \geq 0 \\ (p_1 - p_4) Q_3 + (p_2 - p_T) Q_2], & if \;\; Q_2 < 0 \end{cases} \tag{2.7}$$

In these equations, p_1 is the pump outlet pressure, p_2 and p_4 are the piston-side and rod-side pressures after the control valves, p_3 and p_5 are the piston and rod chamber pressures, and p_T is the return line pressure to the tank. The terms Q_1, Q_2, and Q_3 represent the pump flow rate, piston-side flow rate, and rod-side flow rate, respectively. These variables establish a consistent nomenclature for the energy balance calculations.

With these definitions, the energy distribution for conventional and IEHEC-based systems can be compared, as follows.

In a conventional hydraulic system, the total input energy $E_{in.1}$ supplied by the prime mover is distributed among useful actuator energy (E_{out}) and the primary loss components: valve losses (E_{valve}), hose losses (E_{hose}) and pump inefficiencies ($E_{pump,loss}$). This relationship can be expressed as:

$$E_{in.1} = E_{out} + E_{valve} + E_{hose} + E_{pump,loss} \tag{2.8}$$

Thus, the efficiency of the conventional system is

$$\eta_{conventional} = \frac{E_{in.1} - (E_{valve} + E_{hose} + E_{pump,loss})}{E_{in.1}} \quad (2.9)$$

In contrast, the IEHEC-based system replaces many hydraulic components with electrical ones, as shown in Figure 2-2, introducing new forms of losses, including generator (E_{gen}), cable (E_{cable}), frequency converter (E_{fq}), and internal conversion losses (E_{IEHEC}). However, because energy conversion occurs close to the actuator, pressure drops, and throttling losses are eliminated. The energy balance for this system can be expressed as:

$$E_{in.2} = E_{out} + E_{gen} + E_{es} + E_{fq} + E_{cable} + E_{IEHEC} \quad (2.10)$$

and its corresponding efficiency is:

$$\eta_{IEHEC} = \frac{E_{in.2} - (E_{gen} + E_{es} + E_{fq} + E_{cable} + E_{IEHEC})}{E_{in.2}} \quad (2.11)$$

Although the IEHEC introduces new electrical losses, these are generally smaller than the combined hydraulic losses found in conventional systems. By reducing throttling and hose pressure losses, the total input energy demand decreases. The efficiency improvement is reflected in the difference between $E_{in.1}$ and $E_{in.2}$, normalized by the original input energy. This demonstrates that localized electro-hydraulic energy conversion allows the IEHEC architecture to achieve more efficient and sustainable operation without compromising actuator performance.

2.2 Enhancing Hydraulic Efficiency with Direct Electric Drive Pump Control

In the previous section, the Integrated Electro-Hydraulic Energy Converter (IEHEC) was presented as an effective solution for reducing long-line losses in boom hydraulics by relocating energy conversion closer to the actuators. While that approach addresses transmission inefficiencies, another critical source of energy loss in conventional hydraulic systems is the servovalve. Traditional hydraulic actuation often depends on servo or proportional valves to regulate lifting and lowering operations. These valves operate by restricting fluid flow, which results in significant throttling losses and excessive heat generation. The wasted energy not only

increases fuel consumption and operational costs but also limits opportunities for energy recovery during load-lowering phases.

To overcome these challenges, a Direct Electric Drive Pump Control system has been developed in which a permanent magnet synchronous motor (PMSM) is directly coupled to a bidirectional hydraulic pump. In this configuration, the PMSM eliminates the need for servovalves, as motor torque and speed directly regulate pump displacement and flow. This direct-drive architecture eliminates throttling losses and enables efficient bidirectional energy conversion. When lifting, the motor supplies torque to pressurize the hydraulic fluid and raise the load. During lowering, the load drives the pump into motoring mode, converting hydraulic energy into shaft rotation. The PMSM, acting as a generator, then converts this rotation into electrical energy.

The concept has been further advanced through integration with a Potential Energy Recovery System (PERS), particularly in forklift applications. Figure 2-5 shows the combined hydraulic and electric system with PERS. In this design, the PMSM and hydraulic pump are controlled by a Direct Torque Control (DTC)-based servo drive, which maintains constant switching frequency for efficient and precise control. The use of modern electric drives also replaces conventional lead-acid batteries with more advanced energy storage systems, thereby improving overall performance. A two-way normally closed poppet valve ensures safety by preventing unintended load descent, while sensors continuously measure pressure, current, voltage, and cylinder position to provide accurate monitoring and control of the system.

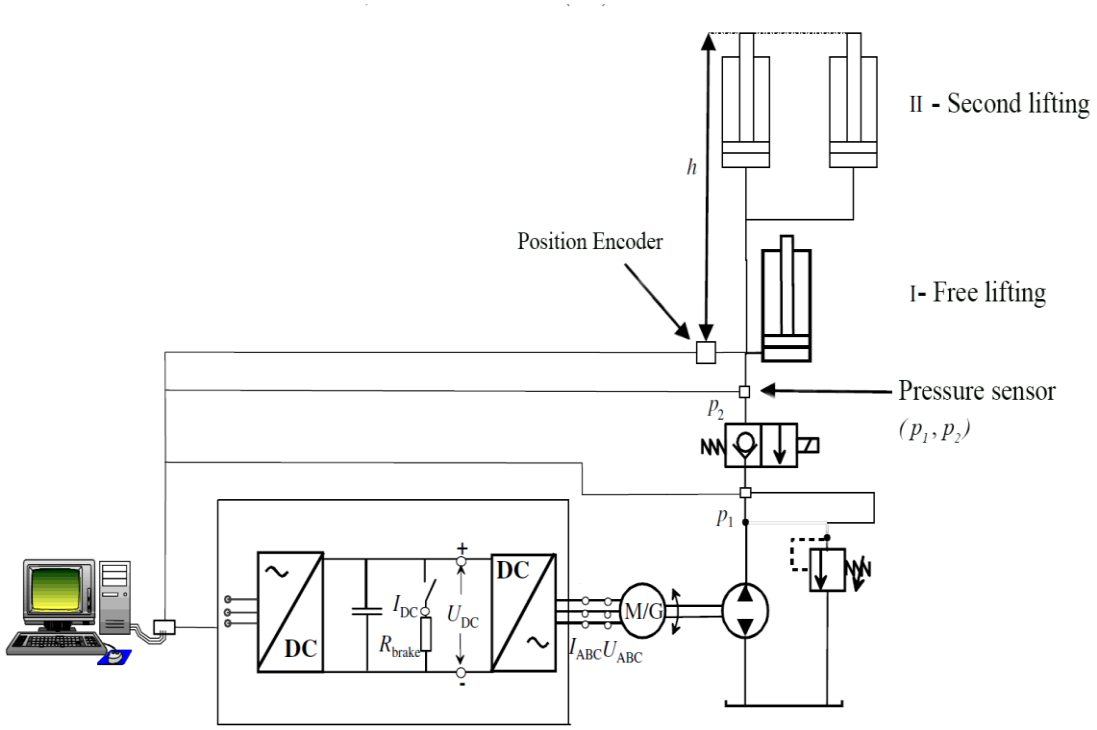

Figure 2-5: Integrated electric-hydraulic circuit for lift function with energy regeneration (reproduced from [8], © 2013 Elsevier Ltd., with permission. License No. 6135270673483).

The forklift's lifting mechanism operates in two mechanically sequenced stages, eliminating the need for independent cylinder control. Figure 2-6 shows the roller chain pulley system that controls the lifting process. In the free lift zone, the first hydraulic cylinder, which has a slightly larger piston cross-sectional area, is activated. This stage raises the forks and load to a moderate height without extending the outer mast. By limiting hydraulic use to a single cylinder, energy losses are reduced, and the system enables smoother, more efficient lifting. During lowering in this zone, the potential energy of the descending load is captured by the bidirectional pump, which acts as a hydraulic motor. The PMSM converts this energy into electricity and directs it to the storage system for reuse.

Once the free lift cylinder is fully extended, the second lift zone begins, where additional cylinders engage to extend the mast and lift the load to its maximum height. This stage requires higher flow and pressure because the cylinders must lift both the mast assembly and the load over a greater vertical distance. However, the increased lifting height also raises the load's gravitational potential energy. As a result, when the load is lowered from this stage, a larger amount of hydraulic energy becomes available for recovery. As the load descends, the pump again works in motoring mode, and the PMSM channels the regenerated energy into the storage system. The sequential operation

of the cylinders ensures that hydraulic power is only applied where necessary, thereby reducing wastage. Importantly, because servovalves are eliminated, throttling losses are avoided altogether, improving efficiency compared with conventional designs.

Figure 2-6: Forklift lift function: (a) Free lift zone, and (b) Full height lifting.

The energy performance of the forklift system with the Potential Energy Recovery System (PERS) can be assessed through efficiency calculations that consider both lifting and lowering operations. This evaluation requires balancing the input energy supplied to the system and the useful energy recovered or delivered at the actuator. By quantifying these flows, the overall efficiency of the system can be determined.

The energy efficiency, denoted as η_{cycle}, is defined over the time interval $[t_1, t_2]$ as the ratio of total useful output energy (E_{out}) to total input energy (E_{in}). It is expressed as:

$$\eta_{cycle} = \frac{\int_{t1}^{t2} P_{out}(t)dt}{\int_{t1}^{t2} P_{in}(t)dt} = \frac{E_{out}}{E_{in}} \tag{2.12}$$

Eq. (2.12) provides a precise measure of how efficiently the forklift utilizes energy during both lifting and lowering operations. Now to compare the energy consumption of the forklift with and without the PERS, the term energy-saving ratio (Γ_s). It is defined as:

$$\Gamma_S = \frac{E_{old} - E_{new}}{E_{old}} \tag{2.13}$$

where E_{old} is the energy consumed by the forklift without energy recovery and E_{new} is the energy consumed when equipped with the energy recovery system.

The total input energy for each case is calculated as:

$$E_{old} = E_{motor}/(\eta_{SC} \cdot \eta_{inverter}) \tag{2.14}$$

$$E_{new} = E_{old} - E_{brake} \cdot \eta_{SC} \tag{2.15}$$

where E_{motor} is the input electrical energy supplied to the motor, E_{brake} is energy recovered during lowering the load, η_{SC} is the discharge efficiency of the supercapacitor, η_{inv} is inverter efficiency. The recovered energy, E_{brake} and input energy, E_{motor} are calculated using the following equations [9]:

$$E_{brake} = \int_{t1}^{t2} i_{brake}^2 \cdot R_{brake}\, dt \tag{2.16}$$

$$E_{mot} = \int_{t1}^{t2} (i_a u_a + i_b u_b + i_c u_c) dt \tag{2.17}$$

where *i* and *u* are phase current and voltage, which are measured using sensor probes and R_{brake} is resistance in the braking resistors.

By combining direct electric drive pump control with the ability to capture and store potential energy, the forklift can significantly reduce energy consumption compared to conventional systems. The recovered electrical energy is typically stored in high-power devices, such as supercapacitors, which are well-suited for rapid charge and discharge cycles. This stored energy can then be reused during subsequent lifting operations, reducing the demand on the primary power source and enhancing overall system sustainability. The use of sequential lift zones, the removal of throttling valves, and the integration of modern energy storage technologies show how this approach boosts the efficiency of hydraulic systems in mobile machinery. Ultimately, these architectures represent a move toward more sustainable and reliable fluid power systems that support the goal of minimizing energy losses and extending machine lifespan.

2.3 A New Perspective on Fuel Efficiency in Hydraulic Excavation Machinery

In the previous section, direct electric drive pump control was discussed as a way to reduce throttling losses and recover energy in mobile hydraulic systems. While such methods have been shown to improve efficiency in forklifts and other industrial equipment, the challenge of fuel efficiency is particularly critical in hydraulic excavators. Excavators are among the most fuel-intensive categories of construction machinery, commonly used in industries such as mining, earthmoving, and infrastructure development. Their operation involves high fuel consumption, high operating costs, and considerable environmental emissions.

These inefficiencies arise from several interconnected factors. First, the diesel engines powering excavators are usually oversized to meet peak load demands. As a result, they often operate under partial load conditions where combustion is less efficient, leading to fuel waste. Idling is another major factor, as engines frequently run without performing productive work. Prolonged idling not only wastes fuel but also accelerates component wear, increasing maintenance costs. Secondly, the hydraulic system itself is inherently inefficient. Traditional valve-controlled designs restrict excess flow to match actuator demands, dissipating significant amounts of energy as heat. This not only reduces the proportion of useful power delivered to the actuators but also imposes additional cooling requirements. Lastly, auxiliary drives such as cooling fans, alternators, and hydraulic pumps operate continuously regardless of workload. These parasitic loads consume a noticeable share of the available fuel energy, even when the machine is not performing active digging or lifting tasks.

Improving the fuel efficiency of hydraulic excavators requires a system-level understanding of how energy flows through the engine, hydraulic system, and actuators during a typical duty cycle. The operational cycle of an excavator consists of four primary phases: lifting, digging, swinging, and lowering. Each of these phases both consumes energy and creates opportunities for energy recovery.

During the lifting phase, the hydraulic pump supplies high-pressure fluid to the actuators, which raise the boom and load. Energy is often wasted because pump output does not precisely match actuator demand, and throttling in control valves dissipates the difference as heat. In the digging phase, the machine requires steady hydraulic power to penetrate and move soil. In traditional systems, excess hydraulic flow continues to circulate even when it is not fully needed, resulting in

further losses. The swinging phase involves horizontal rotation of the boom and load. Here, kinetic energy is generated as the boom accelerates; however, during deceleration, this energy is typically dissipated as heat within the hydraulic system. With regenerative braking concepts, however, this kinetic energy could be recovered and converted into usable electrical power. Similarly, in the lowering phase, the boom releases gravitational potential energy. Conventional systems dissipate this energy as heat, but with bidirectional pumps operating in motoring mode, it can be converted into electrical energy and stored for later lifting operations.

A Sankey flow diagram of the excavator energy distribution, shown in Figure 2-7, helps to visualize these dynamics. The diagram illustrates how input diesel energy is partitioned into useful work and losses across different subsystems. A substantial portion of the input energy is lost immediately in the internal combustion engine through incomplete combustion, friction, and heat rejection. Additional energy is consumed by ancillary systems and lost through hydraulic pump inefficiencies, including leakage and friction. Within the hydraulic system, a significant portion of power is wasted through throttling valves and pipeline resistance. The remaining fraction is delivered to the actuators as positive actuator energy, denoted as $E_{Act,pos}$, which represents the energy available for productive tasks such as digging or lifting. However, part of this actuator energy contributes to accelerating or raising the mass of the implement. This portion, called negative actuator energy $E_{Act,neg}$, can in principle be recovered during lowering or deceleration. The difference between these two terms defines the net actuator energy,

$$E_{Act,net} = E_{Act,pos} - E_{Act,neg} \tag{2.18}$$

which represents the actual useful energy delivered to perform productive work.

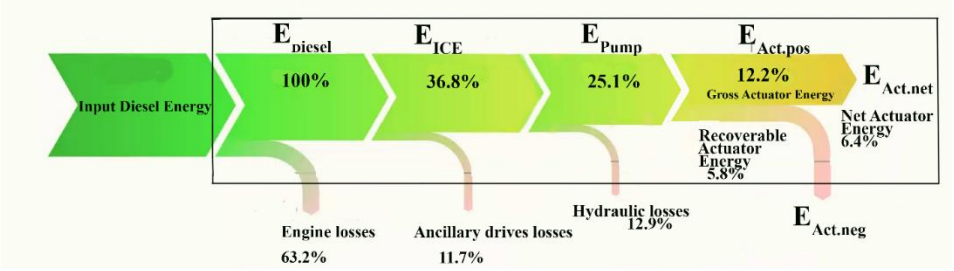

Figure 2-7: Sankey plot of energy flow in a hydraulic system (reproduced from Vukovic et al., Energies, 2017, CC BY 4.0 [10]).

On this basis, the efficiency of the hydraulic system is defined as the ratio of positive actuator energy to the energy delivered by the pump:

$$\eta_{Hyd} = \frac{E_{Act,pos}}{E_{pump}} \tag{2.19}$$

The hydraulic efficiency depends strongly on the circuit design and control method. For example, a single-circuit load-sensing system typically achieves efficiencies up to 50%, whereas dual-circuit positive control systems can reach about 60% [10]. These values highlight the inherent limitations of conventional valve-controlled hydraulics and the need for advanced control strategies to minimize throttling losses.

To extend this concept to the system level, overall fuel efficiency is defined in two complementary ways. Gross efficiency measures how much of the diesel input energy is transformed into gross actuator energy, which is the total positive actuator energy without considering potential recovery. It is defined as

$$\eta_{Tot,Gross} = \frac{E_{Act,pos}}{E_{Diesel}} \tag{2.20}$$

Net efficiency, by contrast, considers the fact that some of the actuator energy can be recovered during lowering and deceleration. By including the recoverable negative actuator energy, the net efficiency offers a more realistic measure of how much diesel input is ultimately transformed into effective useful work:

$$\eta_{Tot,net} = \frac{E_{Act,pos} - E_{Act,neg}}{E_{Diesel}} = \frac{E_{Act,net}}{E_{Diesel}} \tag{2.21}$$

These definitions mark a significant shift in perspective: losses such as gravitational and kinetic energy, once considered unavoidable, are now seen as potential sources of recoverable energy. By implementing advanced pump control strategies and recovery circuits, the overall fuel efficiency of excavators can be significantly improved. This perspective not only clarifies where energy is lost but also provides a framework for assessing how much of it can be reused, laying the foundation for more sustainable excavator designs.

This analysis of excavator operation highlights that a considerable share of fuel energy, traditionally treated as irrecoverable loss, actually exists in the form of recoverable gravitational

and kinetic energy. Recognizing these losses as potential resources reframes the definition of efficiency in hydraulic machinery. Building on this perspective, the next section introduces hydraulic energy regeneration systems. These systems, first explored extensively in the automotive industry, are designed to capture and reuse energy that would otherwise be wasted, thereby improving overall efficiency and sustainability in mobile hydraulics.

2.4 Hydraulic Energy Regeneration System in Automotive Application

As discussed in the previous section, a significant portion of energy in mobile machinery is dissipated as heat, throttling losses, and friction, even though part of this energy exists in recoverable forms such as gravitational and kinetic energy. Section 2.3 showed that energy losses can be recovered, but it did not cover how efficiency is calculated when that energy is reused. This challenge can be illustrated through automotive regenerative braking systems, where kinetic energy that would normally be lost as heat during deceleration is stored in a hydraulic accumulator and later reused to assist during acceleration. In such systems, the feasibility of energy recovery is evident, and it also becomes possible to evaluate efficiency by considering both the recovered energy and the useful work performed. Figure 2-8 illustrates a simplified schematic representation of such a system, showing the interaction of its key components.

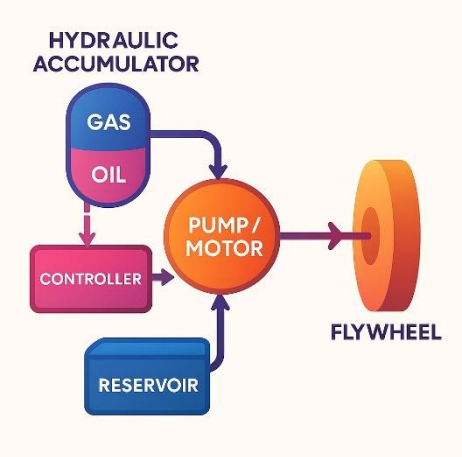

Figure 2-8: Simplified layout of the hydraulic energy regeneration system (reproduced from [11]).

At the core of the system is the hydraulic accumulator, which serves as the primary energy storage device. During deceleration or braking, hydraulic fluid is directed into the accumulator,

compressing the gas inside. This compression process stores potential energy that can be released later to support high-demand operations such as acceleration or lifting. The pump/motor unit allows this two-way energy flow. In pump mode, it transforms the vehicle's kinetic energy into hydraulic energy stored in the accumulator. In motor mode, it reverses the process, drawing energy from the accumulator and converting it back into mechanical power to drive the system.

The flywheel also helps stabilize the system by storing kinetic energy during deceleration and providing inertia during acceleration. This helps reduce fluctuations in energy delivery and results in smoother operation. A hydraulic reservoir keeps a steady fluid supply for the pump/motor unit, while a controller manages the entire process. The controller maximizes energy flow between components, regulates the charging and discharging of the accumulator, and prevents overloading or excessive discharging. By continuously monitoring parameters such as pressure, flow, current, and voltage, the controller ensures efficient recovery and reuse across different operating conditions.

The performance of the hydraulic energy regeneration system can be assessed using efficiency metrics that describe both hydraulic and mechanical performance. Two important parameters are volumetric efficiency and torque efficiency of the pump/motor unit.

Volumetric efficiency represents the ratio of actual flow, Q_a to ideal flow, Q_i. For pumps and motors, it can be expressed as [11]:

$$\eta_v = \frac{Q_a}{Q_i}$$

$$\eta_{v_{pump}} = 1 - \frac{C_s}{xS} - \frac{\Delta p}{\beta} - \frac{C_{st}}{x\sigma} \tag{2.22}$$

$$\eta_{v_{motor}} = \frac{1}{1 + \frac{C_s}{xS} + \frac{\Delta p}{\beta} + \frac{C_{st}}{x\sigma}} \tag{2.23}$$

where C_s and C_{st} are the laminar and turbulent leakage coefficients, respectively, β is the fluid bulk modulus of elasticity, x is the displacement of the pump/motor, and Δp is the pump/motor pressure differential. The term S and σ represent the characteristic coefficient for laminar and turbulent leakage, respectively.

Torque efficiency describes the ratio of the ideal torque (for a frictionless unit) to the actual torque required. It expressed as [11]:

$$\eta_t \equiv \frac{T_i}{T_a}$$

$$\eta_{t_{pump}} = \frac{1}{1 + \frac{C_s}{xS} + \frac{\Delta p}{\beta} + \frac{C_{st}}{x\sigma}} \tag{2.24}$$

$$\eta_{t_{motor}} = 1 - \frac{C_v S}{x} - \frac{C_f}{x} - C_h x^2 \sigma^2 \tag{2.25}$$

where C_v, C_f and C_h are the viscous, frictional, and the hydrodynamic loss coefficients, respectively.

By comparing Eqs. (2.22) - (2.25), the relationship between pump and motor efficiencies can be established:

$$\eta_{v_{motor}} \equiv \frac{1}{2 - \eta_{v_{pump}}} \tag{2.26}$$

$$\eta_{t_{motor}} \equiv 2 - \frac{1}{\eta_{t_{pump}}} \tag{2.27}$$

These equations help quantify the energy losses and inefficiencies in both volumetric flow and mechanical torque transfer, providing a comprehensive understanding of system performance under varying conditions.

Round-Trip efficiency: Round-trip efficiency (η_{rt}) is a measure of how effectively an energy storage system captures and reuses energy over successive operational cycles. It represents the ratio of the energy reused during the reutilization phase to the energy initially stored in the system. In the context of the hydraulic energy regeneration system, round-trip efficiency evaluates the performance of the accumulator and pump/motor unit in minimizing energy losses during the energy storage and release processes. Mathematically, it is expressed as [11]:

$$\eta_{rt}(i) = \left[\frac{N_p(i+1)}{N_p(i)}\right]^2 \tag{2.28}$$

where $N_p(i)$ represents the normalized peak flywheel speed corresponding to the energy stored during cycle i and $N_p(i+1)$ is the normalized flywheel speed associated with the energy recovered in the subsequent cycle. The square arises because the total stored energy in the flywheel is proportional to the square of its rotational speed; therefore, the ratio of recovered energy between two consecutive cycles is obtained by squaring the ratio of their peak speeds. 100% round-trip efficiency indicates that all the stored energy is recovered after reuse, which is an ideal scenario. However, in practical applications, losses due to thermal dissipation, leakage, and mechanical friction reduce this efficiency. Higher round-trip efficiency values reflect better energy retention and reduced losses, indicating a more effective system for energy storage and reutilization.

The study of hydraulic energy regeneration in automotive applications reveals that braking energy, which is usually lost as heat, can be recovered and reused effectively. Besides demonstrating feasibility, these systems also help to define and calculate efficiency when recovery and reuse are considered. Parameters such as volumetric efficiency, torque efficiency, and round-trip efficiency allow the performance of recovery cycles to be measured and compared. While these methods offer useful insights into how energy recovery influences system efficiency, they remain specific to certain applications and do not provide a universal framework.

2.5 Summary

This chapter reviewed existing methods and technologies created to improve energy efficiency in hydraulic systems. Section 2.1 discussed the Integrated Electro-Hydraulic Energy Converter (IEHEC), which reduces line losses by replacing hydraulic hoses with electrical cables and relocating energy conversion closer to the actuators.

Section 2.2 covered Direct Electric Drive Pump Control with Potential Energy Recovery Systems (PERS). By eliminating servo valves and coupling a permanent magnet synchronous motor to a bidirectional pump, this approach reduces throttling losses and allows energy recovery. Forklift applications showed that splitting operations into free-lift and second-lift zones enhances efficiency, with energy savings ratios confirming noticeable reductions in energy consumption.

Section 2.3 examined fuel efficiency in hydraulic excavators. Inefficiencies were identified at the engine, hydraulic, and auxiliary drive levels. The operational cycle analysis, supported by a Sankey flow diagram, showed how fuel energy divides into useful actuator work, irrecoverable losses, and recoverable components such as gravitational and kinetic energy. This reframed efficiency definitions by recognizing that some losses can potentially be recovered.

Section 2.4 focuses on hydraulic energy regeneration in automotive applications. Regenerative braking systems using accumulators, pump/motor units, and controllers demonstrated practical recovery of kinetic energy during deceleration. Efficiency evaluation through volumetric efficiency, torque efficiency, and round-trip efficiency showed how performance can be quantified when recovery and reuse are included. Although effective for specific applications, these methods do not provide a universal framework.

In conclusion, Chapter 2 highlighted both the scale of inefficiencies in conventional hydraulics and the solutions developed to reduce losses through advanced designs and energy recovery systems. Different metrics, such as energy-saving ratios, Sankey flow diagrams, and round-trip efficiency, have been used to evaluate performance. However, a unified metric is still needed to consistently compare diverse system architectures and guide the development of more efficient and sustainable hydraulic technologies.

Chapter 3 A Comprehensive Metric for Energy Evaluation in Hydraulic Systems

To make hydraulic systems more energy efficient and environmentally friendly, it is essential to establish a consistent and reliable method for evaluating their performance. As discussed in Chapter 2, these systems are built with different components, circuit designs, and control strategies, and often use performance evaluation methods that are specific to their design. Because of this, it becomes difficult to compare how well different systems recover and utilize energy fairly. Although some traditional methods account for certain energy losses, they typically focus on specific variables such as flow rate, pressure drop, or input power. As a result, these methods may indicate improvements in system performance, but they fail to reveal the system's true potential for energy optimization. For instance, they do not identify whether certain power losses could be recovered, or whether recovered energy is not reutilized effectively. In some cases, the energy stored in the system is not reused effectively and ends up being lost again due to additional losses such as leakage, friction, or pressure drops.

Given these limitations in traditional evaluation methods, a more complete understanding of energy behaviour is needed. One such approach, known as the Cyclic Performance Index (CPI), has been introduced to provide a more comprehensive evaluation of energy performance [1]. To explain this concept, energy flow is examined using a simple hydraulic system consisting of a single-rod actuator used for lifting and lowering a weight. This example offers a clear view of how energy is delivered, recovered, reutilized, and lost throughout the cycle, and serves as a foundation for introducing a more comprehensive performance metric.

3.1 Concept and Formulation

Because traditional evaluation methods have limitations, it is important to gain a clearer understanding of how energy flows within hydraulic systems. To support this, a simple example is presented to introduce the Cyclic Performance Index (CPI). Figure 3-1 illustrates a single-rod hydrostatic actuator system used for lifting and lowering a load. This setup helps visualize how energy is delivered, recovered, and lost during different phases of operation, making it easier to understand the CPI concept.

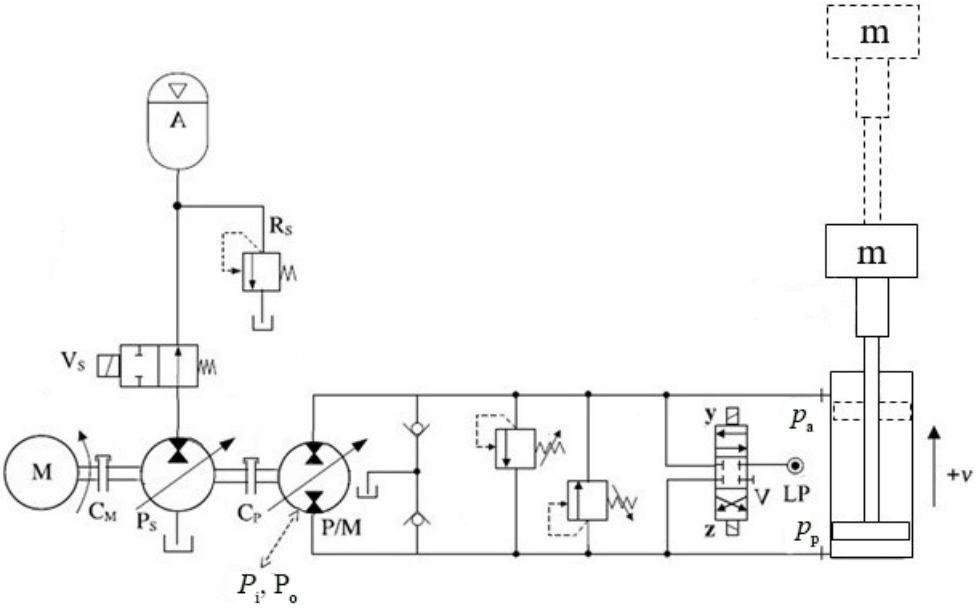

Figure 3-1: A Single-rod hydrostatic actuator for lifting and lowering a weight (reproduced from Costa and Sepehri, Energies, 2024, CC BY 4.0 [1]).

The circuit shown in Figure 3-1 includes key components such as a pump/motor unit, P_S, a relief valve, Rs, an accumulator, A, directional valves V and V_s, and two clutches, C_P and C_M. Clutch, C_M, connects the pump/motor shaft to the prime mover, M, while the clutch, C_P, connects it to the main pump that drives the single-rod actuator. This arrangement allows the system to supply energy during lifting and recover it during lowering. The accumulator stores excess energy, which can be reused later to support the actuator or reduce the load on the prime mover.

To understand the energy flow within the system, a key approach involves analyzing the interaction between the cylinder force, F_R and the cylinder velocity, v. The cylinder force, $F_R = p_p A_P - p_a A_a$, where p_p is the pressure in the piston-side chamber, p_a is the pressure in the rod-side chamber, A_p and A_a are the piston and rod-side areas, respectively. The sign of the product $F_R \,.\, v$, indicates the direction of energy transfer: when positive, energy is delivered to the load (pumping); when negative, energy is returned from the load to the system (motoring) [12], [13]. This behaviour is illustrated in Figure 3-2.

As shown in Figure 3-1, assume that the pump /motor rotation is controlled in such a way that the piston extends and retracts at the same velocity. In this scenario, the cylinder operates cyclically, as illustrated in Figure 3-2.

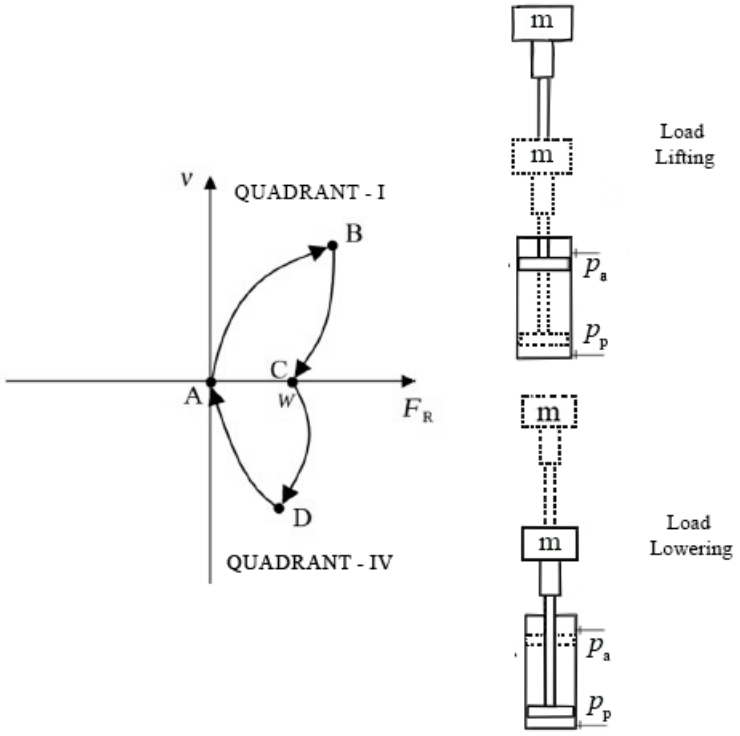

Figure 3-2: Cyclic operations of the actuator using V-F_R diagram (reproduced from Costa and Sepehri, Energies, 2024, CC BY 4.0 [1]).

Figure 3-2 illustrates the relationship between cylinder force and piston velocity during a complete operating cycle of the actuator. The left side of the figure shows a quadrant diagram, while the right side displays the corresponding physical positions of the load during lifting and lowering. At point A, the piston is fully retracted, and both force and velocity are zero. As the piston extends upward to lift the load, the system moves from point A to B through the first quadrant, where both force and velocity are positive ($F_R \cdot v > 0$). This represents the pumping phase, during which the actuator consumes energy to perform positive work. At point C, the piston reaches its maximum extension and temporarily stops. When the load is lowered, the piston retracts from point C to D, entering the fourth quadrant ($F_R \cdot v < 0$). This is the motoring phase, where energy flows back into the system as the load assists the motion, allowing some of its potential energy to be recovered. The curved path through quadrants I and IV demonstrates the continuous transition between energy input and energy recovery during a full cycle.

To assess the performance of this actuator-based hydraulic system, it is useful to compare two configurations using the power-time curves. In the first configuration, the hydraulic system

operates without any form of energy recovery. During the lowering phase, the potential energy released by the load is not stored or reused. It is simply lost through the circuit. This setup is illustrated in Figure 3-3, and its power-time characteristics are shown in Figures 3-4(a) through 3-4(f).

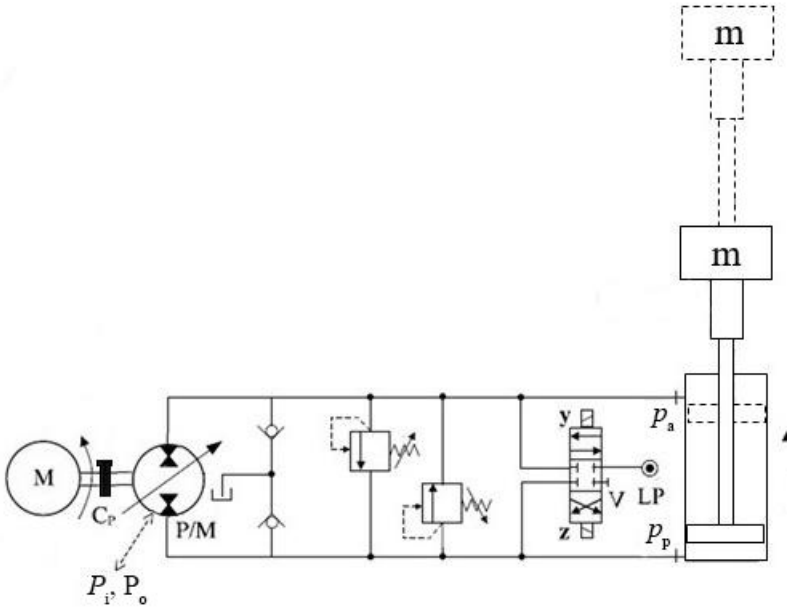

Figure 3-3: Schematic diagram of a Single-rod hydrostatic actuator for lifting and lowering a weight without an energy recovery setup.

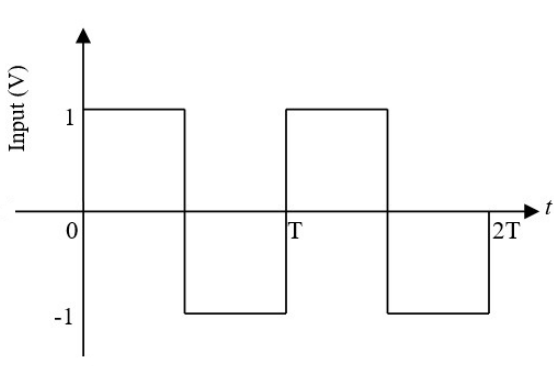

(a). Applied voltage to the prime mover (V).

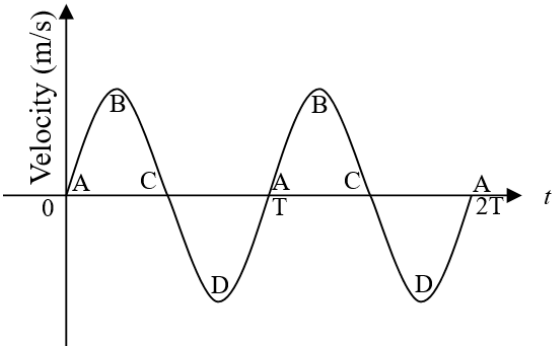

(b). Piston-rod velocity (m/s).

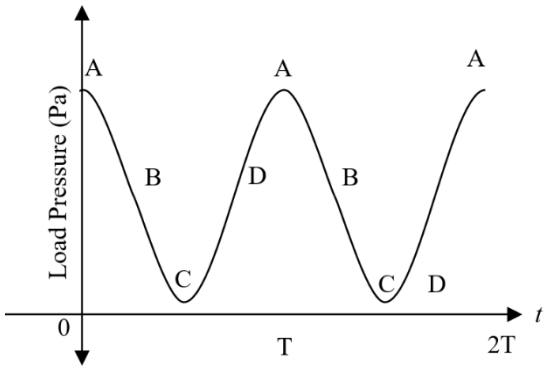

(c). Load pressure (Pa).

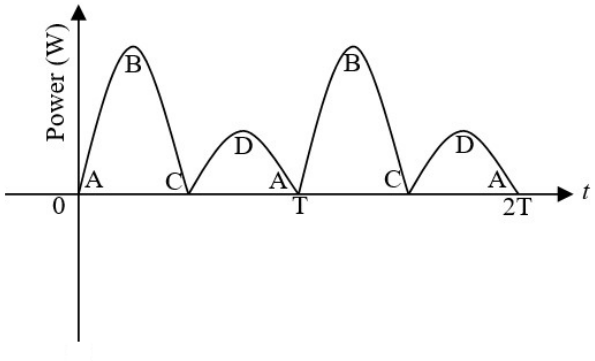

(d). Power input to the pump (W).

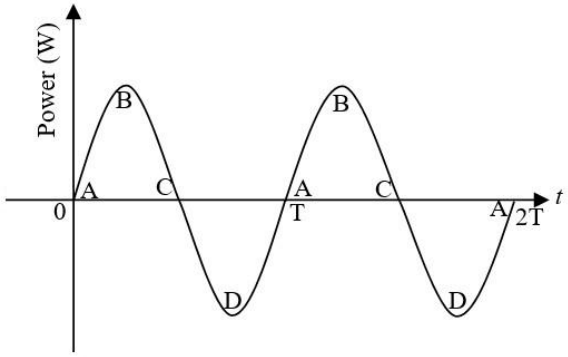

(e). Power output from the actuator (W).

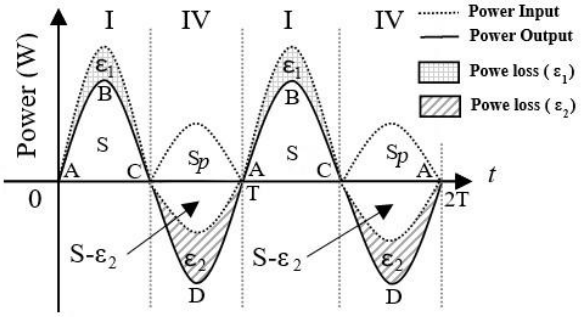

(f). System without energy recovery (W) (adapted from [1]).

Figure 3-4: Power flow analysis for the lifting and lowering system. (a) Applied voltage to the prime mover (V); (b) Piston-rod velocity (m/s); (c) Load pressure, P_L (Pa); (d) Power input to pump (W); (e) Power output from actuator (W); (f) without energy recovery (W) (reproduced from Costa and Sepehri, Energies, 2024, CC BY 4.0 [1]).

The square-wave voltage applied to the prime mover is shown in Figure 3-4(a), which drives the actuator to extend and retract. The resulting piston velocity is shown in Figure 3-4(b). The corresponding load pressure, $P_L = p_p - \frac{A_a}{A_p}\, p_a$, is illustrated in Figure 3-4(c); it reflects the pressure difference across the actuator and varies according to the direction and magnitude of the load during lifting and lowering. Power input and output are presented in Figures 3-4(d) and 3-4(e), respectively. Positive output values represent the lifting phase (quadrant I), while negative values during lowering indicate that energy is returned from the load (quadrant IV), but in this configuration, it is not recovered and is instead lost.

For this setup, illustrated in Figure 3-3, the prime mover supplies a total energy of $S+\varepsilon_1$ during the lifting phase, where S is the useful energy transferred to the load and ε_1 accounts for internal system losses such as friction or leakage. These losses occur during the interval $0 \leq t \leq 0.5T$, when the actuator extends to lift the load. During the lowering phase, from $0.5T \leq t \leq T$, a portion of the released energy is lost, ε_2, while the remaining energy, $S - \varepsilon_2$, must be counterbalanced by additional input from the prime mover, represented as S_p, as shown in Figure 3-4(f). Since the system does not store energy, the prime mover is required to deliver the full energy demand during every cycle.

The pumping efficiency of the system over a cycle for the system represented in Figure 3-4(f) is given by the equation:

$$\eta = \frac{\int_T^{1.5T} P_{out} dt}{\int_T^{2T} P_{in} dt} = \frac{S}{(S + \varepsilon_1) + S_p} \leq 1 \tag{3.1}$$

Here, P_{out} represents the output power at the cylinder, and P_{in} is the input power from the prime mover. These are calculated as:

$$P_{out} = |P_L A_p v| \tag{3.2}$$
$$P_{in} = |T_e \omega_m|$$

where A_p is the piston-side area, v is the velocity of the piston, T_e is the motor torque and ω_m is the servomotor angular speed.

The motor torque, T_e, is determined from:

$$\mathrm{T_e} - T_L = J\frac{d\omega_m}{dt} + B\omega_m \tag{3.3}$$
$$T_L = D_{P/\mathrm{M}}(p_p - p_a)$$

where T_L is the load torque, J is the total moment of inertia of the servomotor and pump-motor (P/M), and B is the viscous damping coefficient.

For Eq. (3.1), the limiting value, $\eta = 1$ represents the case where there are no internal losses at the lifting phase ($\varepsilon_1 = 0$) and no power supplied to counterbalance the load at the lowering phase ($S_p = 0$). It is important to note that the integration limits for the numerator and denominator are

different. The numerator focuses on the energy output at the cylinder during the lifting phase, while the denominator $(S + \varepsilon_1) + S_p$ focuses on the total energy input from the prime mover during the lifting and lowering phases. This difference is essential for accurately evaluating the system's performance.

In the second configuration, an energy storage and reutilization circuit is introduced. The system layout is shown in Figure 3-5.

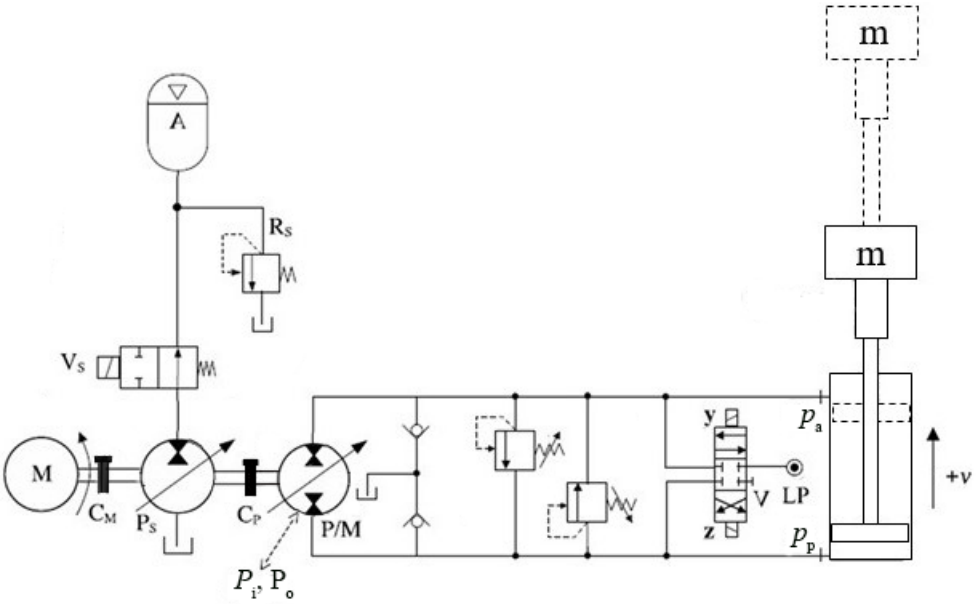

Figure 3-5: Schematic diagram of a Single-rod hydrostatic actuator for lifting and lowering a weight with an energy recovery setup (reproduced from Costa and Sepehri, Energies, 2024, CC BY 4.0 [1]).

Its corresponding power-time behaviour is illustrated in Figure 3-6(a) - Figure 3-6(g), which shows the applied voltage, piston velocity, load pressure, and input/output power profiles under energy recovery conditions.

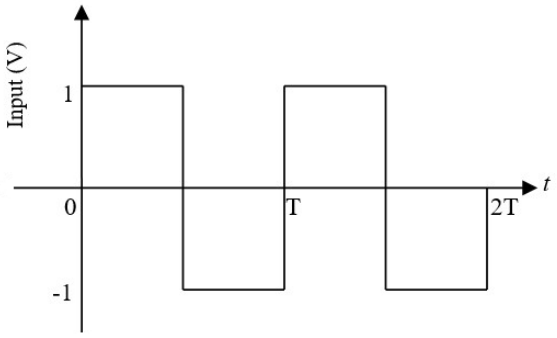

(a). Applied voltage to the prime mover (V).

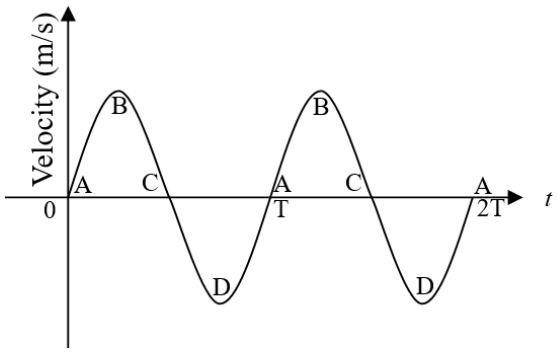

(b). Piston-rod velocity (m/s).

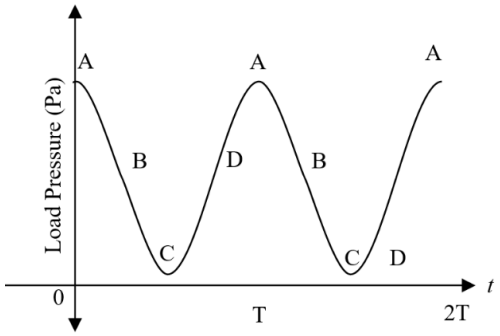

(c). Load pressure (Pa).

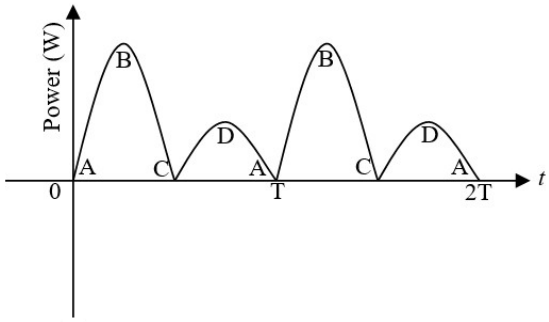

(d). Power input to the pump (W).

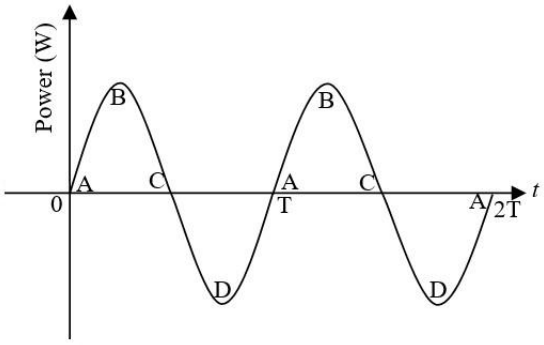

(e). Power output from the actuator (W).

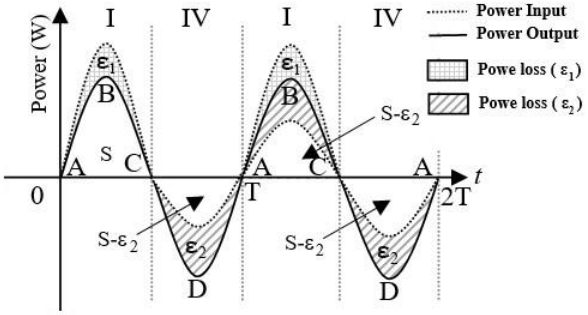

(f). System with energy recovery (W) (adapted from [1]).

Figure 3-6: Power flow analysis for the lifting and lowering system. (a) Applied voltage to the prime mover (V); (b) Piston-rod velocity (m/s); (c) Load pressure, P_L (Pa); (d) Power input to pump (W); (e) Power output from actuator (W); (f) with energy recovery (W) (reproduced from Costa and Sepehri, Energies, 2024, CC BY 4.0 [1]).

Figure 3-6(f) illustrates the power curves for the system with energy storage. As shown in the figure, after the lifting phase (first quadrant), when the system enters the fourth quadrant (lowering phase), the remaining energy, *S*- ε_2 is saved in the accumulator. The energy saved in the first cycle is used in the next cycle. In this case, the cyclic pumping efficiency measured at $T \leq t \leq 2T$ may result in a number greater than 1. Due to this possibility, the Greek letter γ used instead of η and Eq (3.1) is then written as

$$\gamma = \frac{\int_T^{1.5T} P_{out} dt}{\int_T^{2T} P_{in} dt} = \frac{S}{(S + \varepsilon_1) - (S - \varepsilon_2)} = \frac{S}{\varepsilon_1 + \varepsilon_2} \tag{3.4}$$

Here $\varepsilon_1 + \varepsilon_2$ can be directly measured from the power consumed by the prime mover during the interval [T,2T]. As per Eq. (3.4), the prime mover needs to provide just enough energy to compensate for the circuit losses.

The input and output power used in Eq. (3.4) are defined as:

$$P_{out} = |P_L A_p v| \tag{3.5}$$
$$P_{in} = |T_e \omega_{P_s}|$$

where T_e is the total electromagnetic torque delivered by the motor, which is influenced by three key components: the mechanical load torque T_L, the torque associated with energy recovery or supply from the accumulator T_{P_s} and the dynamic characteristics of the motor-pump shaft. This relationship is described by the following equation:

$$T_e - T_L \pm T_{P_s} = J \frac{d\omega_{P_s}}{dt} + B\omega_{P_s} \tag{3.6}$$
$$T_{P_s} = \pm D_{P_s} P_{acc}$$

where D_{P_s} is the displacement of the pump/motor, P_s and P_{acc} is the pressure in the accumulator. The sign depends on whether the accumulator is supplying energy (reutilizing, negative sign) or recovering energy (storing, positive sign).

The only problem with Eq. (3.4) is that in the hypothetical absence of circuit losses, it is possible that $\gamma \rightarrow \infty$. So, using this method γ can obtain $0 \leq \gamma \leq \infty$. Any value of γ greater than one

indicates that the circuit reutilizes some of the input energy to lift the weight again. Moreover, when $\gamma \to \infty$, all the recovered energy is used in the subsequent lifting phase, which is physically not attainable.

Table 3.1 summarizes the various possible values of γ for the circuit shown in Figure 3-1, where we observe six different modes for lifting and lowering the hydraulic system. These values offer insight into how different configurations and conditions influence the energy recovery capabilities of the system.

Table 3.1: Cyclic performance index (γ) for selected circuit losses (ε_1, ε_2) and counteracting motor torque (S_P) relative to Figure 3-1 Circuit (adapted from Costa and Sepehri, Energies, 2024, CC BY 4.0 [1]).

Case	Interpretation	ε_1	ε_2	S_p	γ
1	Perfect lossless circuit	0	0	0	$\gamma = \frac{S}{\varepsilon_1+\varepsilon_2} = \frac{S}{0} = \infty$
2	Some energy is recovered at quadrants II and IV	>0	>0	0	$\gamma = \frac{S}{\varepsilon_1+\varepsilon_2} > 1$
3	No loss, free weight fall (all motoring energy wasted, at quadrants II and IV	0	S	0	$\gamma = \frac{S}{\varepsilon_1+\varepsilon_2} = \frac{S}{S} = 1$
4	Free weight fall (all motoring energy wasted, at quadrants II and IV)	>0	S	0	$\gamma = \frac{S}{\varepsilon_1+\varepsilon_2} = \frac{S}{\varepsilon_1+S} < 1$
5	Weight held by the prime mover (no energy recovery at quadrant II and IV)	>0	>0	S_p	$\gamma = \frac{S}{(S+\varepsilon_1)+S_p} < 1$
6	Weight is too heavy to be moved (pump energy is lost through relief valves)	>>0	0	0	$\gamma = \frac{S}{\varepsilon_1+\varepsilon_2} = \frac{0}{\varepsilon_1} = 0$

Similarly, when a system completes a cycle involving multiple pumping and motoring operations, the Cyclic Performance Index (γ) can be extended to evaluate the overall performance. This generalized definition of CPI accounts for all the energy interactions during the cycle, making it suitable for systems with complex operations. For a system containing N_p pumping quadrants, γ is given by

$$\gamma = \frac{\sum_{K=1}^{N_p}(\int_{t_{1k}}^{t_{2k}} P_o dt)}{\sum_{j=1}^{N}(\int_{t_{1j}}^{t_{2j}} P_i dt)} \tag{3.7}$$

where t_{1k} and t_{2k} represent the start and end times of the k^{th} pumping operation, while t_{1j} and t_{2j} denotes the start and end times of the j^{th} operation, which could be either pumping or motoring. The term P_{out} refers to the output power at the actuator, which is the energy delivered for productive work during the operation. On the other hand, P_{in} represents the input power supplied by the prime mover, which drives the system and facilitates the energy flow required for both pumping and motoring phases.

Eq. (3.7) essentially sums up the energy contributions from all pumping operations and compares them to the total input energy across all phases. It provides a clear measure of how effectively the system recovers and utilizes energy. The cyclic performance index can also be written in terms of energy:

$$\gamma = \frac{\sum_{K=1}^{N_p}(E_{out}^{k})}{\sum_{j=1}^{N}(E_{in}^{j})} \tag{3.8}$$

where E_{out}^{k} is the output energy from the actuator and E_{in}^{j} is the total energy supplied by the prime mover.

This approach helps evaluate system performance when multiple pumping and motoring operations occur within a single cycle. By summarizing the energy contributions from all phases, provides a comprehensive view of how effectively the system uses and recovers energy throughout its operation. This detailed analysis not only identifies areas for improvement but also simplifies the comparison between different systems, making it easier to determine which design performs better in terms of energy efficiency and recovery.

3.2 Summary

This chapter described the Cyclic Performance Index (CPI) as a universal metric to evaluate and compare the energy performance of hydraulic systems. By addressing the limitations of current available methods, the CPI offers a comprehensive approach that considers the entire energy flow, including energy recovery and losses across a system's operational cycle. This ensures that systems with various designs and modes of operation can be effectively compared.

This chapter also demonstrated how analyzing energy flow using the interaction between cylinder force and velocity provides critical insights into the system's performance. In addition, a detailed comparison of a lifting and lowering system with and without energy recovery circuits clarified how energy is stored, reused and analyzed using power versus time curves. Moreover, the Cyclic Performance Indicator (CPI) provides a more detailed evaluation framework for hydraulic systems that involve multiple pumping and motoring operations within a single cycle, offering deeper insights into their performance characteristics.

By highlighting both practical application and theoretical concept, this chapter provides tools to understand better and evaluate hydraulic systems. The insights show that using energy recovery systems and standardized metrics like the CPI makes it easier to assess system performance and helps to create hydraulic systems that are more efficient and sustainable.

Chapter 4 Energy Storage and Reutilization in Electro-Hydrostatic Actuators

4.1 Introduction

Electro-Hydrostatic Actuators (EHAs) play a vital role in modern hydraulic systems. They have a compact design that enhances the system's performance. Often, EHAs integrate the pump and actuator into a single unit or position them close together to avoid long hydraulic lines. This design simplifies the system, boosts response times, and reduces energy losses. EHA systems are commonly used in fields such as aerospace, robotics, and industrial machinery.

Even though EHA systems perform better than traditional systems, energy loss still happens while performing some tasks, like lowering a weight or decelerating a load. These losses occur because potential energy is wasted as heat. To solve this, an Energy Storage and Reutilization (ESR) system can be added. The ESR system captures energy that would typically be wasted and reuses it during subsequent operations.

This chapter presents an analysis of an Electro-Hydrostatic Actuator equipped with a previously developed ESR circuit [14]. The focus is on understanding how energy is stored, transferred, and reused within the system. The main components of the EHA-ESR configuration are described, and its behavior is evaluated using simulation results. Through this examination, the chapter demonstrates the potential benefits of ESR integration in reducing energy losses and improving the efficiency of hydraulic actuation systems.

To support the simulation study presented in this chapter, the same EHA–ESR configuration was implemented and tested on a laboratory test bench. This experimental setup, shown in Figure 4-1, follows the architecture described in [14], provides a physical reference for validating the modelled system. A photograph of the experimental setup is included to illustrate the actual hardware used in the verification process.

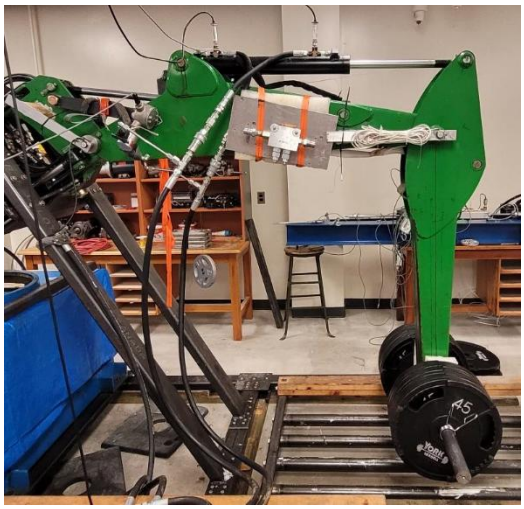

Figure 4-1: Experimental Electro-Hydrostatic Actuator (EHA) test bench used for system validation.

4.2 Electro-Hydrostatic Actuator (EHA)

In this section, the focus shifts to explain the Electro-Hydrostatic Actuator (EHA) in detail, including its components, configuration, and operational modes. The overview will also highlight the foundational equations governing the system's behavior, such as flow and force dynamics, which are critical for evaluating performance and setting the stage for integrating Energy Storage and Reutilization (ESR) systems.

4.2.1 Overview

The Electro-Hydrostatic Actuator (EHA) system consists of several key components, each playing a specific role in its operation. These components contribute to its overall functionality and improve the performance of the system. Figure 4-2 provides a schematic of the EHA circuit, which was designed by Costa and Sepehri [12]. This figure illustrates the system configuration and interactions between the components.

The servomotor, 1, is the primary driver of the EHA system. It provides precise speed and torque to the pump/motor, 2, through a belt transmission. This control allows the system to achieve the desired actuator motion. The servomotor operates in torque mode, where its controller regulates the current to match the torque requirements of the system. This ensures smooth operation during both pumping and motoring operations.

The pump/motor, 2, is a fixed-displacement, bidirectional unit. It converts mechanical energy from the servomotor into hydraulic energy during pumping operations. Conversely, during motoring operations, energy from the load returns to the system and the pump acts as a motor. The servomotor counterbalances this returning energy.

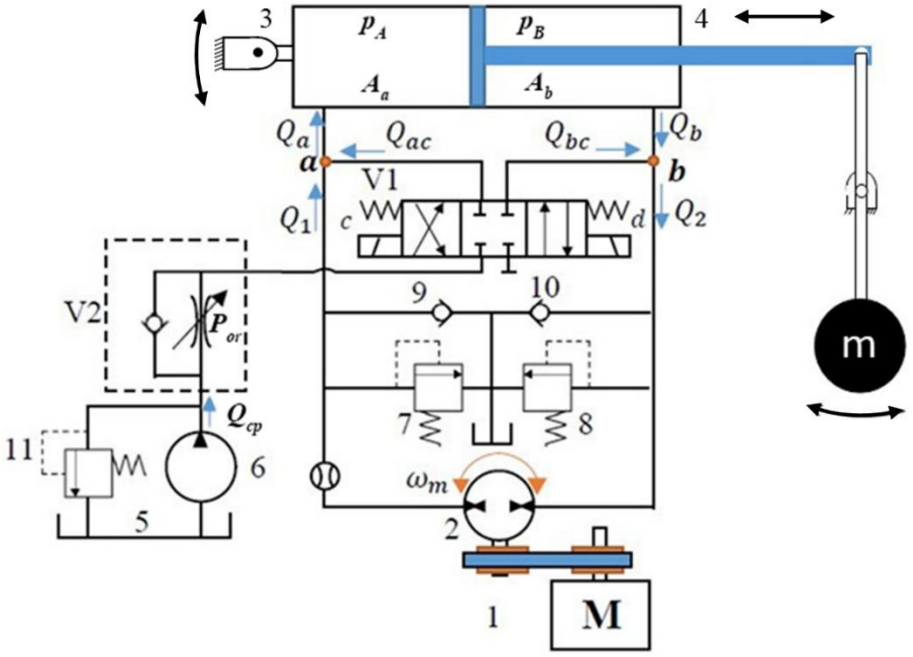

Figure 4-2: Schematic diagram of the EHA (developed from [13]).

The single-rod hydraulic cylinder, 3, is used to move the load, 4. An area difference on both sides of the piston is responsible for different flow rates on the cap and rod sides of the cylinder. To address this imbalance, a compensation circuit is needed to balance the fluid flows on both sides of the pump. The charge-pump, 6, compensates for the differential flow caused by the single-rod actuator. It helps to maintain a consistent flow of hydraulic fluid to ensure smooth operation of the cylinder. Additionally, the charge pump helps prevent cavitation and maintains a minimum system pressure, regulated by the relief valve, 11. Relief valves, 7 and 8, protect the system from overpressure conditions by redirecting excess fluid to the low-pressure side of the cylinder. On the other hand, check valves 9 and 10 are anti-cavitation valves, which prevent the lower circuit pressure from dropping excessively. The directional valve, V1, is a three-position, four-way valve that controls the flow from the charge circuit into either the cap or rod sides of the actuator. The flow-control valve, V2, is a one-way valve with an integrated orifice that provides flow

compensation during both cylinder extension and retraction. Pressure transducers are mounted near the cylinder ports to monitor the cap-side and rod-side pressure, p_a and p_b. An incremental encoder measures the piston position and velocity to calculate the piston speed. These measurements are crucial for evaluating the system's performance and identifying the operational quadrants.

4.2.2 Quadrant-based Operation

The Electro-Hydrostatic Actuator (EHA) operates in four different quadrants based on the direction of cylinder force and velocity. Understanding these quadrants is crucial for analyzing energy flow, determining operational modes, and identifying opportunities for energy recovery. The system's behavior in each quadrant is determined by using the relationship between cylinder force, $F_R = (p_A A_a - p_B A_b)$ and piston velocity (v).

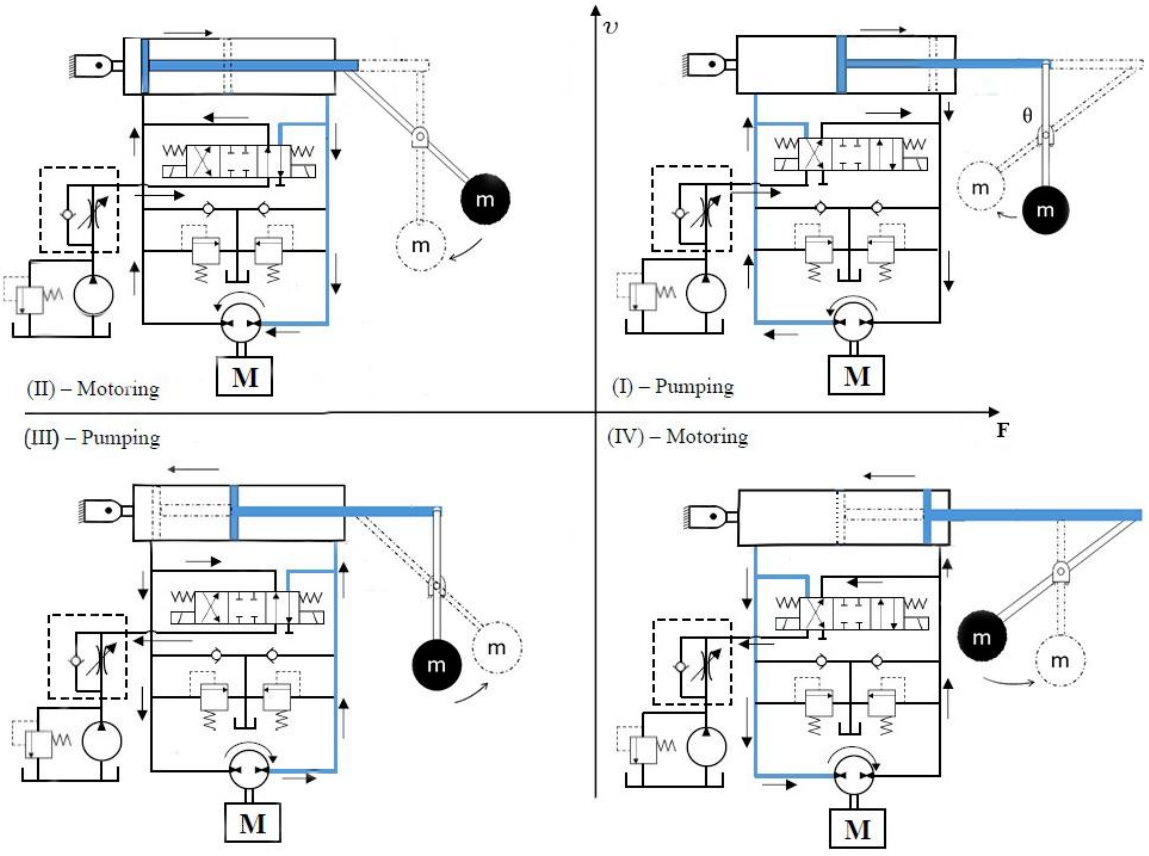

Figure 4-3: Four-quadrant base operations of the EHA (developed from [14]).

Figure 4-3 illustrates the four quadrants of the EHA operation. Each quadrant represents a unique condition based on the direction of force and velocity, which directly impacts the energy flow within the system. The system operates in all quadrants during a complete cycle.

To define the quadrants, a sign conversion is established: the cylinder velocity (v) is considered positive when the piston extends and negative when it retracts. At the same time, the cylinder force (F_R) is defined as positive when the actuator pushes the load and negative when it pulls the load.

Based on these conditions, the four quadrants are categorized as follows:

Quadrant I: Pumping – Cylinder Extension with Load Resistance: The system operates in this quadrant when $F_R > 0$ and $v > 0$. In this quadrant, the piston extends and pushes the load. The prime mover supplies energy to the Pump/Motor (PM_1) and the pump supplies the energy to the actuator. Since energy is flowing from the system to the load, this phase is classified as a pumping operation. During this phase, additional flow is provided by the charge pump through the directional valve to the cylinder rod side, compensating for the differential flow in the single-rod actuator.

Quadrant II: Motoring – Cylinder Extension with Load Assistance: In this quadrant, the cylinder force is negative ($F_R < 0$), but the velocity remains positive ($v > 0$), meaning that the load is assisting the motion of the actuator. Instead of the pump supplying energy, the load drives the actuator and as a result PM_1 operates as a motor. Therefore, it can be said that energy is recovered from the load and fed back into the system. At this quadrant, the charge pump flow is directed into the cylinder cap-side, as shown in Figure 4-3.

Quadrant III: Pumping – Cylinder Retraction with Load Resistance: During this phase, the cylinder force is negative ($F_R < 0$), and velocity is also negative ($v < 0$), meaning the piston retracts under the influence of the prime mover. Similar to Quadrant I, the PM_1 receives energy from the prime mover. Since energy is flowing from the system to the load, this phase is also considered a pumping operation. At this quadrant, the charge pump flow is directed into the cylinder rod-side, as shown in Figure 4-3.

Quadrant IV: Motoring - Cylinder Retraction with Load Assistance: In this quadrant, the cylinder force is positive ($F_R > 0$), but the velocity is negative ($v < 0$), meaning that the piston retracts under

the influence of the load. Similar to Quadrant II, the load assists the actuator's movement. Since energy flows from the load to the system and PM_1 act as a motor; this phase is classified as a motoring operation. At this quadrant, the charge pump flow is directed into the cylinder cap-side, as shown in Figure 4-3.

By analyzing these quadrants, the performance of the EHA system can be evaluated, and opportunities for energy savings can be identified.

4.2.3 Dynamic Modelling

This section presents the main equations governing the Electro-Hydrostatic Actuator (EHA) system, explaining the relationship between energy flow, force and energy efficiency. The equations in this chapter are adopted from the validated models in [14]. These equations are essential for understanding how the system operates under different conditions, including pumping and motoring operations. By defining these fundamental relationships, this section provides a foundation for evaluating the system's performance.

The AC servomotor drives the bidirectional pump/motor, which generates hydraulic pressure to move the actuator. This servomotor is operated in torque mode, which means its output torque is directly controlled by the current supplied through a controller. The relation between the applied voltage (U) and the current (I_{ac}) is given by:

$$U = V_b + RI_{ac} + L\frac{dI_{ac}}{dt} \tag{4.1}$$

where V_b represents the back Electromotive Force (EMF), R and L are the resistance and inductance, respectively. The generated torque, T_e, and the angular velocity of the servomotor, ω_m can be calculated using the following relations:

$$V_b = \omega_m K_B \tag{4.2}$$

$$T_e = I_{ac} K_T \tag{4.3}$$

where K_B is the back EMF constant and K_T is motor torque constant. The servomotor angular speed, ω_m Obtained using Newton's second law for rotation:

$$T_e - T_L = J\frac{d\omega_m}{dt} + B\omega_m \tag{4.4}$$

where J is the total moment of inertia of the combined servomotor and hydraulic pump/motor, PM_1, B is the viscous damping coefficient, and T_L represents the load torque.

The pump/motor converts this energy into hydraulic energy by producing a flow that drives the actuator. The generated flow rate by PM_1 is:

$$Q_1 = Q_2 = D_{PM_1}\omega_m \tag{4.5}$$

where D_{PM_1} is the pump displacement and ω_m is the servomotor angular speed. The hydraulic power supplied by PM_1 is, thus, given by:

$$P_{PM_1} = |Q_1(p_A - p_B)| \tag{4.6}$$

Actuator force and flow equations: The actuator receives hydraulic power from the pump-motor to drive the load. The hydraulic force equation is given by:

$$F_R = p_A A_a - p_B A_b = P_L A_a \tag{4.7}$$

where A_a and A_b are the piston area and piston-rod side areas, respectively. P_L is the load-pressure, which is given by $P_L = p_A - \frac{A_b}{A_a}p_B$. Load torque, T_L, generated by a pump-motor, can be calculated by:

$$T_L = D_{PM_1}(p_A - p_B) \tag{4.8}$$

The flow continuity equations at the cylinder ports are:

$$Q_a = A_a v + \frac{[V_a + \left(\frac{L}{2} + x_p\right)A_a]}{\beta}\dot{p_A} \tag{4.9}$$

$$Q_b = A_b v + \frac{[V_b + \left(\frac{L}{2} + x_p\right)A_b]}{\beta}\dot{p_B} \tag{4.10}$$

where V_a and V_b are the pipe volumes at the cylinder ports, L is the stroke length, and β is the bulk modulus of the hydraulic fluid.

The useful power delivered to the actuator is given by:

$$P_{cy} = |P_L A_a v| \tag{4.11}$$

The charge pump power is given by:

$$P_{cp} = |Q_{cp} p_{or}| \tag{4.12}$$

where Q_{cp} is the charge pump flow and P_{or} is the charge pump pressure.

The flow equations at the junction nodes a and b (Figure 4-1) are:

$$\begin{aligned} Q_a &= Q_1 + Q_{ac} \\ Q_b &= Q_2 - Q_{bc} \end{aligned} \tag{4.13}$$

where Q_{ac} and Q_{bc} represent flow compensation. The compensation flow logic depends on the operating quadrant of the actuator.

When the system operates in Quadrant I or IV, Q_{ac} becomes zero. In Quadrant I, Q_{bc} is equal to the charge pump flow Q_{cp}, while in Quadrant IV, Q_{bc} is calculated as:

$$Q_{bc} = -c_{vi}\sqrt{\frac{(p_b - p_{or})}{sg}} \tag{4.14}$$

where c_{vi} is the valve flow coefficient, p_b is the rod-side pressure, p_{or} is the charge pump relief pressure and sg is the specific gravity of the fluid.

Similarly, when the system operates in Quadrant II or III, Q_{bc} becomes zero. In Quadrant II, Q_{ac} is equal to the charge pump flow Q_{cp}, while in Quadrant III, Q_{ac} is,

$$Q_{ac} = -c_{vi}\sqrt{\frac{(p_a - p_{or})}{sg}} \tag{4.15}$$

where p_a is the cap-side pressure.

Now, based on the traditional definition of efficiency, the system efficiency can be calculated by comparing the useful power output to the total input power [14]. Efficiency is often expressed in terms of power ratios during pumping and motoring modes.

During the pumping operation, the prime mover supplies power to drive the pump, which is used to extend or retract the actuator. The efficiency equation for this operation is:

$$\eta_{pumping} = \frac{P_{cy}}{P_{PM_1} + P_{cp}} \leq 1 \tag{4.16}$$

During motoring operation, the energy flow reverses, and the load assists the cylinder motion by transferring power back to the system. The efficiency equation for this mode is:

$$\eta_{motoring} = \frac{P_{PM_1}}{P_{cy} + P_{cp}} \leq 1 \tag{4.17}$$

Equations (4.16) and (4.17) provide a basic evaluation of the EHA performance by measuring the power usage during pumping and motoring operations. These equations only serve as a reference to compare the results of the EHA with the ESR circuit. In the next section, the energy storage and reutilization system is introduced by explaining its working principle and integration with the EHA. The numerical values adopted for the servomotor, pump/motor, actuator, and hydraulic components used in the dynamic model are listed in Table 4-1.

Table 4-1: Parameters used in the dynamic modelling of EHA [14].

Parameter Name	Symbol	Value
Resistance	R	0.16Ω
Inductance	L	3.99 mH
Back EMF constant	K_B	1.52 V/$\frac{\text{rad}}{\text{s}}$
Motor torque constant	K_T	1.86 Nm/amp
Pump displacement	D_{PM_1}	8×10^{-6} m^3/rev
Piston-cap side area	A_a	3167×10^{-6} m^2
Piston-rod side areas	A_b	2380×10^{-6} m^2
Bulk modulus of the hydraulic fluid	β	689×10^{6} Pa
Charge pump flow	Q_{cp}	6.7×10^{-4} m^3/s
Charge pump pressure	p_{or}	5.5×10^{5} Pa
Specific gravity of the fluid	sg	0.86
Valve flow coefficient	C_{vi}	$1.6\times 10^{-7}\text{m}^3/(\sqrt{\text{Pa}}\ \text{s})$
Charge pump flow rate	Q_{cp}	$6.7\times 10^{-4}\text{m}^3/\text{s}$

4.3 Energy Storage and Reutilization (ESR) Circuit

The Energy Storage and Reutilization (ESR) circuit is designed to improve the performance of the Electro-Hydrostatic Actuator by capturing excess energy during motoring operations and reusing it during subsequent pumping operations. This helps improve the overall system performance by reducing power consumption.

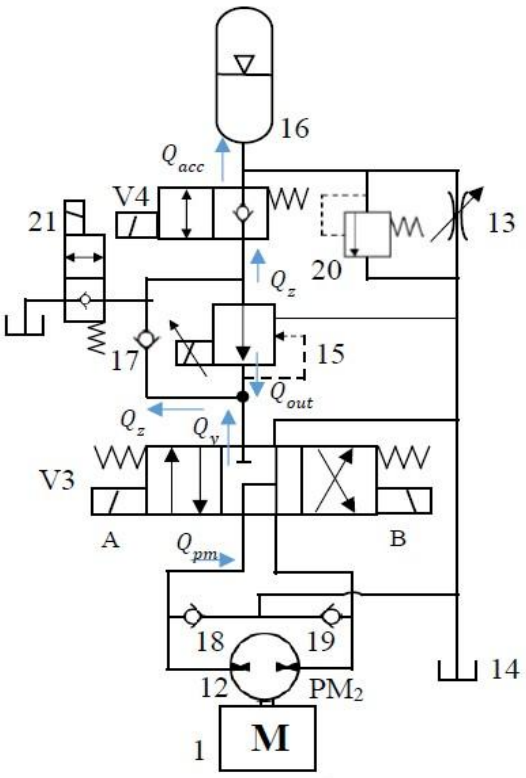

(a)

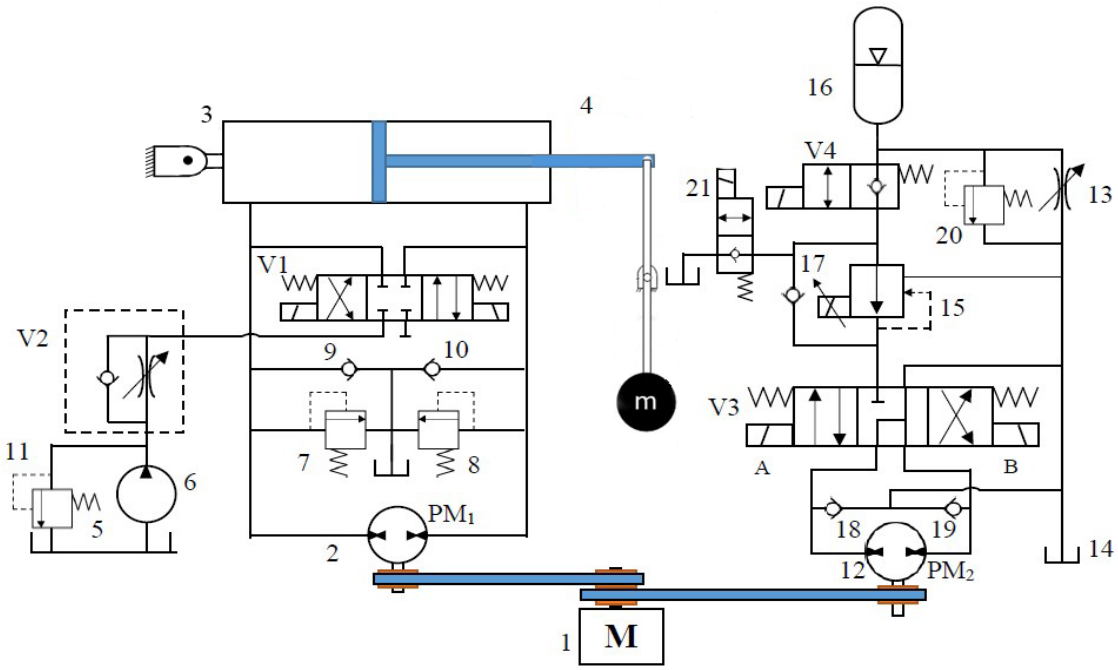

(b)

Figure 4-4: (a) Schematic diagram of the ESR circuit, (b) Integration of the ESR circuit with EHA (developed from [14]).

The ESR circuit consists of several hydraulic components, including a bidirectional pump/motor, PM_2, a hydraulic accumulator, a directional control valve and an electro-proportional pressure-reducing valve (EPPRV). These components work together to store energy during the motoring operation and supply it back to assist the actuator during the next pumping operation.

Figure 4-4(a) shows the ESR circuit with all major components, while Figure 4-4(b) illustrates how the ESR circuit is integrated with the EHA. This section explains how the ESR circuit functions in its different operational modes and the role of each component in managing energy flow.

4.3.1 Components and Configuration

As shown in Figure 4-4(a), the ESR circuit consists of a bidirectional pump/motor, 12, which is mechanically connected to the servomotor via a belt drive, as shown in Figure 4-4(b). This mechanical linkage enables energy transfer between the hydraulic accumulator, 16 and the actuator system. A hydraulic accumulator, 16, stores excess hydraulic energy during motoring operations and releases it when the system needs additional power.

To control the direction and flow of hydraulic fluid, the system integrates directional control valves V_3 and V_4. These valves facilitate switching between energy storage and reutilization modes. The electro-proportional pressure reducing valve (EPPRV), 15, regulates the pressure supplied from the accumulator, ensuring stable and efficient operation. Check valves 17,18, and 19 are used to prevent backflow, maintaining correct flow direction under different operating conditions. The relief valve, 20, protects the system from excessive pressure buildup by discharging excess pressure when needed. Furthermore, a flow discharge valve, 13, is added to safely release stored energy to the reservoir when it is necessary.

By utilizing these components efficiently, the ESR circuit reduces energy losses and enables the reuse of stored hydraulic energy. In the next section, each operation mode of the ESR circuit is duly explained.

4.3.2 Operational Modes

The Energy Storage and Reutilization (ESR) circuit operates in four distinct modes: storage, reutilization, discharge and flow recirculation. These modes control, how energy is stored, transferred and reused to enhance the system performance.

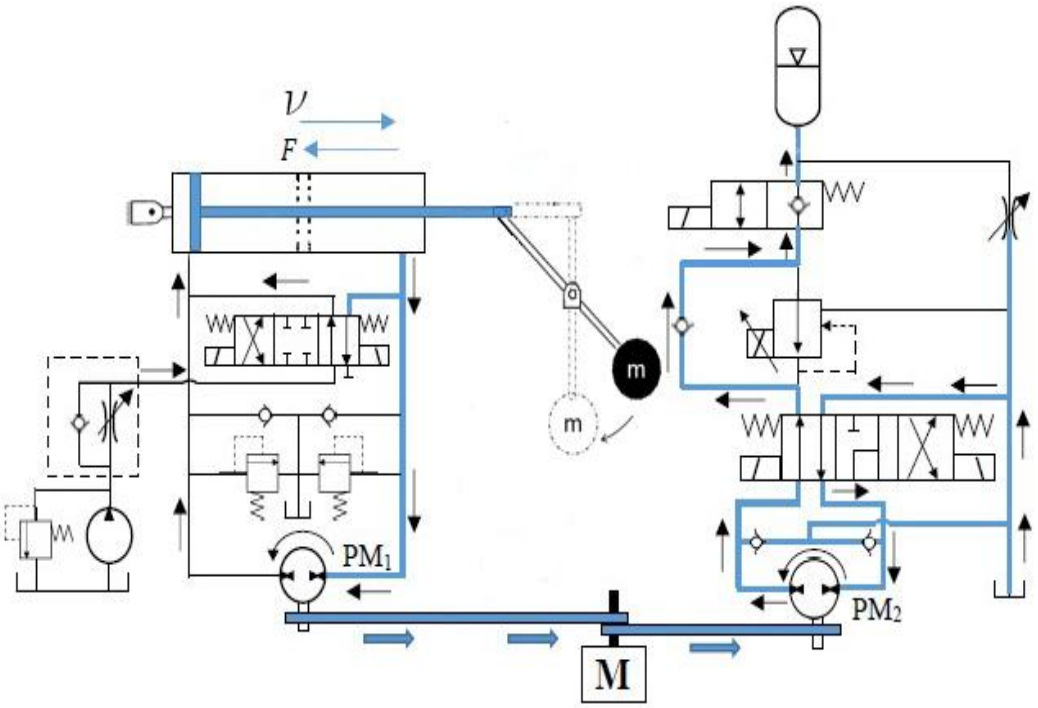

(a)

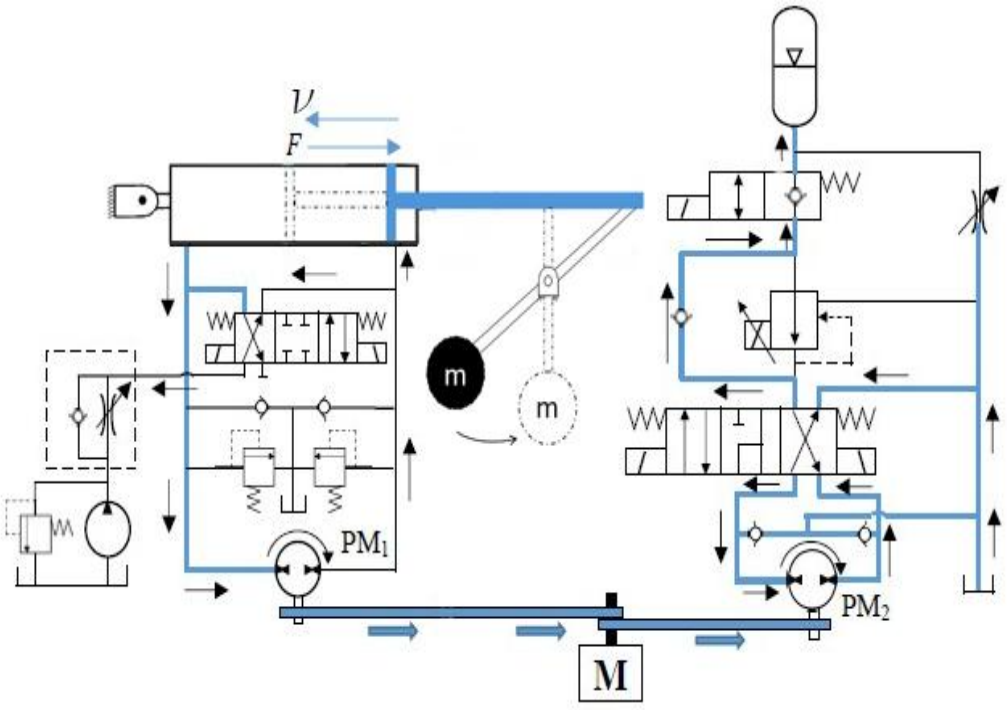

(b)

Figure 4-5: Energy storage during (motoring operation): (a) Second quadrant, (b) Fourth quadrant (developed from [14]).

1. Storage mode: The energy storage mode occurs when the actuator operates in motoring quadrants (Quadrant II and Quadrant IV). In these quadrants, the load force assists the piston and PM_1 operates as a motor. So, instead of allowing the load energy to dissipate, this energy is transferred to the ESR system to charge the hydraulic accumulators.

When the actuator moves in the positive direction and the load assists the motion, the system operates in quadrant II. As discussed before, in this case PM_1 runs as a motor. As shown in Figure 4-5(a), the float-center directional valve, V3 shifts to the left, allowing PM_2 to generate flow towards the storage check valve, 17. This flow reaches the hydraulic accumulator, 16, where energy is stored by compressing gas inside the accumulator using the incoming hydraulic fluid. The reutilization valve, V4, remains deactivated and in the storage position, ensuring that the flow is directed to the accumulator.

Similarly, as shown in Figure 4-5(b), the actuator moves in the negative direction, and again the load assists the motion with the system operating in quadrant IV. During this process, the rotation of both PM_1 and PM_2 is clockwise. Due to that, the float-centre directional valve, V3, shifts to the right, directing the flow towards PM_2, which then transfers energy into the accumulators. The energy storage process continues until the accumulator reaches its predefined pressure limit, set by the relief valve, 20.

2. Energy reutilization mode: The energy utilization mode is activated when the system needs extra power to assist the actuator motion during pumping operation (Quadrant I and Quadrant III). Instead of relying solely on the prime mover, the stored energy in the accumulator is used to drive PM_2, which, in turn, assists the pump PM_1.

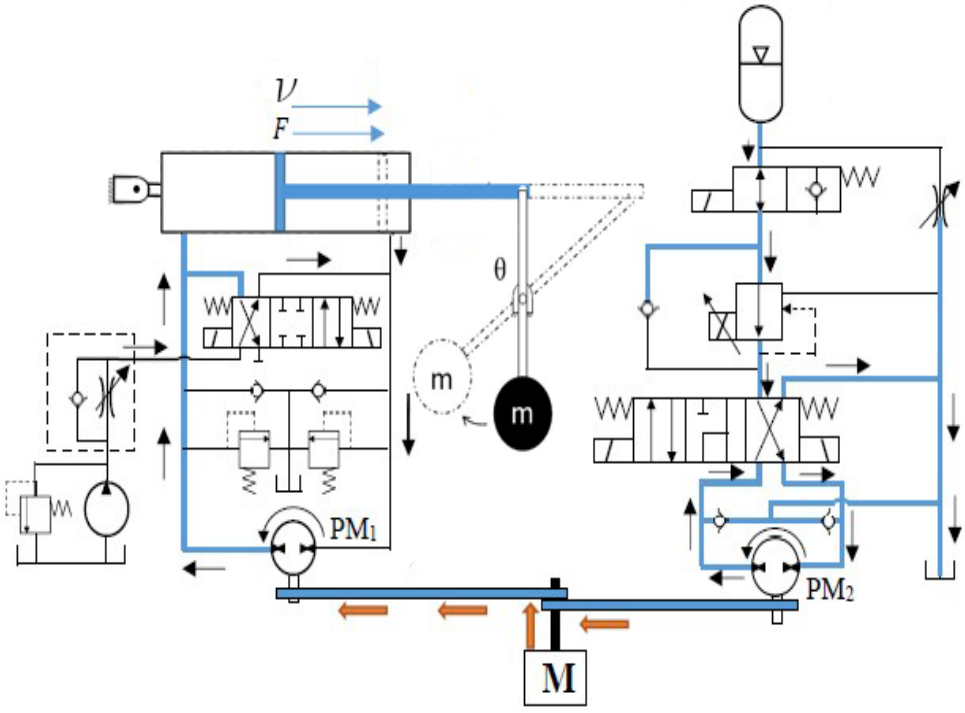

(a)

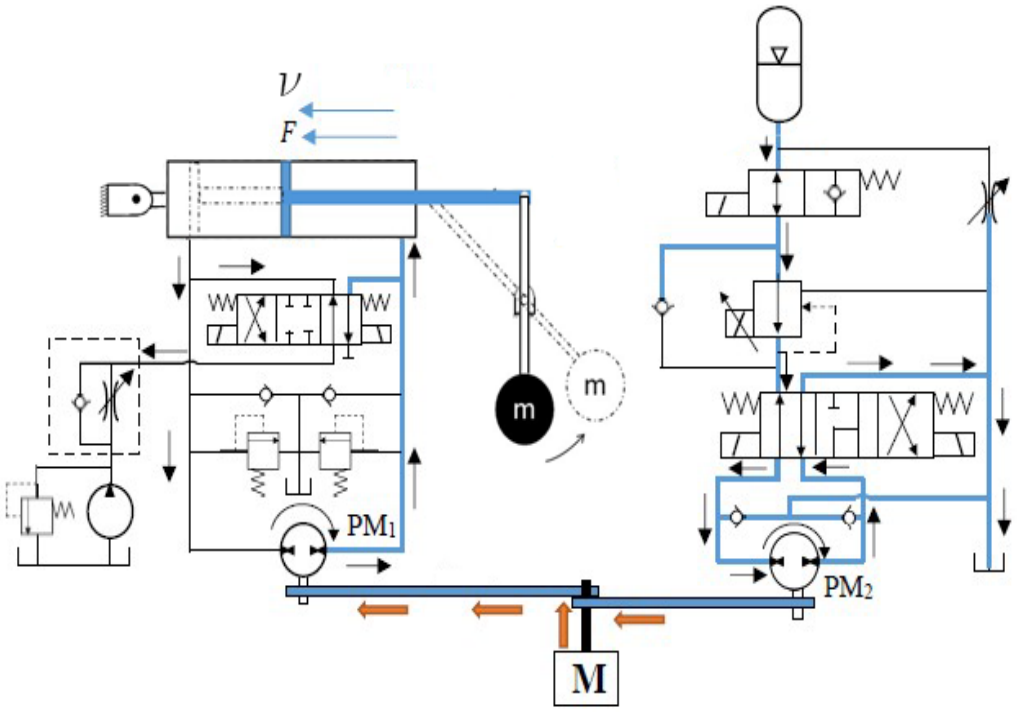

(b)

Figure 4-6: Energy reutilization during (Pumping operations): (a) First quadrant and (b)Third quadrant (developed from [14]).

As shown in Figure 4-6(a), the system operates in pumping mode. During this phase, the actuator extends using energy supplied by PM_1. The reutilization valve, V4, shifts to the reutilization position and releases the stored energy from the actuator into PM_2. Further, the EPPRV regulates this flow by ensuring that a controlled pressure is supplied to PM_2. The float-center directional valve V3 shifts to the right, thus enabling PM_2 and PM_1 to act as motors, reducing the energy demand on the prime mover.

Similarly, in quadrant III, when the actuator retracts in the negative direction, the stored energy is utilized to assist the operation. As shown in Figure 4-6(b), the float-center directional valve,V3 shifts to the left and PM_2, again, assists the system by converting the stored hydraulic energy into mechanical energy, thus helping to drive PM_1.

3. Energy discharge process: The energy discharge mode is used when the ESR circuit needs to be deactivated or when excess stored energy needs to be released for safety or maintenance

reasons. In this process, the hydraulic accumulators are emptied by allowing the stored pressurized fluid to return to the tank.

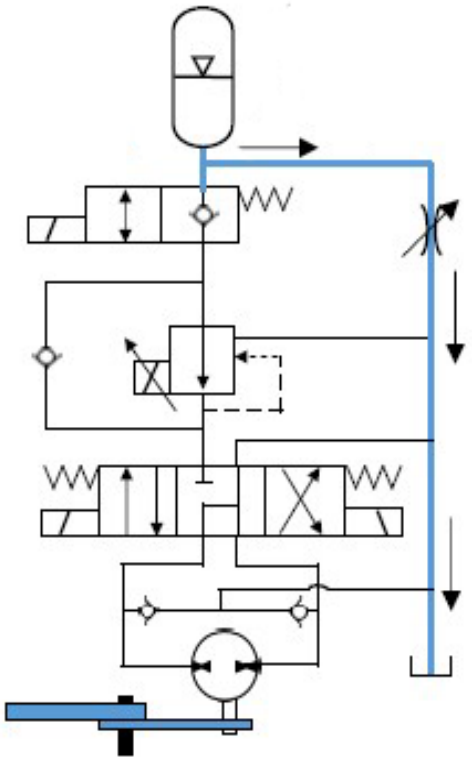

Figure 4-7: Energy discharge process in the ESR circuit (reproduced from [14]).

As shown in Figure 4-7, the flow discharge valve is opened, allowing the stored fluid in the hydraulic accumulators to be released to the tank. This process relieves system pressure and ensures that no residual energy remains in the accumulators. The reutilization valve and the float-center directional valve remain in their rest position, ensuring that no fluid flows back into the circuit. This mode is primarily used when the system is shut down or when it is started for the first time.

4. Flow recirculation process: Flow recirculation mode allows the Electro-Hydrostatic Actuator (EHA) to function independently from the ESR circuit. In this case, stored energy is not reutilized to run the system, and the system operates as a standard hydraulic circuit.

As shown in Figure 4-8, the flow discharge valve remains closed while the float-center directional valve, V3 and the reutilization valve, V4, are set to their neutral positions. In this state, the secondary pump, PM_2 is disconnected from the EHA, and no energy is transferred to or from the accumulators. Due to that, the primary pump, PM_1 operates solely with the energy supplied by the prime mover. This mode is used when energy recovery is not required, such as during low-load conditions or when the stored energy in the accumulators is not sufficient for reutilization.

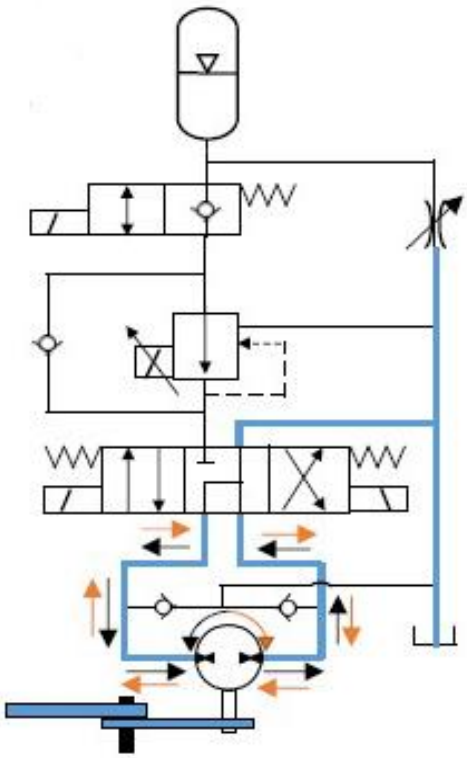

Figure 4-8: Flow recirculation process in the ESR circuit (reproduced from [13]).

By integrating these four operational modes, the system enhances the overall performance and reduces energy demand on the prime mover. This structured energy management approach ensures that the system operates optimally under varying load conditions and makes it more reliable and sustainable.

4.3.3 Dynamic Modelling

To understand the performance of the EHA with Energy Storage and Reutilization (ESR) circuit, it is necessary to analyze its fundamental equations that govern its operation. These equations describe how energy is stored, transferred, and reutilized in the system. These equations are taken from the validated model in [14]. The analysis begins with the flow equation for the pump/motor unit PM_2.

The secondary pump-motor, PM_2 is responsible for transferring energy between the ESR system and EHA. The flow rate through PM_2 can be expressed as:

$$Q_{pm} = D_{pm}.\omega_p \tag{4.18}$$

where Q_{pm} is flow rate, D_{pm} is the displacement, and ω_p is the rotational speed of the secondary pump-motor, PM_2 during the motoring operation.

During energy storage, PM_2 acts as a pump and charges the accumulator. While in reutilization mode, it operates as a motor to assist PM_1 by converting hydraulic energy back into mechanical power. As discussed in the previous section, PM_2 helps to reduce the energy demand on prime movers. The torque balance during energy storage for Figure 4-4 is given by,

$$T_e - T_L - T_{PM_2} = J_e \frac{d\omega_p}{dt} + B_e\omega_p \tag{4.19}$$

$$T_{PM_2} = \begin{cases} D_{PM_2}(P_{acc}) \ \ for\ Quadrant\ \text{II} \\ -D_{PM_2}(P_{acc})\ for\ Quadrant\ \text{IV} \end{cases} \tag{4.20}$$

where T_e is the servomotor torque, T_L is the load torque generated by PM_1 and T_{PM_2} is the secondary pump torque during the energy storage process. J_e and B_e are the moment of inertia and viscous damping coefficient of the servomotor, for PM_1 and PM_2. P_{acc} is the accumulator pressure.

Now, when the reutilization operation starts and PM_2 works as a motor, as shown in Figure 4-5

$$Q_{pm} = D_{pm}.\omega_r \tag{4.21}$$

$$T_e - T_L + T_{PM_2} = J_e \frac{d\omega_r}{dt} + B_e \omega_r \tag{4.22}$$

$$T_{PM_2} = \begin{cases} D_{PM_2}(P_{EPPRV}) \ for\ Quadrant\ \text{I} \\ -D_{PM_2}(P_{EPPRV}) \ for\ Quadrant\ \text{III} \end{cases} \tag{4.23}$$

Here, P_{EPPRV} is the outlet pressure of the electro-proportional pressure-reducing valve (EPPRV) and ω_r is the rotational speed (rev/s) of the secondary pump-motor, PM_2 during the pumping operation.

The power transferred by PM_2 during the energy storage and reutilization is given by,

$$\begin{aligned} P_{PM_2} &= Q_{PM}\,(P_{acc}) \qquad \text{(during quadrants II } and \text{ IV)} \\ P_{PM_2} &= Q_{PM}\,(P_{EPPRV}) \qquad \text{(during quadrants I } and \text{ III)} \end{aligned} \tag{4.24}$$

The hydraulic accumulator is a key component for energy storage, as it holds pressurized fluid that can be used later for assisting the operations. To monitor the available stored energy, a parameter called State of Charge (SOC) is used. The SOC represents the amount of energy available in the accumulator at any given time and can be defined in two ways: volume-based SOC and pressure-based SOC.

The volume-based SOC measures how much oil is stored in the accumulator compared to its total capacity [15]. It is expressed as:

$$SOC_V = \frac{V_{oil}}{V_{total\ oil\ stored}} \tag{4.25}$$

The pressure-based SOC evaluates the stored energy by comparing the current accumulator pressure to its minimum and maximum values:

$$SOC_P = \frac{P_{acc} - P_{min}}{P_{max} - P_{min}} \tag{4.26}$$

where P_{acc} is the current accumulator pressure, P_{min} is the pre-charge pressure (1.55×10^6Pa) and P_{max} is the maximum accumulator pressure.

Now, to prevent the stored energy from being wasted away, one condition is created, by which $SOC_P \geq SOC_{RTH}$, where SOC_{RTH} is the reutilization limit, predefined as 0.65. This condition

indicates when the stored energy should be released during the pumping operation. Also, to prevent the accumulator from being overcharged, another limit is defined as SOC_{STH}, referred to as "storage limit", which is then set to 0.9.

By using Eq. (4.6), (4.11), (4.12) and (4.24), the system efficiency of the hybrid system during pumping operation is given by,

$$\eta_{pumping} = \frac{P_{cy}}{P_{PM_1} - P_{PM_2} + P_{cp}} \leq 1 \tag{4.27}$$

The system efficiency of the hybrid system during motoring operation [16] is given by,

$$\eta_{motoring} = \frac{P_{PM_1} + P_{PM_2}}{P_{cy} + P_{cp}} \leq 1 \tag{4.28}$$

4.4 Performance Comparison Between the EHA With and Without the ESR Circuit

To understand the effect of energy storage and reutilization, the performance of an Electro-Hydrostatic Actuator (EHA) with and without the ESR circuit is compared. This section presents simulation results for both cases, focusing on power supply, power consumption during operation and overall system performance. The comparison clearly illustrates the performance improvements achieved through energy recovery and reutilization

The results for an Electro-Hydrostatic Actuator (EHA) are shown in Figure 4-9. This figure represents various performance parameters, including input voltage, displacement, velocity, torque, flow rate, power consumption and efficiency. The system operates in a sequence of quadrants III-II-I-IV to complete one full cycle.

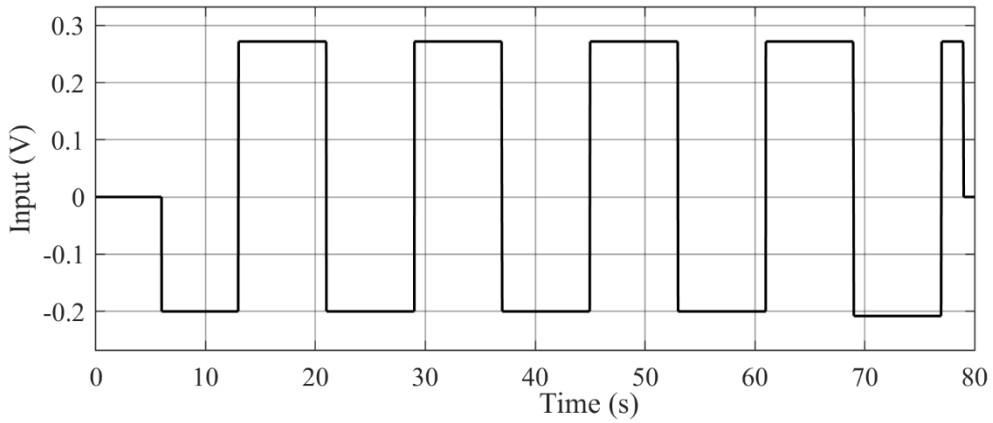

(a) Input (V) vs Time (s)

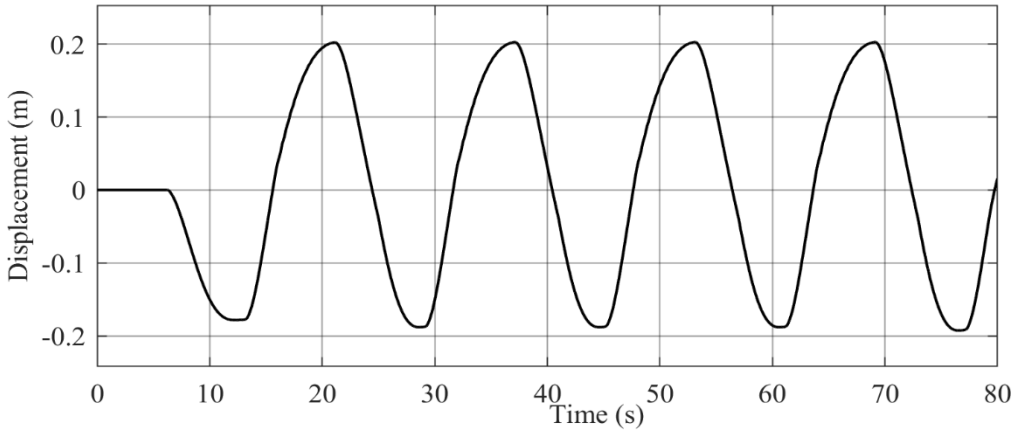

(b) Displacement (m) vs Time (s)

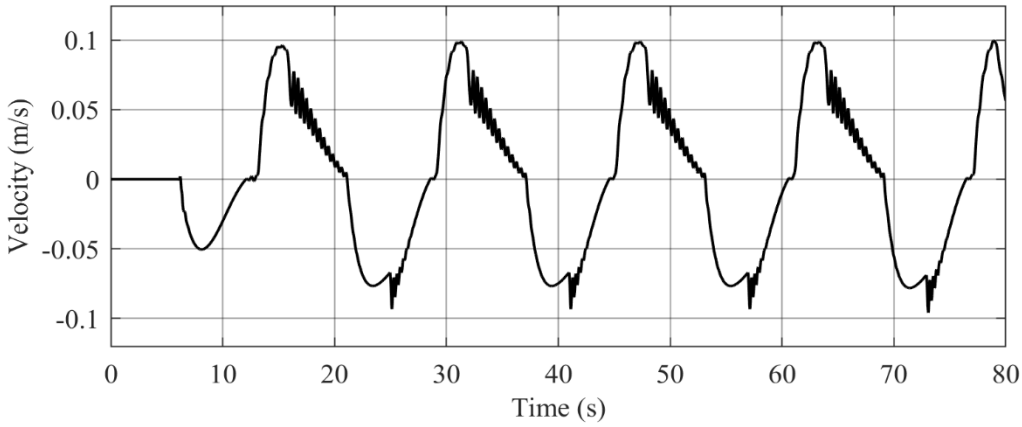

(c) Velocity (m/s) vs Time (s)

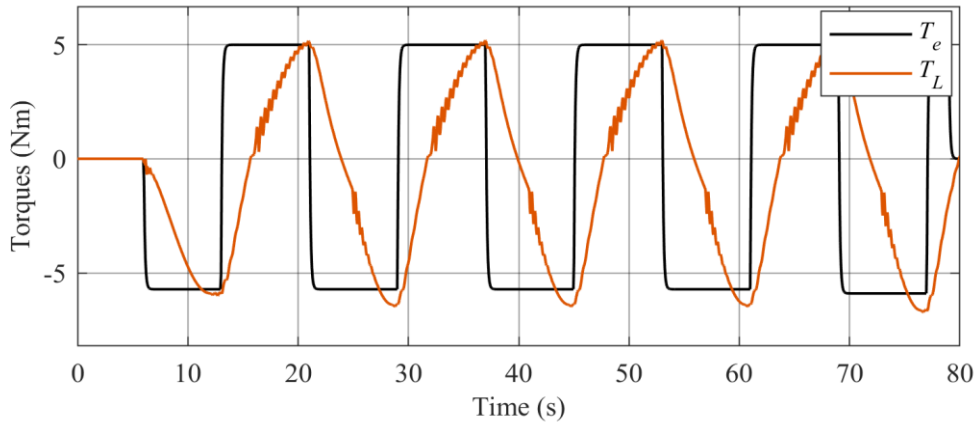

(d) Torque (Nm) vs Time (s)

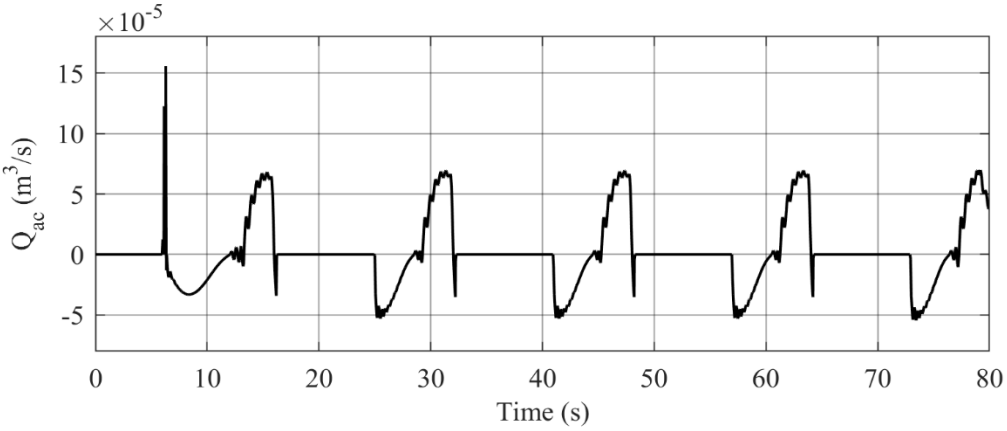

(e) Flow rate Q_{ac} (m^3/s) vs Time (s)

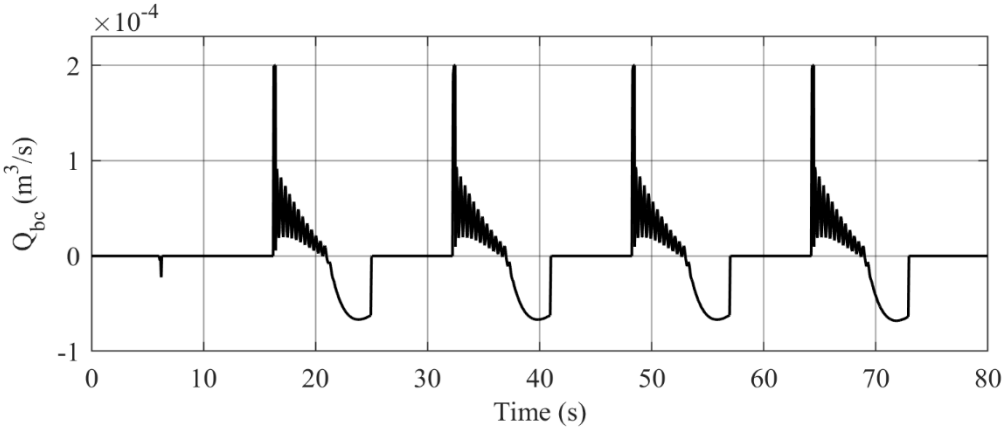

(f) Flow rate Q_{bc} (m^3/s) vs Time (s)

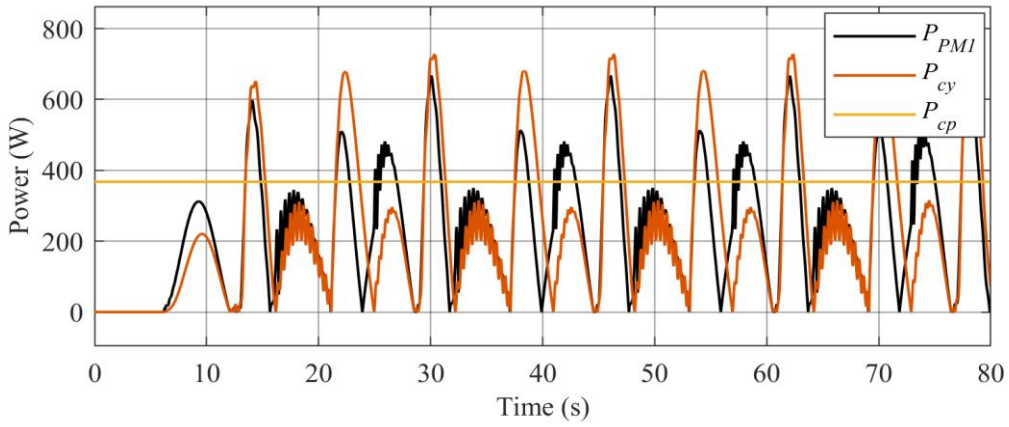

(g) Power (W) of P_{PM_1}, P_{cp} and P_{cy} vs Time (s)

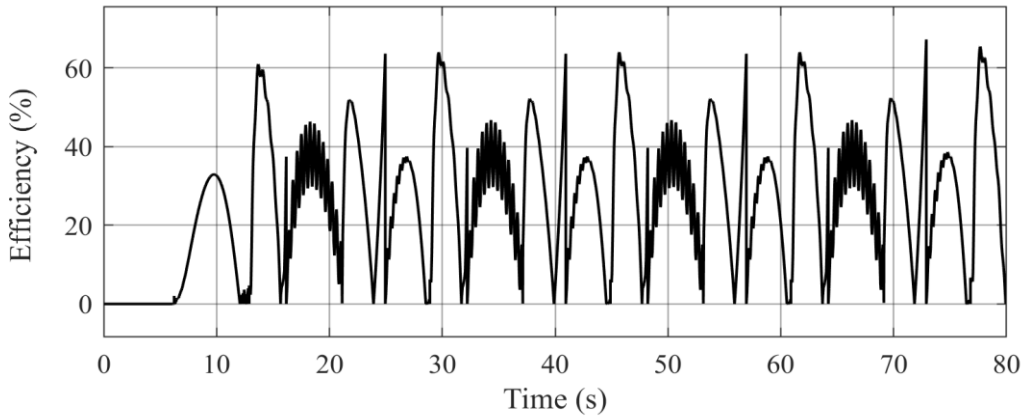

(h) Efficiency (%) vs Time (s)

Figure 4-9: (a)Voltage input (V); (b) Piston displacement (m); (c) Piston velocity (m/s); (d) Servomotor and load Torque (Nm); (e) Flow rate Q_{ac} (m^3/s); (f) Flow rate Q_{bc} (m^3/s); (g) Power (W) of PM_1, charge pump (P_{cp}) and cylinder power(P_{cy}); and (h) EHA efficiency (%).

Figure 4-9(a) represents the input voltage supplied to the servomotor, which directly influences the actuator movement and the overall system performance. Variation in input energy shows how the system responds to different operational demands. Figure 4-9(b) shows the actuator motion by highlighting the piston displacement, while Figure 4-9(c) shows the piston velocity, which indicates acceleration and deceleration during extension and retraction. Figure 4-9(d) illustrates the system reaction under different load conditions by presenting the prime mover torque and the load torque. Figure 4-9(e),(f) shows the flow rate at both sides of the actuator. Using Eq. (4.6) and

Eq. (4.11) to Eq. (4.17), the hydraulic power of the primary pump, charge pump, the cylinder power and the efficiency for each operation are determined and represented in Figures 4-9(g) and (h). As shown in Figure 4-9(g), cylinder power is higher during motoring operation; for that reason, to balance the load, extra resistive power ($P_{cy} - P_{PM_1}$) is provided by the prime mover. Moreover, Figure 4-9(h) shows that the pumping efficiency is between 40% and 50%, while motoring efficiency is between 50% and 60%. The reason is that the output power P_{PM_1} is greater in motoring operation when compared to pumping operation,

Now the ESR circuit has been added to the main system as shown in Figure 4-4(b) and tested under the same voltage input and load conditions applied to the EHA. The following results, shown in Figure 4-10(a) to Figure 4-10(j), demonstrate how the addition of the ESR circuit affects system performance by storing and reutilizing the energy.

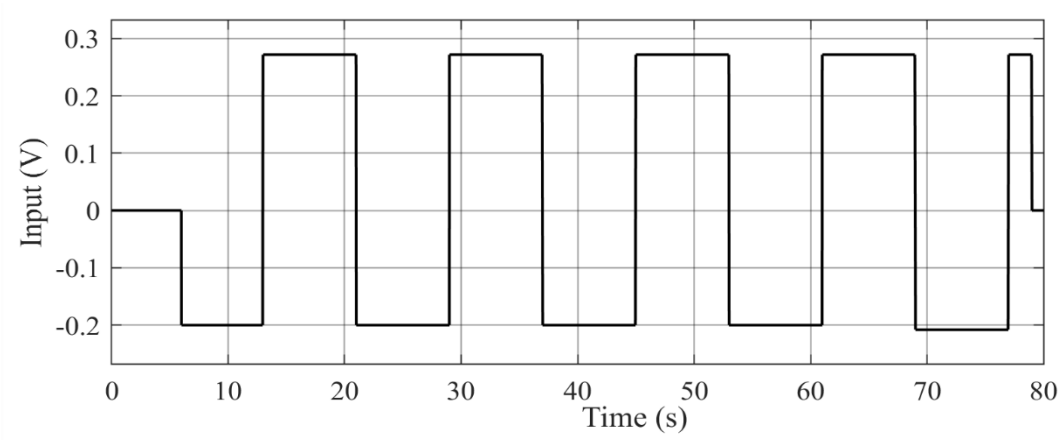

(a). Input (V) vs Time (s)

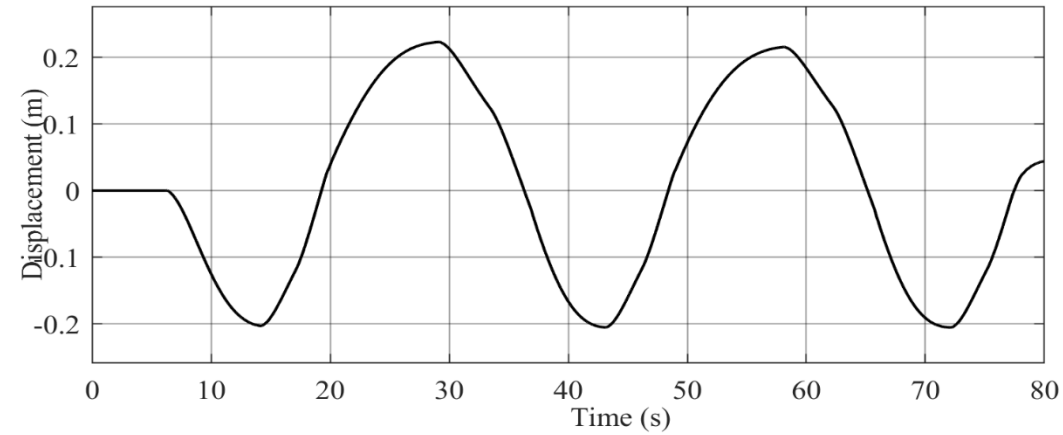

(b). Displacement (m) vs Time (s)

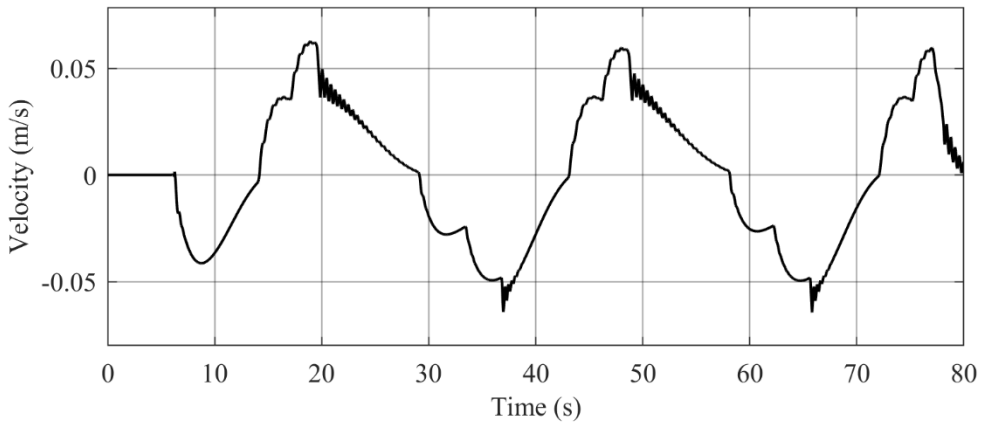

(c). Velocity (m/s) vs Time (s)

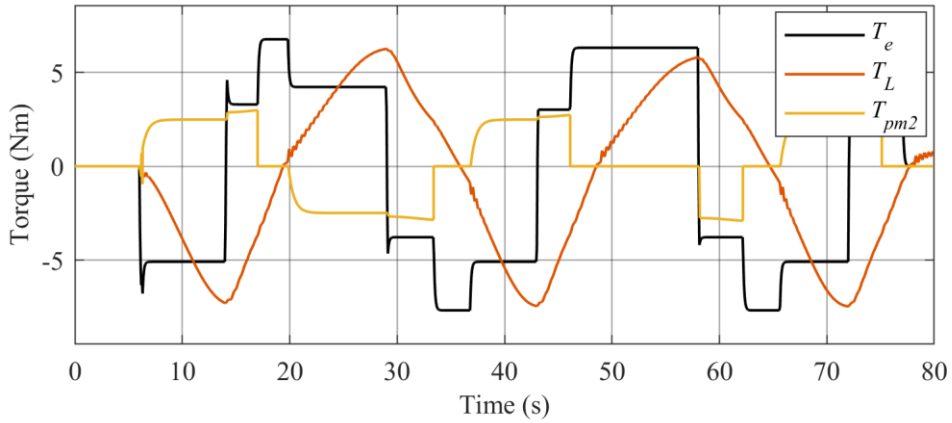

(d). Torque (Nm) vs Time (s)

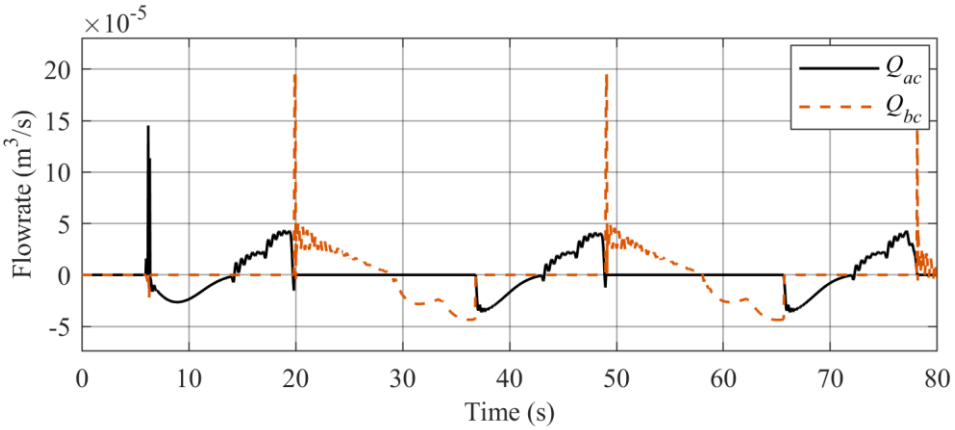

(e). Flowrate (m^3/s) vs Time (s)

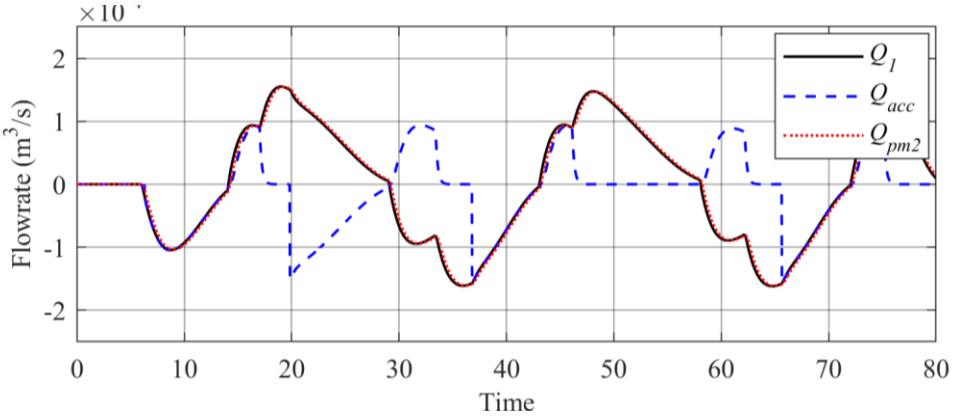

(f). Flowrate (m^3/s) vs Time (s)

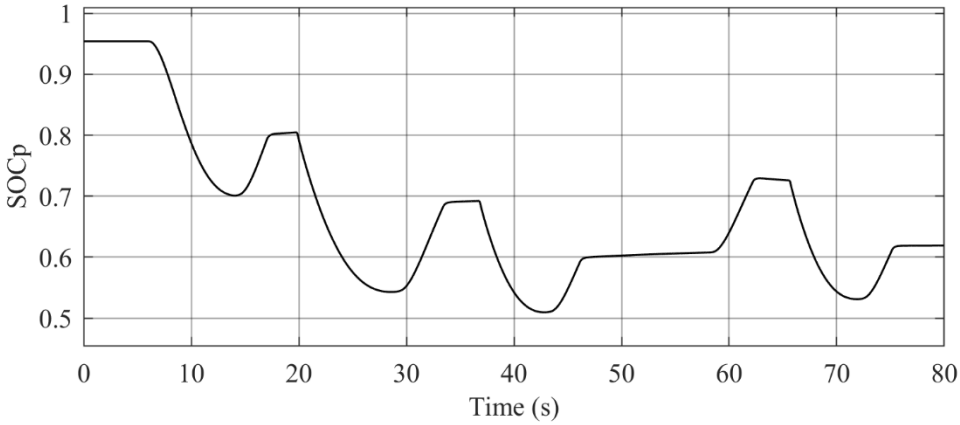

(g). State of charge-pressure vs Time (s)

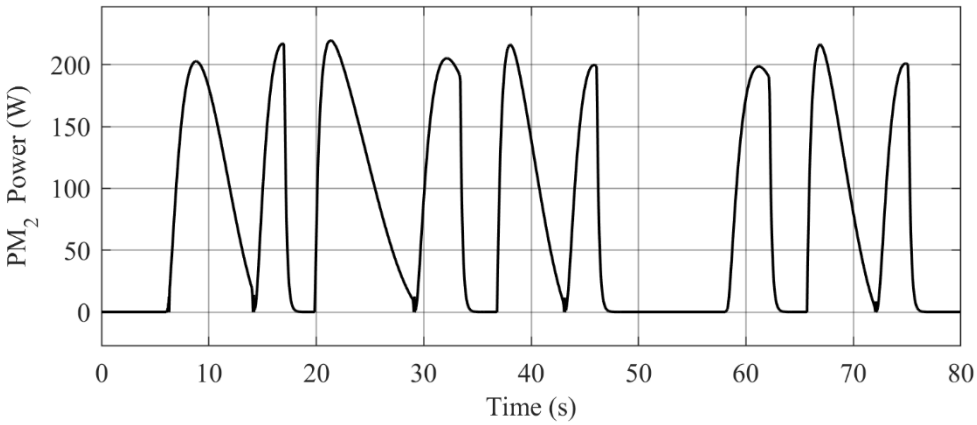

(h). Power (W) vs Time (s)

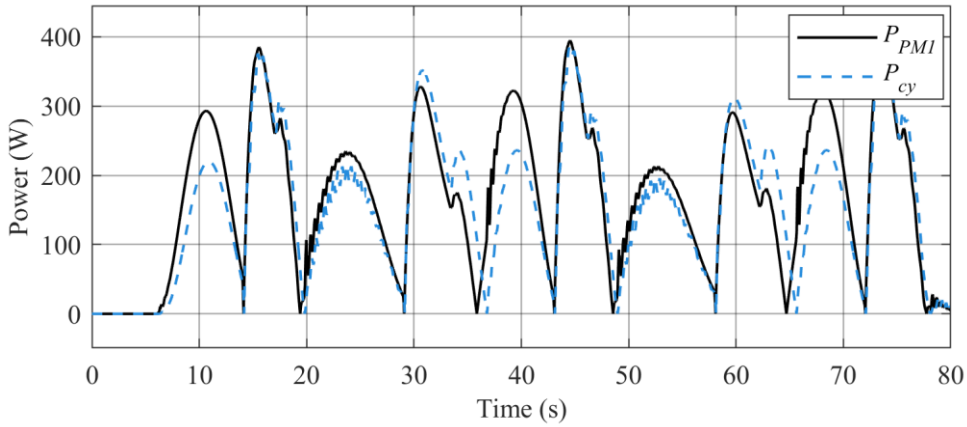

(i). Power (W) vs Time (s)

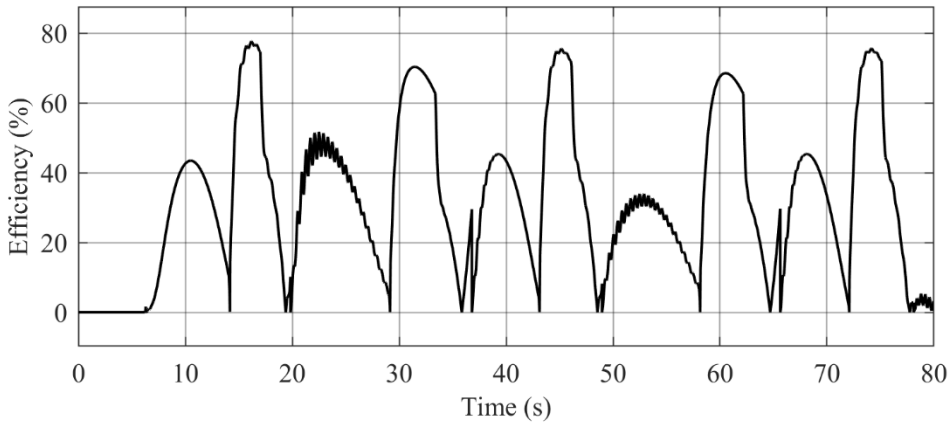

(j). Efficiency (%) vs Time (s)

Figure 4-10: Performance of the EHA with ESR circuit: (a) Voltage input (V) to servomotor; (b) Piston displacement (m); (c) Piston velocity (m/s); (d) Servomotor torque (T_e), load torque (T_L), and secondary pump (T_{PM_2}) torque (Nm); (e) Flow rate at both sides of the actuator (Q_{ac} and Q_{bc}); (f) Flow rates of $\mathrm{PM}_1, \mathrm{PM}_2$ and accumulator; (g) state of charge-pressure; (h) PM_2 power; (i) Power of P_{PM_1} and P_{cy}; and (j) Efficiency (%) of each operation.

The simulation results are shown in Figure 4-10. The current input to the servomotor is shown in Figure 4-10(a). The displacement and rod velocity of the cylinder are shown in Figure 4-10(b) and (c). The torque acting on $\mathrm{PM}_1, \mathrm{PM}_2$ and the servomotor shafts are shown in Figure 4-10(d). The flow through valve V1 is shown in Figure 4-10(e). The flows through $\mathrm{PM}_1, \mathrm{PM}_2$ and the accumulator are shown in Figure 4-10(f). The state of charge pressure at the accumulator is illustrated in Figure 4-10(g). As seen in this figure, between times 49s and 58s, the stored energy

is not sufficient for reutilization. Because of that, the ESR circuit is inactive, and EHA is driven by the servomotor alone. The hydraulic power of P_{PM_2}, P_{PM_1} and P_{cy} are shown in Figure 4-10(h) and (i), respectively. The system efficiency is shown in Figure 4-10(j). The efficiency of the EHA has improved by nearly 15-18% when the ESR circuit is added, as it helps recover and reuse energy.

4.5 Summary

This chapter described how the Energy Storage and Reutilization (ESR) circuit enhances the performance of an Electro-Hydrostatic Actuator (EHA). First, it described the electro-hydrostatic actuator, including its components, working principles, and its operation in four quadrants. The energy flow across different quadrants was examined to understand how energy is supplied and recovered during actuator operation.

Next, the ESR circuit was introduced as a way to store and reuse energy that would otherwise be lost. The system components, such as the secondary pump/motor, hydraulic accumulators, and control valves, were explained. The EHA with energy storage and reutilisation circuit operates in four modes: storage, reutilisation, discharge, and flow recirculation. Each mode helps manage energy efficiently based on system requirements.

The chapter also presented key equations for EHA with and without an energy storage and reutilisation circuit. These equations define power distribution, flow balance, and efficiency calculations, which help in simulating system performance. Simulations were used to compare the EHA with and without the ESR circuit. The results demonstrated the impact of adding the ESR system on torque, power consumption, and efficiency. The efficiency improved by 15-18% for the tests shown here due to energy recovery and reuse.

In conclusion, integrating the ESR circuit with the EHA reduces power demand and improves overall performance. The findings demonstrate that an energy recovery system can enhance the efficiency and sustainability of hydraulic systems while preserving their functionality.

Chapter 5 Comparative Analysis of Traditional Methods and the Proposed CPI Approach on an Electro-Hydrostatic Actuator

5.1 Introduction

Evaluating energy performance in hydraulic systems is essential, especially when comparing different systems. Many traditional methods have been used to calculate efficiency, but these methods depend on the specific design and working principles of each system. This makes it difficult to compare two different systems, especially when the systems include an energy storage and reutilization circuit.

In Chapter 4, the performance of the Electro-Hydrostatic Actuator (EHA) was analyzed with and without the ESR circuit. The results showed that adding an ESR circuit can improve efficiency, but current efficiency methods do not fully capture this improvement. This is because most traditional methods only focus on input and output power, without adequately considering stored and reused energy.

As shown in Chapter 2, various hydraulic systems use different energy evaluation methods; traditional efficiency calculations are not suitable for comparing systems with energy recovery circuits. This creates a need for a standard performance indicator that can be applied across different systems. The Cyclic Performance Index (CPI), introduced in Chapter 3, addresses this issue. The CPI provides a standardized and straightforward method for accurately assessing energetic performance, enabling fair comparisons between systems with varying designs.

The objective of this chapter is to:

1. Review traditional efficiency evaluation methods.
2. Apply these traditional methods to the EHA systems with or without ESRs, to understand their limitations.
3. Investigating CPI approach as a more effective method for evaluating efficiency, especially in systems that store and reuse energy.
4. Compare the results from traditional methods with those obtained with the CPI to demonstrate how the CPI provides a more precise and more accurate assessment of energy performance.

By the end of this chapter, it will be evident that the CPI is a more reliable and standardized method for measuring and comparing the efficiency of hydraulic systems, particularly when energy recovery is involved.

5.2 Comparative Study of Traditional Methods for Energy Performance Evaluation

This section reviews three commonly used methods for measuring efficiency: (1) energy saving ratio, (2) relative efficiency analysis, and (3) the concept of the Sankey diagram.

5.2.1 Energy Saving Ratio

In this method, the energy-saving ratio (Γ_s) measures the improvement in energy efficiency achieved by a system equipped with an energy storage and reutilization circuit, compared to one that operates without it. It provides a quantitative assessment of the energy savings achieved when an energy recovery mechanism is integrated into a hydraulic system. The energy-saving ratio can be calculated as follows:

$$\Gamma_s = \frac{E_{old} - E_{new}}{E_{old}} \tag{5.1}$$

where E_{old} is the energy consumption of the system without energy saving and E_{new} is the energy consumption of the system with energy recovery. In simpler terms, an energy-saving ratio shows the amount of energy saved when a recovery system is implemented. A higher value of Γ_s indicates a more effective energy recovery system, in reducing overall energy consumption [8].

Consider the hydraulic lifting system operated by an electric servomotor, as shown in Figure 5-1.

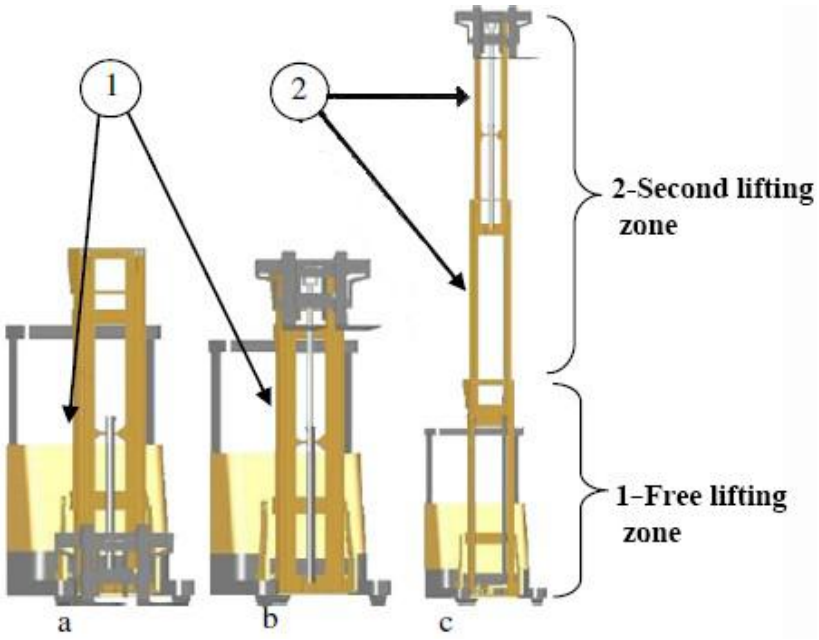

Figure 5-1: Lifting function of the forklift, (a) First stage, all cylinders in the initial position, (b) Free lifting zone, (c) Free lift zone and second cylinder zone (developed from [17], © 2013 Elsevier Ltd., with permission. License No. 6135270673483).

In such systems, most of the energy is consumed during mast operations and vehicle traction. The lifting function, due to gravitational potential, offers more opportunity for energy recovery compared to traction. To analyze this, two zones of mast movement are considered: the free lift zone and the second lift zone. In the free lift zone, the forks are raised without extending the mast. This is achieved by a primary hydraulic cylinder connected to a roller chain pulley mechanism, which lifts the carriage and forks within the outer mast. The chain system doubles the fork movement relative to the cylinder stroke, making it efficient for low-height operations. In contrast, the second lift zone involves extension of the inner mast section to achieve greater lifting heights, resulting in higher energy recovery potential due to elevation.

To quantify the energy performance across both lift zones, the total energy consumption is calculated by integrating the power supplied by the electric servomotor over time. This is expressed as:

$$E = \int_{t_1}^{t_2} \mathrm{P}\,(t)dt \tag{5.2}$$

Here, $P(t)$ is the instantaneous power of the servomotor during the lifting operation between times t_1 and t_2. Using this equation, E_{old} corresponds to the energy consumed by the lifting system without an energy recovery circuit, and E_{new} represents the energy consumed when recovery is enabled. Substituting these values into Eq. (5.1) allows the energy saving ratio Γ_s to be calculated for both the free lift and second lift zones, reflecting the effectiveness of the energy recovery system in each case.

To assess the effectiveness of this method and identify its limitations, Eq. (5.1) is applied to the simulation models of the EHA shown in Figure 4-2 and Figure 4-4(b). This will help determine how well the method captures energy savings and whether it provides an accurate comparison between the EHA and the EHA integrated with the ESR circuit. By applying this approach, its suitability for evaluating energy performance in hydraulic systems with energy storage and reutilization can be examined.

Simulation Experiment:

To apply the energy-saving ratio definition to the Electro-Hydrostatic Actuator (EHA) and EHA integrated with an Energy Storage and Reutilization (ESR) circuit, it is necessary to select appropriate performance parameters and justify their relevance. As discussed earlier, the power supplied by the servomotor is a suitable parameter for this evaluation. The servomotor serves as the primary energy source for both the EHA and the EHA with ESR circuit. In the ESR configuration, the energy stored in the accumulator during motoring operations is reused in subsequent pumping operations. This stored energy assists the servomotor, thereby reducing the total energy it needs to supply. Consequently, the servomotor power effectively reflects the influence of energy reutilization and serves as a reliable basis for assessing energy savings. Based on this reason and applying the energy saving ratio defined in Eq (5.1), the following expression is used:

$$\eta = \frac{E_{Ps_{old}} - E_{Ps_{new}}}{E_{Ps_{old}}} \times 100 \tag{5.3}$$

where E_{Ps_old} is the total energy supplied by the servomotor to complete a full cycle of the EHA, and E_{Ps_new} is the total energy supplied by the servomotor to complete a full cycle of the EHA integrated with the ESR circuit.

The total energy consumed in each case is calculated by integrating the instantaneous servomotor power over the operating time interval. In this study, the servomotor power is obtained as the product of electromagnetic torque and the motor angular speed, expressed as $Ps = T_e\omega_m$. The total energy supplied in each configuration is then determined using

$$E_{Ps_{old}} = \int_{t_1}^{t_2} Ps_{old}\,(t)dt\,, \text{and} \quad E_{Ps_{new}} = \int_{t_1}^{t_2} Ps_{new}\,(t)dt \tag{5.4}$$

The values of Ps_{old} and Ps_{new} are illustrated in Figure 5-2, where Ps_{old} corresponds to the EHA without energy recovery, and Ps_{new} represents the EHA with the ESR circuit.

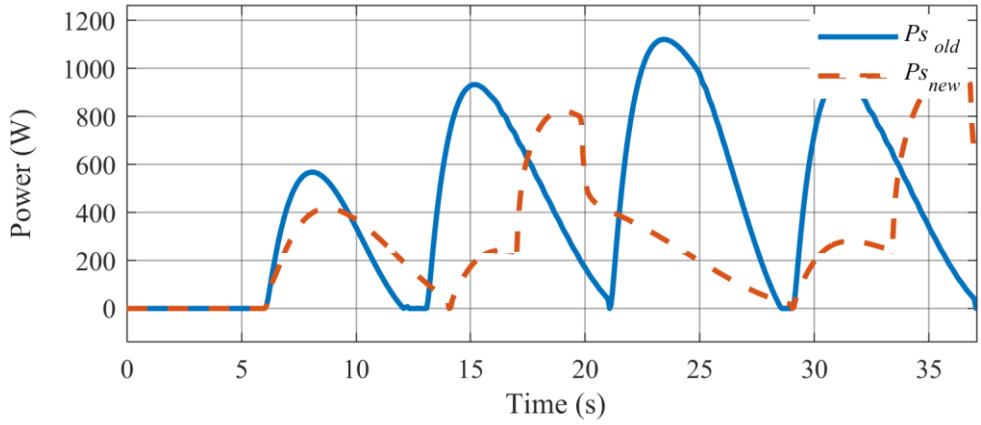

Figure 5-2: Power of the servomotor in EHA, with and without the ESR circuit.

Figure 5-2 demonstrates a clear reduction in power demand when the ESR circuit is used, owing to the assistance provided by the reused energy stored in the accumulator. By using Eq. (5.3) and (5.4), the energy consumption for each configuration is determined, and the corresponding energy-saving ratio is evaluated. These results are based on one complete operating cycle spanning 0–37.5s.

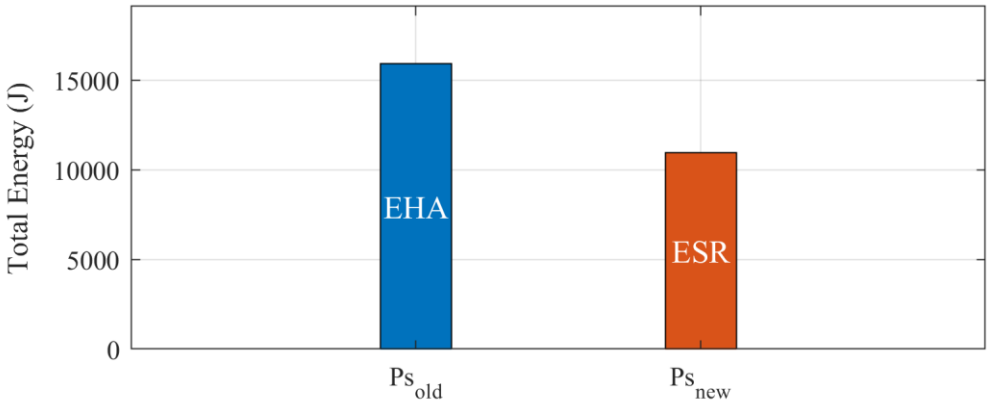

Figure 5-3: Energy comparison of EHA, with and without the ESR circuit.

As shown in Figure 5-3, the total energy consumption from the servomotor for operating the standalone EHA is 15.95 kJ. When the ESR circuit is integrated, this energy is reduced by 4.97 kJ. This corresponds to a 31.19% improvement in energy efficiency, highlighting the effectiveness of the ESR circuit in enhancing overall system performance.

Limitations of the Energy Saving Ratio Method

The energy-saving ratio offers a simple way to measure the reduction in energy consumption when an energy recovery system is added to a hydraulic circuit. It is especially useful when comparing a system without energy recovery to one with it. However, its value lessens when both systems feature energy recovery. With energy recovery in both systems, the ratio only reflects net consumption differences and does not indicate the actual energy recovered. Consequently, this metric cannot determine whether improvements are due to increased recovery, decreased internal losses, or both.

A significant drawback of this definition is that it fails to consider energy losses during transfer. When energy moves from the actuator to the pump or motor and then to the accumulator, some is inevitably lost due to mechanical friction, fluid leakage, and pressure drops within the hydraulic components. These intermediate losses reduce the actual benefit of energy recovery but are not reflected in the calculated energy-saving ratio.

Furthermore, such transfer losses contribute to internal inefficiencies within the system, including volumetric losses, mechanical losses, and flow imbalances. Even when an energy recovery circuit is used, these inefficiencies may cause the servomotor to supply more energy than theoretically

necessary. While energy storage can reduce the load on the servomotor, it does not eliminate the inherent losses within the hydraulic circuit, which can lead to an overestimation of the actual improvement in system efficiency.

Given these limitations, the energy-saving ratio is not well suited for evaluating hydraulic systems that include energy storage and reutilization circuits. Its inability to account for transfer losses, differentiate between recovered and wasted energy, or consider internal inefficiencies such as volumetric, mechanical, and flow imbalances results in an incomplete view of system performance. Without a detailed breakdown of where losses occur and how recovered energy is utilized, the method can overestimate efficiency gains. Therefore, while the energy-saving ratio can indicate general reductions in energy consumption, it cannot serve as a definitive or comprehensive measure of the actual effectiveness of energy recovery in complex hydraulic systems.

5.2.2 Relative Efficiency Analysis for Pump-Controlled Circuits

The relative efficiency assessment is another method used to evaluate the performance of hydraulic systems, concentrating on the flow rate between the pump and motor. This method has been used in previous studies to assess hydraulic circuits and compare their efficiencies under different operating conditions. In reference [18], the term “Relative efficiency” was introduced to define the efficiency of the circuit shown in Figure 5-4.

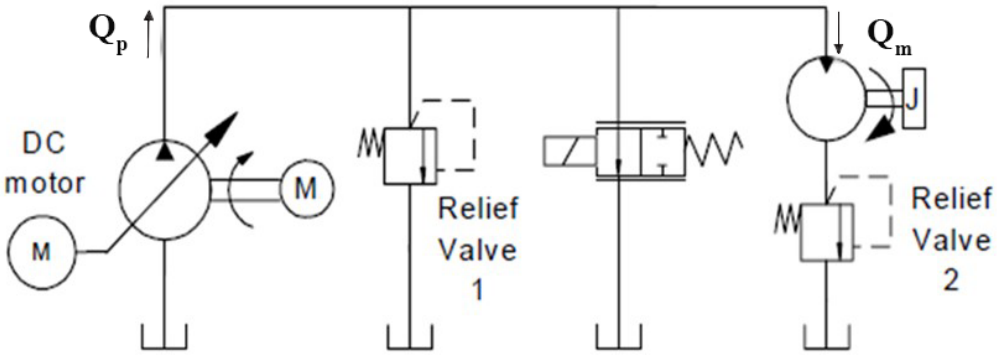

Figure 5-4: Pump-controlled system with bypass flow control (developed from [18]).

In reference [18], the term “relative efficiency” was used to describe the power efficiency of pump-motor open circuit, specifically under the assumption that mechanical and conduit losses are

negligible. This simplified evaluation focuses on the section between the pump outlet and the motor inlet, where it is assumed that the pressure at both points is the same. In this context, the pump and motor are the primary components of interest. So, the relative efficiency of the pump-controlled motor system is given by

$$\eta = \frac{\overline{Q_m}}{\overline{Q_p}} \tag{5.5}$$

where $\overline{Q_m}$ is the average flow rate of the motor at the motor input and $\overline{Q_p}$ is the average flow rate of the pump at the pump output.

To examine whether the concept of relative efficiency can be applied to an EHA and an EHA with an energy storage and reutilization circuit, a similar pump-controlled closed-circuit system was considered to evaluate how well the original definition holds under these conditions.

(a) Closed-Circuit of a Pump-Controlled System

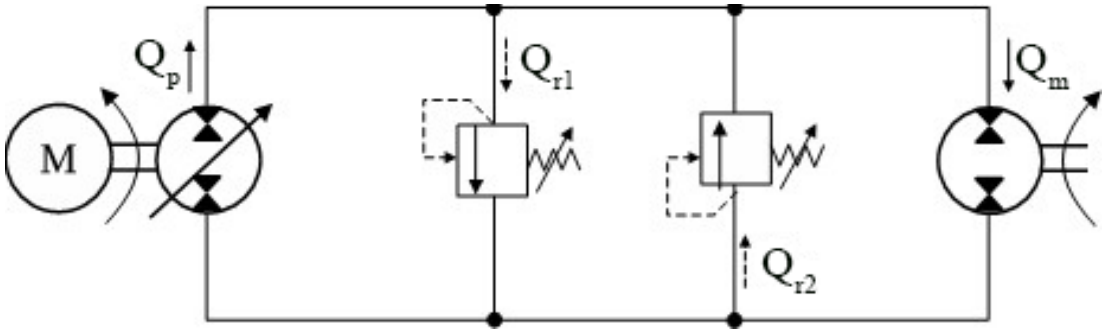

Figure 5-5: Closed circuit of pump-controlled system (adapted from [1]).

As per Eq. (5.5), the relative efficiency of the given system can be provided by

$$\eta = \frac{\overline{Q_p} - Q_{r1} + Q_{r2}}{\overline{Q_p}} \tag{5.6}$$

Now consider the same system but with an energy storage system as shown in Figure 5-6.

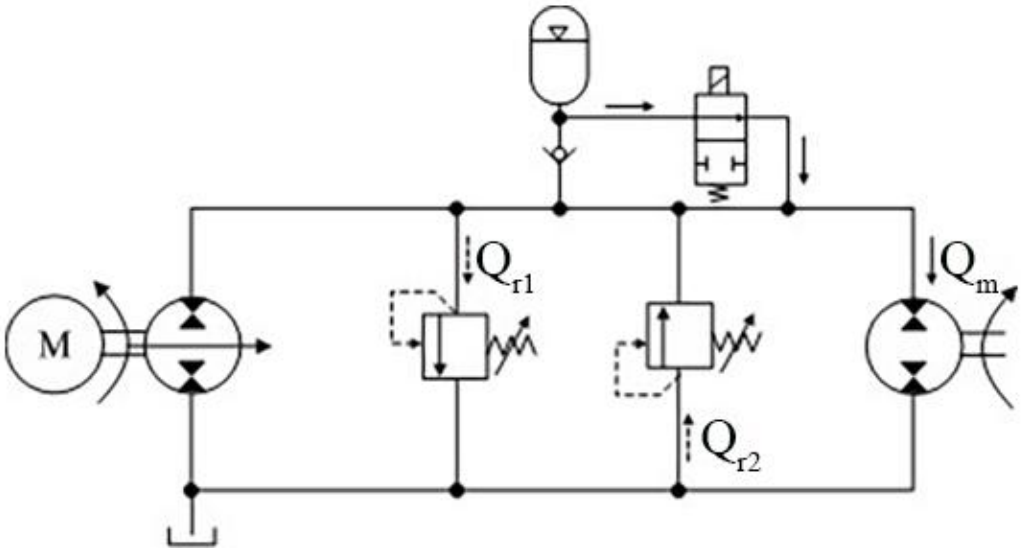

Figure 5-6: Closed circuit of pump-controlled system with energy storage circuit [1].

As shown in Figure 5-6, when the pump displacement is either positive or negative, energy is stored inside the accumulator, and when the pump displacement is zero, that previously stored energy is used to run the motor. In this case, Eq. (5.6) gives $\eta \rightarrow \infty$, because the input flow rate, $\overline{Q_p}$, becomes 0.

Simulation Experiment

To evaluate whether the relative efficiency concept from Eq. (5.5) can be applied to the Electro-Hydrostatic Actuator (EHA) and the EHA equipped with an Energy Storage and Reutilization (ESR) circuit, the closed-circuit configuration shown in Figure 4-2 is considered. In this system, the primary pump (Pump-1) is mechanically driven by a servomotor (M). The volumetric flow entering pump-1 during both pumping and motoring operations is denoted as Q_1.

Due to the asymmetric piston and rod areas of the actuator, a charge pump is required to compensate for the volumetric flow imbalance. The flow provided by the charge pump is represented as Q_{cp}. The net flow required to drive the actuator is denoted as Q_{cy}.

If the original open-circuit relative efficiency definition is adapted for this closed-circuit configuration, the efficiency during pumping and motoring modes can be expressed as:

$$\eta_p = \frac{Q_{cy}}{Q_1 + Q_{cp}} \tag{5.7}$$

$$\eta_m = \frac{Q_1}{Q_{cy} + Q_{cp}} \tag{5.8}$$

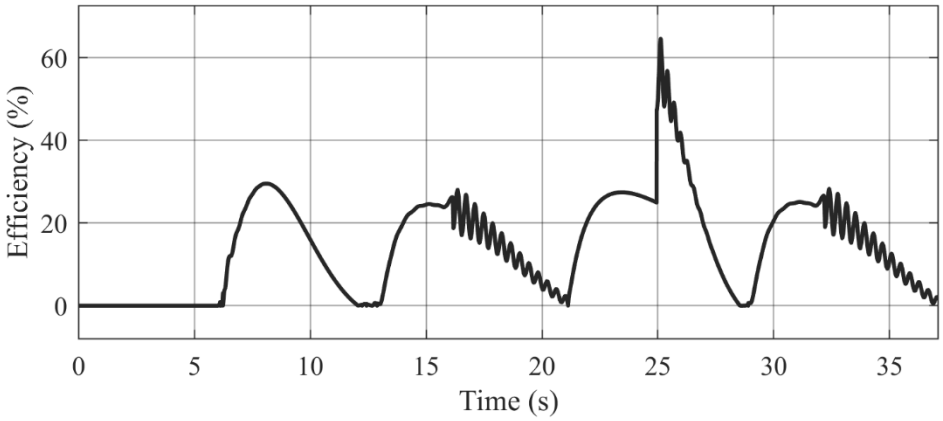

Figure 5-7: Efficiency of EHA using the relative efficiency definition.

The efficiency relationships expressed in Eqs. (5.7) and (5.8), as illustrated in Figure 5-7, raise several concerns about their applicability to the electro-hydrostatic actuator (EHA). These equations assume equal pressures and neglect mechanical losses or energy interactions between components-assumptions that were valid for the simplified pump-motor circuit shown in Figure 5-4, but do not hold for the more complex actuator configuration in Figure 4-1. The EHA includes multiple interacting components, an asymmetric actuator, and non-uniform pressure zones. In the EHA, the cap-side and rod-side pressures differ because the piston areas are not equal, so the actuator does not operate under a single pressure level as assumed in the simplified model. In this context, the flow from the charge pump (Q_{cp}) is not a direct energy input but a compensation flow used to balance volumetric differences in the actuator. Additionally, the mechanical energy transferred from the servomotor M to pump-1 is not fully captured by flow measurements alone, and internal losses further complicate energy tracking. As a result, applying the same flow-based efficiency definitions leads to questionable accuracy. Nevertheless, using Eq. (5.7) and (5.8), the relative efficiency of the electro-hydrostatic actuator was calculated to be between 38% and 42%. However, when the same definition is applied to define the efficiency of the electro-hydrostatic actuator with energy regeneration, the relative efficiencies are given by the following equations:

$$\eta_p = \frac{Q_{cy}}{Q_1 - Q_{pm} + Q_{cp}} \tag{5.9}$$

$$\eta_m = \frac{Q_1 + Q_{acc}}{Q_{cy} + Q_{cp}} \tag{5.10}$$

where Q_{pm} is the flow entering in PM_2, and Q_{acc} is the flow entering the accumulator.

When these equations were applied, the energy storage and reutilization circuit showed an efficiency of around 30%, which is lower than that of the electro-hydrostatic actuator alone. This result contrasts with the findings presented in Section 4.4, where the ESR circuit was predicted to improve EHA efficiency by about 20%. The lower calculated value suggests that the relative efficiency method does not fully capture the benefits of energy recovery in such systems.

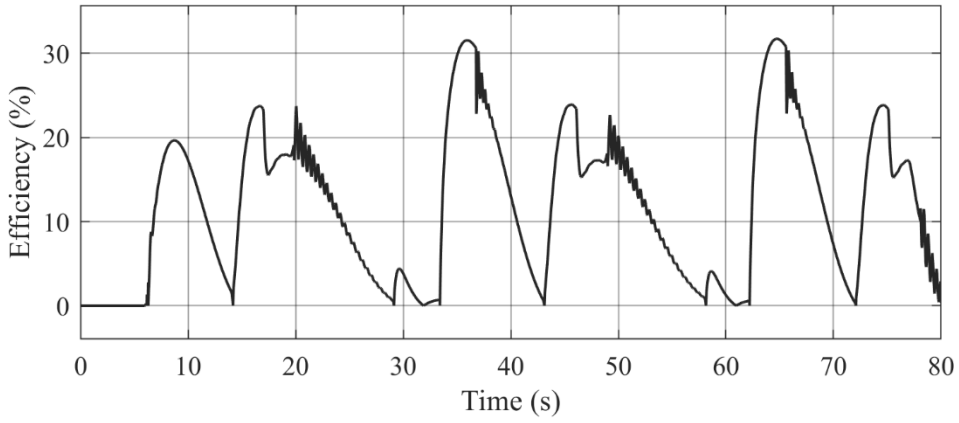

Figure 5-8: Efficiency of EHA with ESR circuit using relative efficiency definition.

The corresponding efficiencies for the EHA with ESR circuit, calculated using Eqs. (5.9) and (5.10) are illustrated in Figure 5-8. From this comparison, it can be seen that the method is not applicable for systems as shown in Figure 4.1 and Figure 4-3(b). During analysis, all underlying assumptions were critically reviewed and tested on both systems. The assumption that the pressure at the inlet and outlet of the system is the same was particularly problematic. In EHA with an ESR circuit, the pressure at various points was found to differ significantly, as shown in Figure 5-9. The pressure at the inlet of pump 1, the actuator, and the charge pump were nearly the same. However, the pressure difference between the EHA and ESR circuit was significant, around 4 MPa. This discrepancy makes the definition of relative efficiency unsuitable for the EHA with an ESR circuit.

From Figure 5-9, the pressure difference between the actual system (EHA) and the sub-system (ESR circuit) is noticeable. This indicates that a system like the energy storage and reutilization (ESR) circuit is dependent on the main EHA for its operation. Specifically, the circulation of fluid

differs between the EHA and ESR systems. The two systems exchange energy via mechanical transmission, not directly through hydraulic flow.

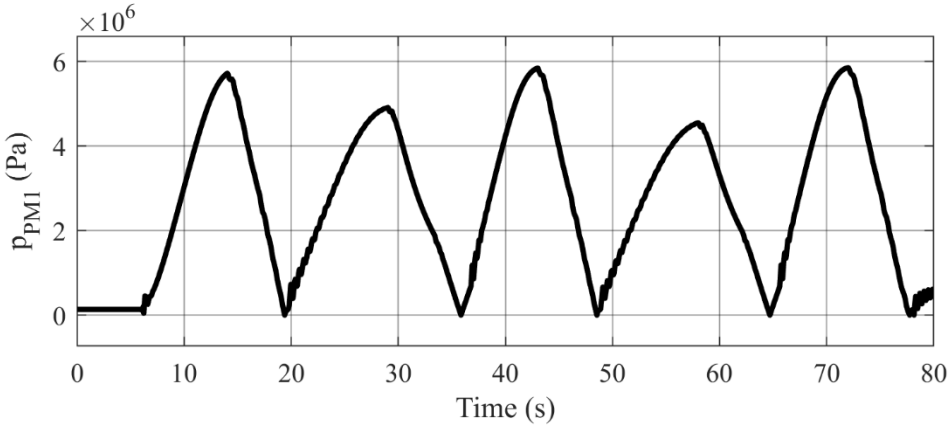

(a). p_{PM_1}(Pa) vs Time (s)

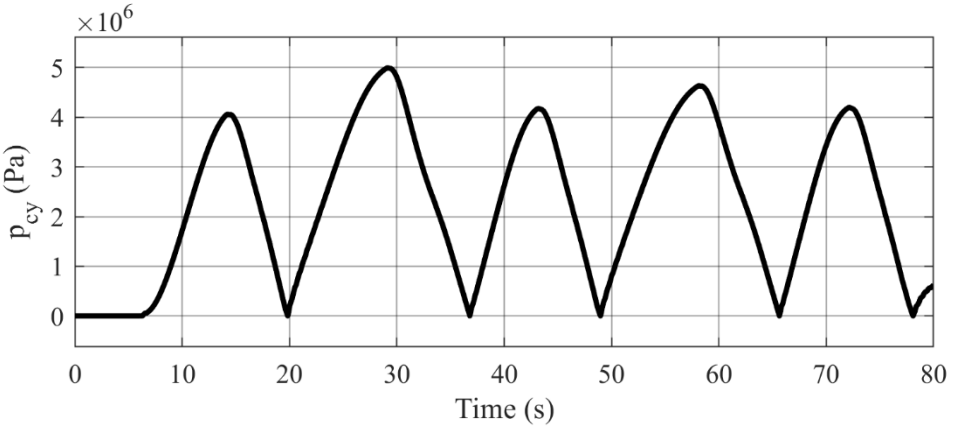

(b). p_{cy} (Pa) vs Time (s)

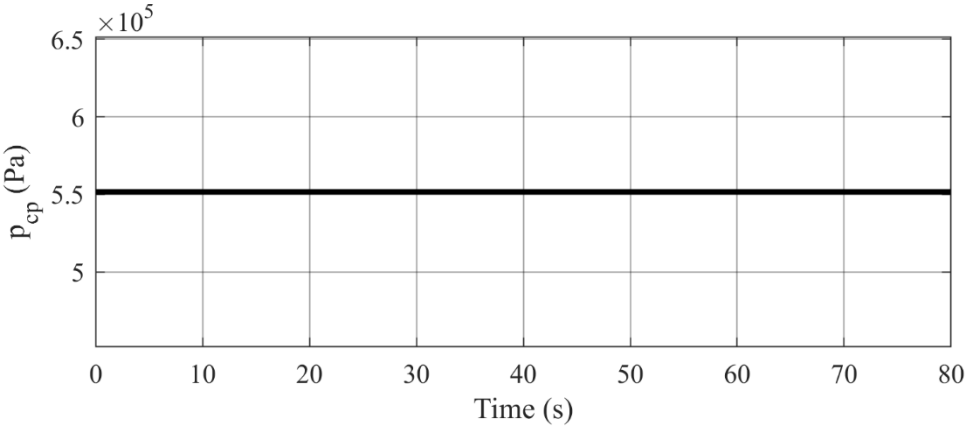

(c). p_{cp} (Pa) vs Time (s)

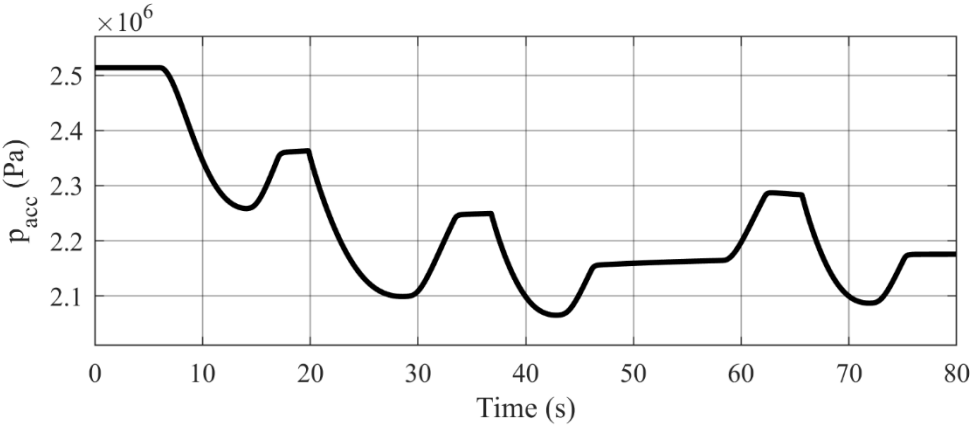

(d). p_{acc} (Pa) vs Time (s)

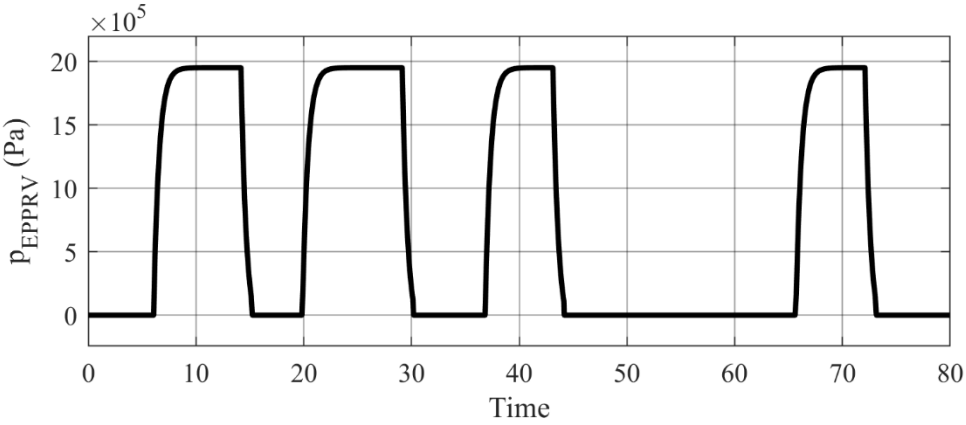

(e). p_{EPPRV} (Pa) vs Time (s)

Figure 5-9: Pressure comparison of Pump-1 (p_{PM_1}), actuator (p_{cy}), charge-pump (p_{cp}), accumulator (p_{acc}) and secondary pump (p_{EPPRV}).

In the ESR system, the pressure depends on parameters such as the accumulator's storage capacity and its maximum pressure handling capabilities. On the other hand, in the EHA, pressure varies with the force required to move the actuator. Because of these differences, the operating pressures of the two systems are distinct. As a result, it is incorrect to assume that the inlet and outlet pressures of both pumps are the same in the EHA and the ESR circuit.

Due to this variation in operating pressures, the method for defining relative efficiency does not apply to the system that incorporates energy storage and reutilization, such as the ESR circuit.

Limitations of the relative efficiency concept

The concept of relative efficiency does not work well for evaluating systems equipped with Energy Storage and Reutilization (ESR) circuit because it only considers the direct hydraulic flow between the pump and the actuator. It fails to include the portion of energy that is stored and reused. This leads to inaccurate efficiency calculations. In some cases, it even gives unrealistic results, like $\eta \rightarrow \infty$, when the pump input flow rate is zero while energy is still being supplied from the accumulator.

Another important limitation is the assumption that the pressures at the pump outlet and actuator inlet are identical. This assumption is not valid for the energy storage and reutilization (ESR). As seen in Figure 5-9, a substantial pressure difference exists between the components of the Electro-Hydrostatic Actuator (EHA) and ESR, which makes this assumption incorrect. This variation means that the calculated efficiency value does not accurately represent actual system performance.

Additionally, the ESR circuit transmits energy not only through hydraulic flow but also mechanically between components. For example, energy can be transferred from the primary pump to the secondary pump via a belt drive. The relative efficiency method does not account for such mechanical energy transfers, leading to an incomplete representation of the system's energy flow.

Given these issues, the relative efficiency method does not provide an accurate comparison of systems with energy storage. A more suitable approach is needed that accounts for both stored and reused energy to properly assess system performance.

5.2.3 Sankey flow diagram- based efficiency method

The Sankey flow diagram-based efficiency method is used to analyze the energy distribution in hydraulic systems by visually representing the relationship between input energy, useful work, and losses. This approach has been applied in previous studies to evaluate fuel consumption and efficiency in heavy-duty machinery such as hydraulic excavators [10]. By mapping energy losses at various stages, this method provides a comprehensive overview of system inefficiencies and highlights the points at which energy is dissipated as heat.

One of the main contributions of this method is the clear introduction of the concept of recoverable energy. In this context, recoverable energy refers to the part of the actuator output during motoring phases that can potentially be returned to the system. The method calculates efficiency by considering these recoverable energy losses separately from other losses, thereby providing a more accurate efficiency measure.

In a previous study [10], the method was used to analyze the efficiency of an excavator performing a dig and dump cycle, as shown in Figure 5-10.

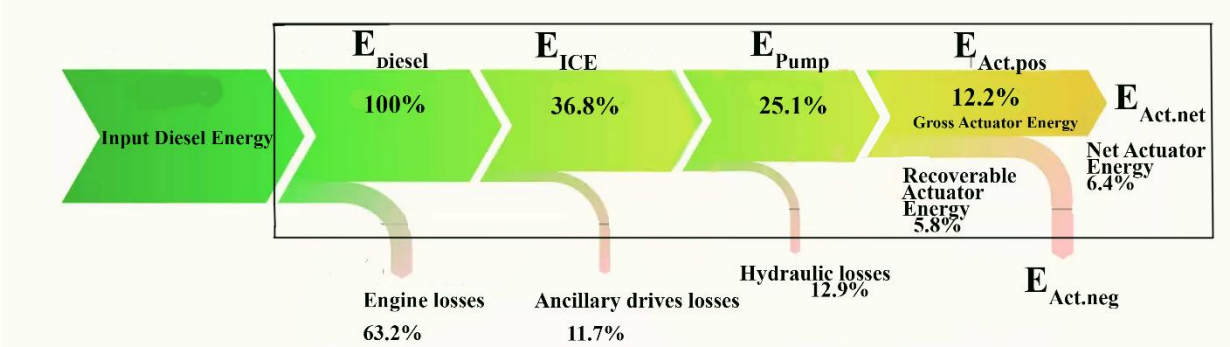

Figure 5-10: Sankey diagram illustrating energy flow through an excavator during dig and dump processes (reproduced from Vukovic et al., Energies, 2017, CC BY 4.0 [10]).

The diagram shows the energy paths through various components, identifying where losses occur and quantifying the efficiency of each stage. In heavy-duty machines, the analysis reveals that a significant portion of the total energy is lost during combustion, with only a small fraction reaching the actuators. Further losses occur within auxiliary systems, and these losses are not recovered but are instead dissipated as heat. Based on this analysis, the hydraulic system efficiency can be defined as:

$$\eta_{hyd} = \frac{E_{act,pos}}{E_{pump}} \tag{5.11}$$

There are two different ways to define total system efficiency. First, we may consider how much of the energy entering the system is delivered to the actuator:

$$\eta_{tot,Gross} = \frac{E_{act,pos}}{E_{Diesel}} \tag{5.12}$$

On the other hand, if energy generated by the actuator during the motoring phase has the potential to be recovered but is not stored or reutilized, it is considered a loss. In this case, the efficiency is defined as:

$$\eta_{tot,Net} = \frac{E_{act,pos} - E_{act,neg}}{E_{Diesel}} = \frac{E_{act,net}}{E_{Diesel}} \tag{5.13}$$

This method is intended for a comprehensive analysis of the entire machine, especially when the objective is to lower fuel consumption. The key point is that relying solely on traditional efficiency definitions, such as hydraulic efficiency, may not give a full view of the system's actual performance. This is because traditional hydraulic efficiency calculations often focus only on the hydraulic subsystem, without considering losses in other components of the machine. The Sankey flow diagram approach addresses this limitation by showing the complete energy flow from the primary energy source to the final useful output. Therefore, in Eq. (5.12) and Eq. (5.13), the total energy supplied by the diesel engine (E_{Diesel}) is taken as the system input, allowing the evaluation to include both hydraulic and non-hydraulic losses.

Now, in the following simulation experiment, this concept is applied to the Electro-Hydrostatic Actuator (EHA) to evaluate its efficiency and examine the distribution of recoverable energy losses within the system.

Simulation Experiment

To evaluate the applicability of the Sankey flow diagram-based approach to hydraulic systems, the method was applied to the Electro-Hydrostatic Actuator (EHA) configuration shown in Figure 4-1. In this arrangement, the total input power to the system is the sum of the power supplied to Pump-1 (P_{PM1}) and the charge pump power (P_{cp}). The output power corresponds to the actuator power (P_{cy}). So, from Eq. (5.11), the hydraulic efficiency during pumping and motoring operations is expressed as:

$$\eta_{hyd} = \frac{P_{cy}}{P_{PM1}+P_{cp}} \quad \text{(for pumping operation)}$$

$$= \frac{P_{PM1}}{P_{cy}+P_{cp}} \quad \text{(for motoring operation)} \tag{5.14}$$

Eq. (5.14) defines the efficiency of the electro-hydrostatic actuator (EHA) based on power flow during the pumping and motoring operations. When the piston is at the central position (x = 0), the system is in a neutral state with no net power transfer. As the piston moves away from this position in either the positive or negative direction (+ x or − x), the actuator is in the pumping mode, during which the prime mover supplies power to drive the load. Conversely, when the piston returns toward the central position, the actuator operates in the motoring mode. In this phase, the load drives the actuator, and part of the mechanical energy is returned to the system. This returned energy is referred to as "recoverable actuator energy" because, in principle, it could be captured and reused. However, in the present method, this energy is treated as a loss when calculating net efficiency, thereby providing a more conservative estimate of system performance. Therefore, using Eq. (5.13), the hydraulic net efficiency of the EHA can be expressed as:

$$\eta_{hyd.net} = \frac{P_{cy}}{P_{PM1}+P_{cp}} \quad \text{(for pumping operation)}$$

$$= \frac{P_{PM1}-P_{cy}}{P_{cy}+P_{cp}} \quad \text{(for motoring operation)} \tag{5.15}$$

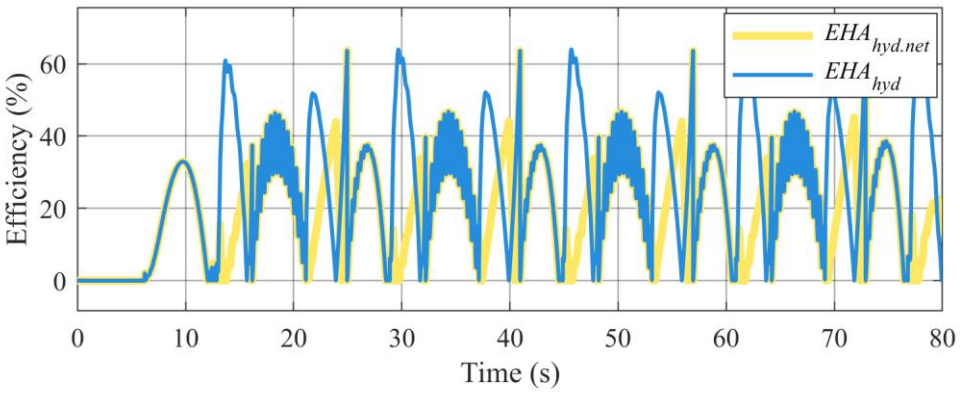

Figure 5-11: Comparison of hydraulic efficiency and net hydraulic efficiency for the electro-hydrostatic actuator.

Figure 5-11 compares the hydraulic efficiency and the net hydraulic efficiency of the Electro-Hydrostatic Actuator (EHA). During the pumping phase, both measures show similar results, with efficiencies of about 45%. However, in the motoring phase, the net hydraulic efficiency is about 15% lower than the standard hydraulic efficiency. This reduction occurs because the net efficiency considers recoverable actuator energy as a loss, which reduces the calculated value. Specifically, when the recoverable energy losses are included, the motoring efficiency drops from around 55% to 40%. This adjustment offers a more realistic representation of the EHA's actual performance.

Limitations of the Sankey flow Diagram-based efficiency method

A key strength of the Sankey flow diagram-based method is that it identifies and quantifies recoverable actuator energy as a distinct loss. This allows for a more accurate evaluation of the EHA, as none of the previously discussed methods explicitly addressed this factor; they mainly focused on efficiency improvement without isolating potential recoverable energy losses. However, this advantage becomes a limitation when assessing an EHA equipped with an ESR circuit. While the method can determine the amount of recoverable energy that is not utilized, it does not evaluate the subsequent storage and reutilization processes. As a result, it cannot provide a complete evaluation of the performance of hydraulic systems that incorporate energy storage and recovery mechanisms.

Given these limitations, there is a clear need for a performance evaluation method that not only measures recoverable energy losses but also considers the efficiency of energy storage and reutilization. The Cyclic Performance Index (CPI) approach, discussed in the next section, addresses this gap by providing a comprehensive framework for analyzing the complete energy flow within the EHA, including both recovery and reuse phases.

5.3 Cyclic Performance Index (CPI) Approach

After reviewing several existing methods, such as energy saving ratio, relative efficiency, and the Sankey flow diagram approach, it became clear that these methods have limitations when applied to systems incorporating energy storage and reutilization. They do not provide a complete or accurate representation of how energy is consumed, recovered, and reused within such systems. The main shortcomings can be summarized as follows:

Incomplete Energy Tracking: Many methods overlook the energy lost during transfer and storage stages, making it impossible to determine the actual amount of energy conserved accurately.

Limited Application to complex systems: Some approaches rely on assumptions like constant pressure or steady operating conditions, which are valid for simpler circuits but not suitable for systems with multiple interacting components, such as those incorporating accumulators for energy storage.

Narrow Focus on Individual Components: Existing methods often concentrate on the efficiency of a single part, such as a motor or a pump, without considering the overall system's functionality. This makes it hard to see how energy is being used or wasted throughout the system.

Because of these issues, a new approach is needed that provides a clearer picture of how energy flows, where losses occur, and how efficient the system is, especially in systems that reuse stored energy.

To address this, it is essential to consider that many hydraulic systems operate in two different modes within a single cycle: (a) pumping mode and (b) motoring mode. In such cases, the general efficiency definition cannot be applied. For systems that experience both phases within the same cycle, the appropriate measure is the cyclic efficiency. Cyclic efficiency represents the ratio of the total useful output energy to the total input energy evaluated over one complete operating cycle. For this system, the efficiency is given by,

$$\eta_{cyclic\ efficiency} = \frac{\int_0^T P_o dt}{\int_0^T P_i dt} \tag{5.16}$$

where P_i is the system input power, and P_o is the system output power within the time period, T.

However, in systems where two different operation modes (pumping and motoring) occur, inputs and outputs will vary within each cycle. In such cases, it is necessary to consider separate inputs and outputs and calculate the efficiency for each operation individually. Therefore, the following steps should be followed to determine the cyclic performance.

Step-1: **Identify the operational cycles:** The first step in defining the Cyclic Performance Index (CPI) is to identify the different operational modes that occur within a complete working cycle of the electro-hydrostatic actuator (EHA). In such systems, a complete cycle consists of alternating pumping and motoring operations, which can be distinguished by examining the relationship between the actuator force, F_R and the piston velocity ν.

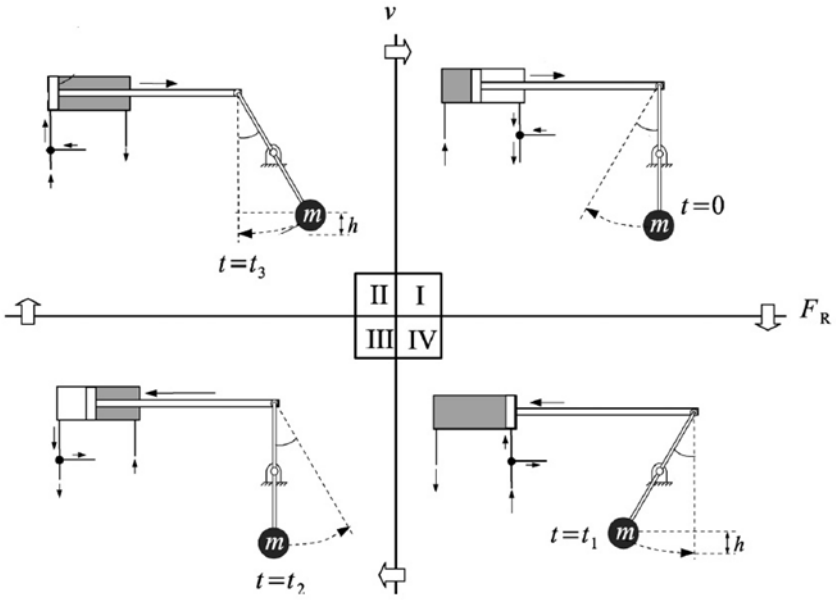

Figure 5-12: Four-quadrant operation of EHA [12].

Pumping operation occurs when the actuator moves against a resistive load, causing energy to flow from the prime mover to the actuator. This is observed when $F_R > 0$, and $\nu > 0$, corresponding to Quadrant I, and when $F_R < 0$, and $\nu < 0$, corresponding to Quadrant III. Conversely, motoring operation takes place when the actuator moves under the influence of an assisting load, returning energy to the system. This occurs when $F_R < 0$, and $\nu > 0$, in Quadrant II, and when $F_R > 0$, and $\nu < 0$ in Quadrant IV. For the EHA configuration shown in Figure 4-1, the system transitions sequentially through the quadrants in the order III → II → I → IV. The correct identification of these modes is essential for accurately assigning input and output power in the subsequent efficiency calculations.

Step-2: Measure input and output power: Having identified the operational phases in Step-1, the next step is to determine the input and output power for each part of the cycle. This distinction

is crucial because, in the EHA with and without an ESR circuit, a complete cycle involves four distinct operations: two pumping phases and two motoring phases, each with a different direction and nature of energy flow.

During the pumping phases, energy is transferred from the prime mover (servomotor driving Pump-1) to the actuator. The power supplied by the prime mover represents the input energy, while the output energy is the mechanical power that the actuator uses to move the load or perform the intended task.

During the motoring phases, stored potential energy in the load is released and returned to the hydraulic circuit. In this process, the actuator acts as the source of input energy. However, the prime mover may still supply additional power to maintain smooth motion or counterbalance forces, meaning that input and output are not as clearly defined as they are in pumping mode.

Because of these differences, applying a single efficiency definition to both modes is problematic. Instead, the power flows must be assessed separately for each operation, ensuring that the effect of energy recovery in motoring is accurately represented. In this approach, the analysis is carried out from the perspective of the cylinder power, which simplifies the identification of input and output flows.

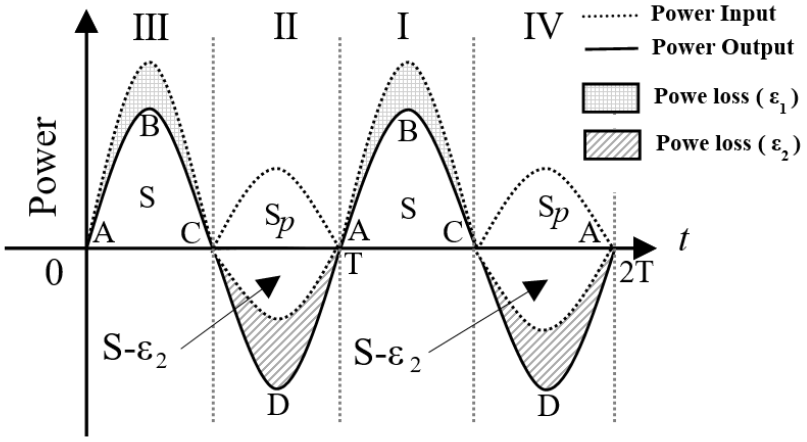

Figure 5-13: Power curves of the system similar to the EHA (reproduced from Costa and Sepehri, Energies, 2024, CC BY 4.0 [1].)

Consider the Electro-Hydrostatic actuator (EHA) as illustrated in Figure 4-1, which completes one cycle as shown in Figure 5-13, spanning 2T, and travelling through four operational quadrants

(III–II–I–IV). Pumping occurs in quadrants III and I (0→0.5T and T→1.5T), while motoring occurs in quadrants II and IV (0.5T→T and 1.5T→2T).

Energy flow in pumping operation: During the pumping phase (0 to 0.5T and T to 1.5T), the energy supplied by the prime mover to the main Pump-1 is denoted as $S + \varepsilon_1$, where S is the cylinder output power and ε_1 represents system losses, including mechanical friction, leakage, and pressure drops. This relationship can be written $S_p = S + \varepsilon_1$, where S_p is the total input energy from the prime mover. At the end of this operation, S amount of energy is stored as potential energy in the load.

Energy flow in motoring operation: During the motoring phase (0.5T to T and 1.5T to 2T), the stored energy S is returned to the system but reduced by losses ε_2. The energy returning to the main Pump-1 is $S - \varepsilon_2$. This energy is considered as "recoverable energy" and might be lost during motoring operation. In such cases, additional energy, S_p, can be supplied by the prime mover to ensure controlled motion of the load. This input can be equal to $S - \varepsilon_2$.

Step-3: Calculate the Cyclic Performance Index: With the input and output power flows established for both pumping and motoring operations, the next step is to evaluate the overall system performance using the Cyclic Performance Index (CPI). The Cyclic Performance Index (CPI) serves as a systematic tool for evaluating the performance of the hydraulic circuit. By separating pumping and motoring phases, it offers a comprehensive measure of how energy flows through the system and how losses affect overall performance. Unlike traditional efficiency definitions, which apply only to single-mode operation, the CPI accommodates systems such as the Electro-Hydrostatic Actuator (EHA), where both pumping and motoring operations occur within the same cycle.

For the EHA shown in Figure 4-1, the CPI is calculated based on the input and output power determined in Step-2. The CPI is expressed as:

$$\gamma = \frac{\int_0^{0.5T} P_o\, dt + \int_T^{1.5T} P_o dt}{\int_0^{0.5T} P_i\, dt + \int_{0.5T}^{T} P_i\, dt + \int_T^{1.5T} P_i\, dt + \int_{1.5T}^{2T} P_i\, dt} \qquad (5.17)$$

$$= \frac{S + S}{2(S + \varepsilon_1) + 2S_p} \quad \leq 1$$

where P_o is the output power of the cylinder during the pumping operation, representing the energy delivered to the actuator and P_i is the input power from the prime mover during pumping and motoring operations. The term S represents the useful output energy of the actuator, ε_1 denotes system losses during pumping, and Sp is the additional input energy supplied by the prime mover during motoring phases to maintain smooth motion. To validate this expression, simulation data for EHA were used:

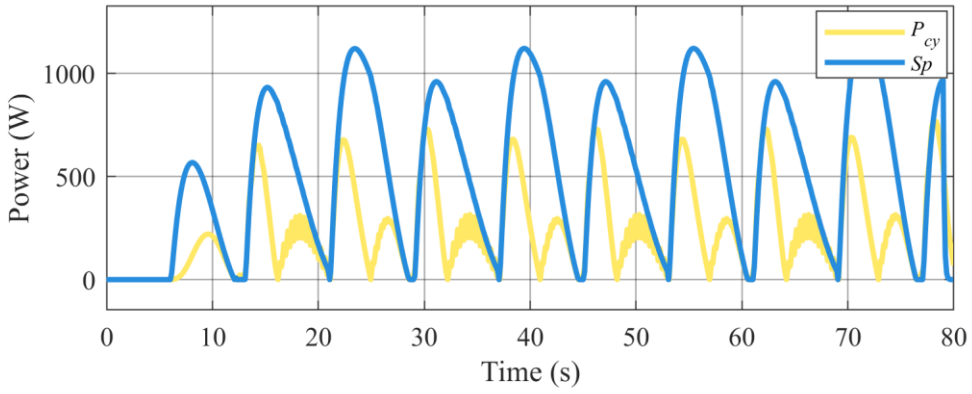

(a)

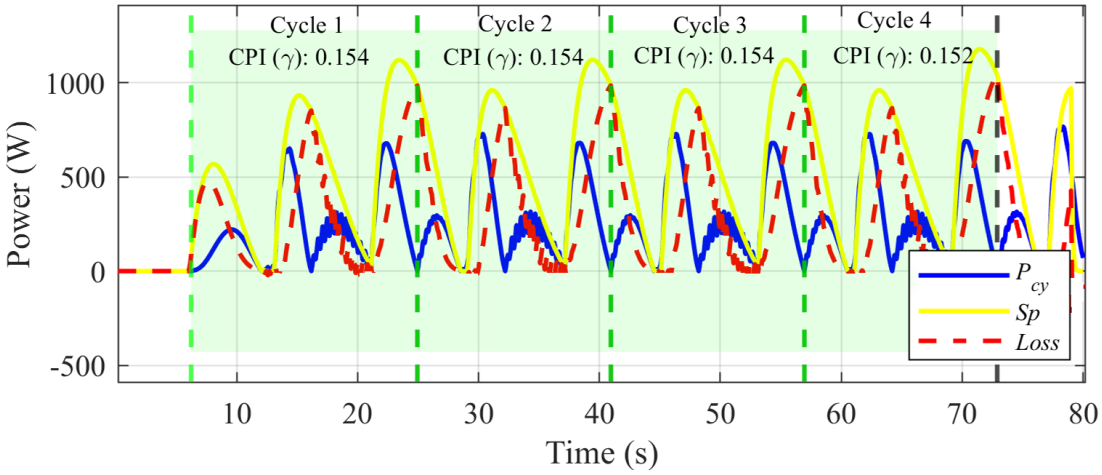

(b)

Figure 5-14: (a) Power curves of cylinder power vs Prime mover power, (b) Cylinder power vs prime mover power vs loss and energy performance of EHA in each Cycle.

Figure 5-14(a) shows the power curves for both the actuator and the servomotor, while Figure 5-14(b) illustrates four complete operating cycles over a period of 80 seconds. The cycle intervals were identified as: 6.2350 – 24.9460 s for cycle 1, 24.9470 – 40.9450 s for cycle 2, 40.9460 – 56.9450 s for cycle 3, and 56.9460 – 72.8920 s for cycle 4.

The efficiency for each cycle was calculated using the CPI concept, as defined in Eq. (5.17). This involved numerically integrating the actuator output power (cylinder power) and the input power from the servomotor over each cycle interval, using simulation data obtained from MATLAB/Simulink. Energy losses were considered during both pumping and motoring operations. These were calculated using the relations $S_p = s + \varepsilon_1$ during pumping, and $S_p = s - \varepsilon_2$ during motoring. Using this approach, the calculated CPI for the respective cycles were 0.154, 0.154, 0.154 and 0.152, resulting in an average CPI (γ) of 0.15, which is less than 1, satisfying the condition outlined in Eq. (5.17).

Up to this point, the CPI framework has been used to evaluate the performance of the EHA. This provides a consistent basis for assessing energy use and losses across entire operating cycles. The next step extends this framework to the EHA with an Energy Storage and Reutilization (ESR) circuit, allowing for a more meaningful comparison of energy recovery and reutilization performance across different system configurations.

Step-4: Compare Results: While the CPI provides a meaningful evaluation of the EHA, its application to systems incorporating energy storage and reutilization needs further refinement. In the ESR configuration, part of the energy released during motoring phases is not lost; instead, it is stored in an accumulator and later reused in the subsequent pumping phases. This distinction must be captured to avoid underestimating system performance.

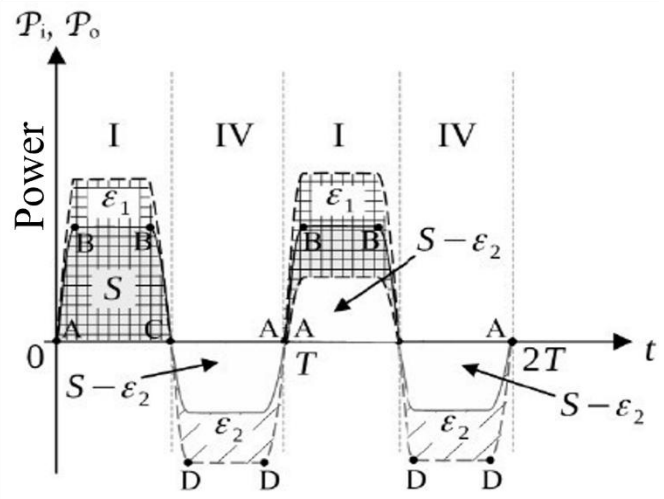

Figure 5-15: Power curves of an Idle energy storage and reutilization system [1].

As shown in Figure 5-15, during the motoring quadrant, the energy recovered from the load (S - ε_2) remains within the circuit rather than being wasted or counterbalanced by the prime mover. It is assumed that there is no power loss during storage and reutilization. The recovered energy is utilized in the subsequent pumping quadrant. In such cases, the cyclic performance index may exceed unity, indicating effective energy recovery and reuse. Due to this possibility, it is required to introduce a new indicator "γ".

The behaviour is captured by redefining the performance indicator using the CPI, expressed for the first cycle as:

$$\gamma = \frac{\int_0^{0.5T} P_o \, dt}{\int_0^{T} P_i \, dt} = \frac{S}{(S+\varepsilon_1)-(S-\varepsilon_2)} = \frac{S}{\varepsilon_1+\varepsilon_2} \tag{5.18}$$

where γ is the CPI, indicating how effectively the system manages energy, $\varepsilon_1 + \varepsilon_2$ are the total circuit losses, measured as the power consumed by the prime mover during the interval [0, T], and S is the energy remaining from the load after losses.

Unlike the efficiency, η, which is always bounded between 0 and 1, the CPI can exceed 1, representing cases where energy recovery significantly enhances system performance. This makes the CPI a more suitable metric for comparing the energy performance of the EHA with an ESR circuit.

Using this method, the system shown in Figure 4-3 is analyzed. The system completes a full cycle by operating across four distinct quadrants. The corresponding energy flows in the circuit are illustrated in Figure 5-16. It should be noted that Figure 5-16 does not represent experimental results but rather a conceptual framework of the possible energy flow in an EHA equipped with an ESR circuit. The diagram extends the cyclic representation of the EHA shown earlier in Figure 5-13 and illustrates how energy can be stored during motoring phases and reused during subsequent pumping phases, thereby reducing the demand on the prime mover.

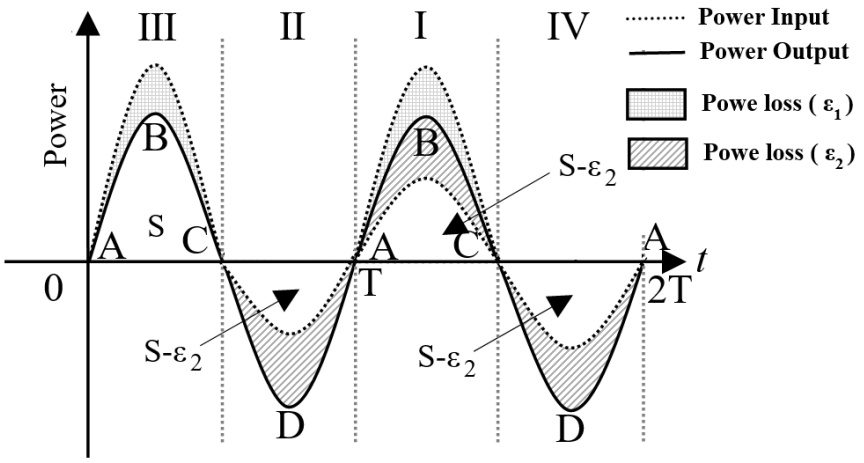

Figure 5-16: Energy flows in an EHA with ESR circuit (reproduced from Costa and Sepehri, Energies, 2024, CC BY 4.0 [1]).

As shown in Figure 5-16, the system transitions through four operational quadrants, labelled I, II, III and IV:

Motoring Quadrants (II and IV): Energy returns from the load to the system in these quadrants. The energy recovered is partially stored $(S - \varepsilon_2)$ and later reused during the subsequent pumping quadrants. It is also assumed that an additional S_p amount of energy is supplied by the prime mover in these quadrants to help control the motion of the weight, ensuring a stable operation.

Pumping Quadrants (I and III): During these quadrants, the prime mover supplies additional energy to compensate for the main circuit losses (ε_1). It is assumed that the energy stored in the previous motoring quadrants $(S - \varepsilon_2)$ assists the pump in driving the cylinder, reducing the overall energy demand on the prime mover. The performance of the ESR systems across the complete cycle is evaluated using the cyclic performance index (γ), calculated as follows:

$$\gamma = \frac{\int_{0.25T}^{0.5T} P_o\, dt + \int_{0.75T}^{T} P_o\, dt}{\int_0^T P_i\, dt} = \frac{2S}{2[(S+\varepsilon_1)-(S-\varepsilon_2)]+S_p} = \frac{2S}{2(\varepsilon_1+\varepsilon_{2)+S_p}} \quad (5.19)$$

where P_o is the cylinder output power, P_i is the input power from the prime mover, ε_1 is energy loss during pumping, ε_2 is energy loss during motoring, and S_p is additional energy supplied by the prime mover during motoring and pumping quadrants.

Simulation results and CPI calculation for EHA with ESR circuit

The performance of an Electro-Hydrostatic Actuator (EHA) equipped with an Energy Storage and Reutilization (ESR) circuit was evaluated using MATLAB. The primary objective was to determine the Cyclic Performance Index (CPI) and assess whether recoverable energy was properly reutilized or not.

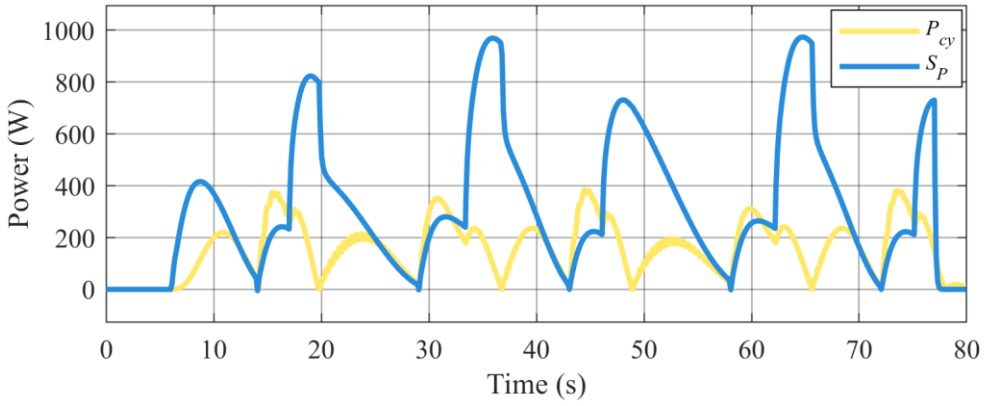

Figure 5-17: Power curves of cylinder power (P_{cy}) vs Prime mover power (S_P).

Figure 5-17 displays the power curves for the cylinder power versus prime mover power during simulation, which was conducted for 80 seconds. In Eq. (5.19), P_o representing the output power delivered by the actuator during the pumping phase, and P_i denotes the input power supplied by the servomotor across the entire cycle.

To apply this concept, the actuator power was integrated during two distinct pumping intervals $[t_1, t_2]$ and $[t_3, t_4]$. This corresponds to the numerator in the CPI equation. The denominator,

representing the total energy supplied by the servomotor, was calculated by integrating the input power curve (P_i) from $t=0$ to $t=t_4$. Thus, Eq. (5.19) simplifies to:

$$\gamma = \frac{\int_{t_1}^{t_2} P_o\, dt + \int_{t_3}^{t_4} P_o\, dt}{\int_0^{t_4} P_i\, dt} = \frac{\int_{t_1}^{t_2} P_{cy}\, dt + \int_{t_3}^{t_4} P_{cy}\, dt}{\int_0^{t_4} S_p\, dt} = \frac{2S}{S_p} \tag{5.20}$$

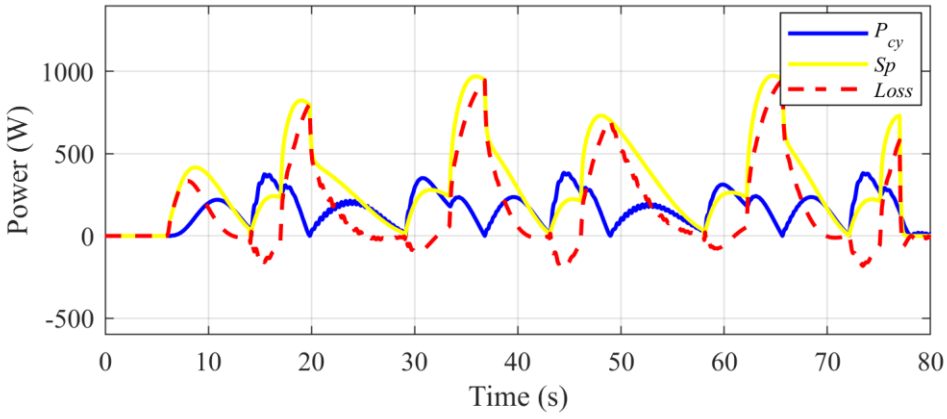

(a)

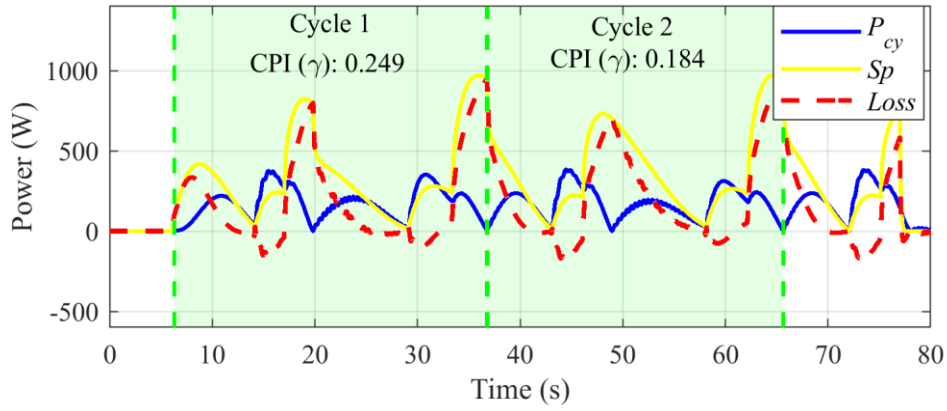

(b)

Figure 5-18: (a) Power curves of the cylinder power vs Servomotor power vs Loss, (b) Energy performance of the EHA with ESR circuit using CPI.

As shown in Figure 5-18(b), the system completed two cycles during the 80-second simulation. The start and end times for each cycle were identified as 6.2980s – 36.7920s for cycle 1, and 36.7930s – 65.6380s for cycle 2. Using Eq. (5.20), the Cyclic Performance Index (CPI) for each

cycle was calculated and is shown in Figure 5-18(b). The Cyclic Performance Index (CPI) for the respective cycles were found to be 0.249 and 0.184, with an average value of 0.2165, which is less than 1. The simulation results showed that the EHA system's performance improved by 44.33% due to the addition of the ESR circuit. However, it was observed that a significant portion of the stored energy was not fully reutilized within the system or no energy recovery at Quadrant IV, suggesting there is room for optimization.

To better interpret what is happening in the system based on the calculated Cyclic Performance Index (CPI) values, Table 5.1 provides a clear framework. After determining the CPI, this table can be used to identify the underlying energy dynamics in the system. By comparing the calculated CPI with the cases represented in Table 5.1, one can diagnose the system behaviour and efficiency:

Table 5.1: Cyclic Performance Index (γ) for selected circuit configurations.

Case	**Interpretation**	$\boldsymbol{\varepsilon_1}$	$\boldsymbol{\varepsilon_2}$	$\boldsymbol{S_p}$	$\boldsymbol{\gamma}$
1	Perfect lossless circuit	0	0	0	$\Gamma = \frac{S}{\varepsilon_1+\varepsilon_2} = \frac{S}{0} = \infty$;where $(\boldsymbol{S_1 = S_2 \cong S})$
2	Some energy recovered at quadrants II and IV	>0	>0	0	$\Gamma = \frac{S}{\varepsilon_1+\varepsilon_2} > 1$; where $(\boldsymbol{S_1 = S_2 \cong S})$
3	No, loss, free weight fall (all motoring energy wasted, at quadrants II and IV	0	S	0	$\Gamma = \frac{S}{\varepsilon_1+\varepsilon_2} = \frac{S}{S} = 1$; where $(\boldsymbol{S_1 = S_2 \cong S})$
4	Free weight fall (all motoring energy wasted, at quadrants II and IV)	>0	S	0	$\Gamma = \frac{S}{\varepsilon_1+\varepsilon_2} = \frac{S}{\varepsilon_1+S} < 1$; where $(\boldsymbol{S_1 = S_2 \cong S})$
5	Weight held by the prime mover (no energy recovery at quadrant II and IV)	>0	>0	S_p	$\Gamma = \frac{S}{(S+\varepsilon_1)+S_p} < 1$; where $(\boldsymbol{S_1 = S_2 \cong S})$
6	**Some energy is recovered at quadrants II and IV**	**>0**	**>0**	**S_p**	$\boldsymbol{\Gamma = \frac{S_1}{[(S_1+\varepsilon_1)-(S_2-\varepsilon_2)]+S_p} < 1}$ **where $(\boldsymbol{S_1 < S_2})$**

7	Weight to heavy to be moved (pump energy lost through relief valves)	>>0	0	0	$\Gamma = \frac{S}{\varepsilon_1+\varepsilon_2} = \frac{0}{\varepsilon_1} = 0$; where $(\boldsymbol{S_1 = S_2 \cong S})$

The current simulation results align with case 6, where the system operates with circuit losses (ε_1,$\varepsilon_2 > 0$) and requires additional energy input (S_p) from the prime mover. In this case, some energy is recovered in Quadrants II and IV, but due to the losses and input demands, the CPI (γ) remains less than 1. The condition $S_1 < S_2$ is indicating that the cylinder energy (S_2) during motoring operation is greater than the cylinder energy (S_1) at pumping operation. As a result, during motoring operation, to counterbalance the cylinder energy, more energy is supplied by the servomotor.

This table and its analysis provide a clear framework for interpreting CPI values and diagnosing system performance under different configurations. By comparing the calculated CPI to the cases outlined in Table 5.1, specific areas of inefficiency can be identified, guiding further optimization efforts.

5.4 Summary

This chapter evaluated different approaches for analyzing the energy performance of hydraulic systems, particularly those with Energy Storage and Reutilization (ESR) circuits. The study highlighted the limitations of traditional efficiency calculation methods and introduced the Cyclic Performance Index (CPI) as a more suitable alternative.

The analysis began with current methods, the Energy Saving Ratio, Relative Efficiency and Sankey Flow Diagram-based efficiency evaluation. Each method was applied to an Electro-Hydrostatic Actuator (EHA), both with and without an ESR circuit, to understand how well they capture energy recovery and reutilization. The Energy Saving Ratio proved useful for comparing systems with and without recovery capabilities but was unable to provide reliable results when both systems incorporated ESR. The Relative Efficiency method relies on flow rate comparisons but was unsuitable for systems with energy storage due to varying pressure conditions. The Sankey Flow Diagram method provided a visual representation of energy flow but lacked precision in tracking recoverable energy.

To address these limitations, the Cyclic Performance Index (CPI), developed by Costa and Sepehri [1], was presented as a standardized metric for evaluating energy performance. Unlike traditional methods, CPI considers energy storage, transfer and reutilization by providing a more precise and more accurate assessment. It accounts for energy losses in different stages of the system and identifies how much stored energy is effectively reused.

Simulation results confirmed that CPI provides a more reliable way to measure efficiency in hydraulic systems with ESR circuits. The comparison between CPI and current methods demonstrated that CPI gives a better understanding of system performance and energy recovery. This chapter concludes that CPI is a more accurate and practical tool for evaluating the performance of hydraulic systems, especially when energy reuse is involved.

Chapter 6 Conclusion

This thesis presented and applied the concept of the Cyclic Performance Index (CPI) to evaluate the energy performance of Electro-Hydrostatic Actuators (EHA) both with and without the integration of an Energy Storage and Reutilization (ESR) circuit. The CPI method, originally developed by Costa and Sepehri [1], was shown to provide a more comprehensive and accurate framework for performance evaluation, as it explicitly includes stored and reutilized energy in the analysis.

Previously developed efficiency measurement methods, such as Energy Saving Ratio, Relative Efficiency, and Sankey Flow Diagram, were analyzed in this thesis and found to have limitations when applied to systems with energy recovery. These methods failed to fully account for stored and reused energy, leading to incomplete or misleading efficiency assessments.

The CPI approach addressed these challenges by evaluating system performance over full operational cycles, which include both pumping and motoring phases. This dual-mode consideration allows CPI to reflect the realities of energy recovery and reutilization, offering a more balanced and accurate evaluation of system efficiency. Simulation studies showed that adding an ESR circuit improved the EHA's energy performance by about 44.3%, with CPI values increasing from 0.15 to 0.21. The analysis also indicated that Quadrant IV exhibited incomplete energy recovery, suggesting that not all stored energy was effectively reused and that further optimization of the EHA with an ESR circuit design is needed.

The findings of this study emphasise the importance of adopting a unified, standardised performance indicator for hydraulic systems, especially those with energy recovery features. The CPI not only measures recoverable energy but also reveals inefficiencies at various stages of operation, allowing for more accurate system assessments. By applying the CPI approach to real-world scenarios, this research enhances understanding of energy flows, losses, and reutilization in fluid power systems, and establishes a strong groundwork for developing energy-efficient and sustainable hydraulic technologies.

6.1 Thesis Contributions

The main contributions of this thesis are summarized as follows:

1. A detailed review of previously developed efficiency measurement methods Energy Saving Ratio, Relative Efficiency, and Sankey Flow Diagram) was conducted, highlighting their limitations when applied to systems with energy storage and reutilization.
2. The Cyclic Performance Index (CPI) [1], introduced as a recent development in hydraulic system analysis, was examined and applied in this study as a new performance indicator. It provides a comprehensive framework for analyzing energy flow and system performance of the systems with ESR circuits.
3. The CPI was applied to a newly developed Electro-Hydrostatic Actuator through detailed simulation experiments. The results showed that the integration of an Energy Storage and Reutilization (ESR) circuit improved energy utilization, with CPI confirming a 44.3% increase in efficiency. These findings validate the CPI as an effective tool for capturing energy recovery and reutilization, underscoring its value as a performance evaluation method for hydraulic systems.

6.2 Future Work

This research provided a foundation for improving energy performance evaluation in hydraulic systems. Future work could focus on the following items listed below.

- Testing CPI in more complex hydraulic systems with multiple actuators to assess its effectiveness in large-scale applications. This would help confirm its usefulness in various system designs and working conditions.
- Creating standardized testing methods based on CPI to compare the energy efficiency of hydraulic systems in different industries. A common framework would allow fair comparisons and help improve system design and performance.

Further refining and expanding the CPI approach will support understanding and the development of more energy-efficient and sustainable hydraulic systems.

References

[1] G. K. Costa and N. Sepehri, "A New Approach for Measuring and Comparing the Energy Performances in Hydraulic Systems," *Energies (Basel)*, vol. 17, no. 24, Dec. 2024, doi: 10.3390/en17246397.

[2] C. WILLIAMSON, "Efficiency Study of an Excavator Hydraulic System Based on Displacement-Controlled Actuators," *Proceedings of the Bath/ASME Symposium on Fluid Power and Motion Control (FPMC), 2008*, pp. 291–307, 2008, Accessed: Jan. 01, 2025. [Online]. Available: https://cir.nii.ac.jp/crid/1573387449821871616.bib?lang=en

[3] C. Morton, V. Pickert, and M. Armstrong, "Self-Alignment Torque as a Source of Energy Recovery for Hybrid Electric Trucks," *IEEE Trans Veh Technol*, vol. 63, no. 1, pp. 62–71, Jan. 2014, doi: 10.1109/TVT.2013.2271049.

[4] A. Marouf, M. Djemai, C. Sentouh, and P. Pudlo, "A New Control Strategy of an Electric-Power-Assisted Steering System," *IEEE Trans Veh Technol*, vol. 61, no. 8, pp. 3574–3589, Oct. 2012, doi: 10.1109/TVT.2012.2209689.

[5] P. Immonen *et al.*, "Energy saving in working hydraulics of long booms in heavy working vehicles," *Autom Constr*, vol. 65, pp. 125–132, May 2016, doi: 10.1016/j.autcon.2015.12.015.

[6] P. Ponomarev, *Tooth-Coil Permanent Magnet Synchronous Machine Design for Special Applications*. [Online]. Available: https://www.researchgate.net/publication/275890030

[7] P. Ponomarev, M. Polikarpova, and J. Pyrhönen, "Design of integrated electro-hydraulic power unit for hybrid mobile working machines," 2011. [Online]. Available: https://www.researchgate.net/publication/252044947

[8] T. A. Minav, L. I. E. Laurila, and J. J. Pyrhönen, "Analysis of electro-hydraulic lifting system's energy efficiency with direct electric drive pump control," *Autom Constr*, vol. 30, pp. 144–150, 2013, doi: 10.1016/j.autcon.2012.11.009.

[9] "Parker, Hydraulic Motor/Pump Series F11/F12. [Internet]," http://www.parker.com2007.

[10] M. Vukovic, R. Leifeld, and H. Murrenhoff, "Reducing fuel consumption in hydraulic excavators-a comprehensive analysis," *Energies (Basel)*, vol. 10, no. 5, 2017, doi: 10.3390/en10050687.

[11] A. Pourmovahed, N. H. Beachley, and F. J. Fronczak, “Modeling of a Hydraulic Energy Regeneration System-Part I: Analytical Treatment,” 1992. [Online]. Available: http://asmedigitalcollection.asme.org/dynamicsystems/article-pdf/114/1/155/5527843/155_1.pdf

[12] G. K. Costa and N. Sepehri, “Four-quadrant analysis and system design for single-rod hydrostatic actuators,” *Journal of Dynamic Systems, Measurement and Control, Transactions of the ASME*, vol. 141, no. 2, 2019, doi: 10.1115/1.4041382.

[13] G. K. Costa and N. Sepehri, “A critical analysis of valve-compensated hydrostatic actuators: Qualitative investigation,” *Actuators*, vol. 8, no. 3, Sep. 2019, doi: 10.3390/ACT8030059.

[14] “Energy Storage and Reutilization for a Single-Rod Electro-Hydrostatic Actuator System,” 2022.

[15] J.-S. Chen, “Energy Efficiency Comparison between Hydraulic Hybrid and Hybrid Electric Vehicles,” *Energies (Basel)*, vol. 8, no. 6, pp. 4697–4723, 2015, doi: 10.3390/en8064697.

[16] S. Qu, D. Fassbender, A. Vacca, and E. Busquets, “A High-Efficient Solution for Electro-Hydraulic Actuators with Energy Regeneration Capability,” *Energy*, vol. 216, Feb. 2020, doi: 10.1016/j.energy.2020.119291.

[17] K. K. Ahn, T. Hung, and T. Dinh, “A Study on Energy Saving Potential of Hydraulic Control System Using Switching Type Closed Loop Constant Pressure System,” *Proceedings of the JFPS International Symposium on Fluid Power*, vol. 2008, Jan. 2008, doi: 10.5739/isfp.2008.317.

[18] T. Shang, “Improving Performance of an Energy Efficient Hydraulic Circuit,” 2004.